Università degli Studi di Padova

DIPARTIMENTO DI INGEGNERIA DELL'INFORMAZIONE
Corso di Laurea Magistrale in Bioingegneria

Tesi di laurea Magistrale

Comparison of muscle activity detection techniques during underwater gait of patients with Parkinson's disease

Laureanda:
Matilde Righetto

Relatore:
Prof.ssa Zimi Sawacha

Correlatori:
Elena Pegolo
Marco Romanato

Anno Accademico 2021–2022

Ai miei nonni

Abstract

In recent years underwater rehabilitation has gained popularity in the treatment of Parkinson's disease. Moreover, the study of muscular electrical activity of pathological subjects during walking have shown important results in clinical applications. One of the issues of analysis of electromiographic signal is the correct detection of muscle on and off states during movements execution. However, many different detection techniques have been implemented to identify muscle activity. The aim of this thesis was to compare results obtained by the application of two different muscle activity detection techniques to the signal acquired during underwater walking of patients with Parkinson's disease.

Sommario

Negli ultimi anni la riabilitazione in acqua ha guadagnato popolarità nel trattamento della malattia di Parkinson. Inoltre, lo studio dell'attività elettrica dei muscoli di soggetti patologici durante la camminata ha riportato risultati importanti nell'applicazione clinica. Una delle difficoltà dell'analisi del segnale elettromiografico è il corretto rilevamento degli stati di attivazione e disattivazione muscolare durante l'esecuzione dei movimenti. Tuttavia, esistono diverse tecniche di rilevamento che sono state implementate per identificare tale attività. Lo scopo di questa tesi è stato quindi quello di confrontare i risultati ottenuti dall'applicazione di due diverse tecniche di rilevazione dell'attività muscolare al segnale acquisito per la camminata in acqua di pazienti con morbo di Parkinson.

Contents

List of Figures

Introduction

Comparison of gait between healthy and pathological subjects has been extensively studied over the years. In addition, information about instants of muscle activation with respect to the gait cycle has proven to be of paramount importance in many clinical situations, including improvements in management of neuromuscular disabilities [2].

Parkinson's disease is one of the most common neurological disorder that affects the movement. PD walking has been extensively analyzed. Indeed, Parkinson's disease is a motor disorder widespread throughout the world and to date, there is no definitive cure for this disease. However, along with several pharmacological and non-pharmacological treatments, one treatment that is gaining popularity is water rehabilitation, specifically under water walking performance. Therefore, a thorough understanding of muscle activity during under water walking in Parkinson's patients can be a useful tool for the analysis, diagnosis and possible effects of this treatment on the disease.

Currently, acquisitions of muscle activity under water can be directly performed due to the technology development of recent years. However, being the acquisition of EMG signal under water a more recent technique, it is still under investigation.

The aim of this thesis was therefore to compare two different methods applying two different filtering techniques for the identification of muscle activity on the EMG signal of Parkinson's patients walking under water. In addition, these methods were also applied to land-based walking signals of healthy subjects to

test their detection efficacy.

Chapter 1 describes the epidemiology, symptoms, and treatment of Parkinson's disease. Chapter 2 illustrates the state of the art in gait analysis with a focus on gait cycle phases, under water walking, and pathological walking in patients with Parkinson's disease. Chapter 3 describes in detail surface EMG, the most common noise artifacts of this signal, the possible processing and filtering techniques and the confounding factors of the EMG signal under water. Chapter 4 presents the subjects involved in the study, the experimental setup and the two different methods used to identify muscle activity. Chapter 5 reports the results obtained both for healthy and Parkinson's disease subjects with the application of the muscle activity detection algorithm. Finally, in chapter 6 conclusions, limitations, and possible future developments of this thesis are described.

Chapter 1

Parkinson's disease

Parkinson's disease (PD) is a neurodegenerative disorder of the Central Nervous System (CNS) characterized by slowness of motion, muscles stiffness, tremors, and, from a morphological point of view, by the degeneration of neurons in the substantia nigra of the compact zone of ventral midbrain. PD is the second most common degenerative disorder, after Alzheimer, and it is one of the common causes of neurological disability, involving 1% of the global population over 55 years old [3].

1.1 Epidemiology

Parkinson's disease epidemiology can be a useful tool to understand the widespread of the disorder and its possible causes. Epidemiology can be divided into two different categories: descriptive epidemiology, which outlines the occurrence of the disease, and analytical epidemiology, which instead deals with the determinants of the disease, i.e. all those factors that may play a role in the causal chain underlying disease mechanisms.

1.1.1 Descriptive epidemiology

In descriptive epidemiology the occurrence of new cases of disease, injury, or other medical conditions over a specified time period is called incidence, while prevalence includes both new and existing cases. Consequently incidence measures the strength of the disease in the population and represents the rate of disease occurrence, while prevalence measures the disease burden in the population and increases as the incidence and duration of the disease increases.
In 2019 the incident number of PD was about 1 million cases worldwide, which has increased by 159.73% since 1990 whereas the global prevalent number has reached 8 million cases showing an increment of 155.5% from 1990 [4]. Moreover, recent studies [5, 6] predicted that the burden of PD will grow substantially in future decades.
The age-specific analysis of prevalence allows to state that PD is dominant in age classes over 65 and that the largest increasing percentage occurred in the group aged over 80. Moreover, specific rates among gender shows a slight prevalence of the disease on men instead of women: this is possibly due to the neuroprotective effects of estrogen for females and also to the higher occupational factors or unhealthy lifestyles in males [4].
There are many indexes that can help with the description of Parkinson's disease epidemiology, some of the most common ones are listed below:

- Years lived with disability (YLD): is an index that measures the average lifespan of incident cases until rehabilitation or death and the disability due to the status. It is widely used to evaluate the health loss caused by PD;

- Age-standardized rate (ASR): is a summary measure of the rate that a population would have if it had a standard age structure and it's necessary when the data exist for different age groups in multiple populations over time. This rate can be computed for different variables, like incidence, prevalence and YLD;

- Estimated annual percentage change (EAPC): is an index that describes the trend of ASR, and it is calculated using a linear regression model. Positive EAPC highlights that there is an increasing trend while a negative index states for a decreasing trend.

Zejin Ou et al. [4] analyzed the PD burden worldwide from 1990 to 2019, and they showed how incident and prevalent cases vary from country to country. Figure 1.1 reports the incidence of PD in terms of ASR in 2019, percentage changes between 2000 and 2019 and the EAPCs of each country. Figure 1.2 describes the prevalence of PD in terms of ASR in 2019, percentage changes between 2000 and 2019 and the EAPCs of each country. It can be seen that there is a heterogeneous distribution between countries that varies for both incidence and prevalence. Italy, for example, shows a decreasing trend of ASR for incidence and prevalence, while United States of America shows an increasing index. In some cases, an increasing trend can be justified by the PD dependence on aging, correlated with a sound health system and a decreasing fertility rate. Whereas, the decreasing trend of Italy may be due to the Mediterranean diet, since it was demonstrated it reduced the risk for PD. Nevertheless, Parkinson's epidemiology data and studies [4, 5, 6] highlight the necessity to find effective strategies to decrease the overall burden of PD, that cover pharmacological treatment [3, 7], neurosurgery [8] and rehabilitation [9] as well.

1.1.2 Analytical epidemiology

Analytical epidemiology is constantly trying to find out the cause-effect relation of the diseases. As a consequence, since the discovery of PD, many researchers have been trying to identify a single cause of the disease. However, more recent research suggests the presence of multiple causes [3].
In 1878 Charcot identified stress as the possible cause of the onset of PD, and over the years the possibility of a hereditary and infectious cause was taken into consideration and analyzed [3]. Only more recent studies have found that forms of familiar PD in which inheritance follows a Mendelian pattern are extremely

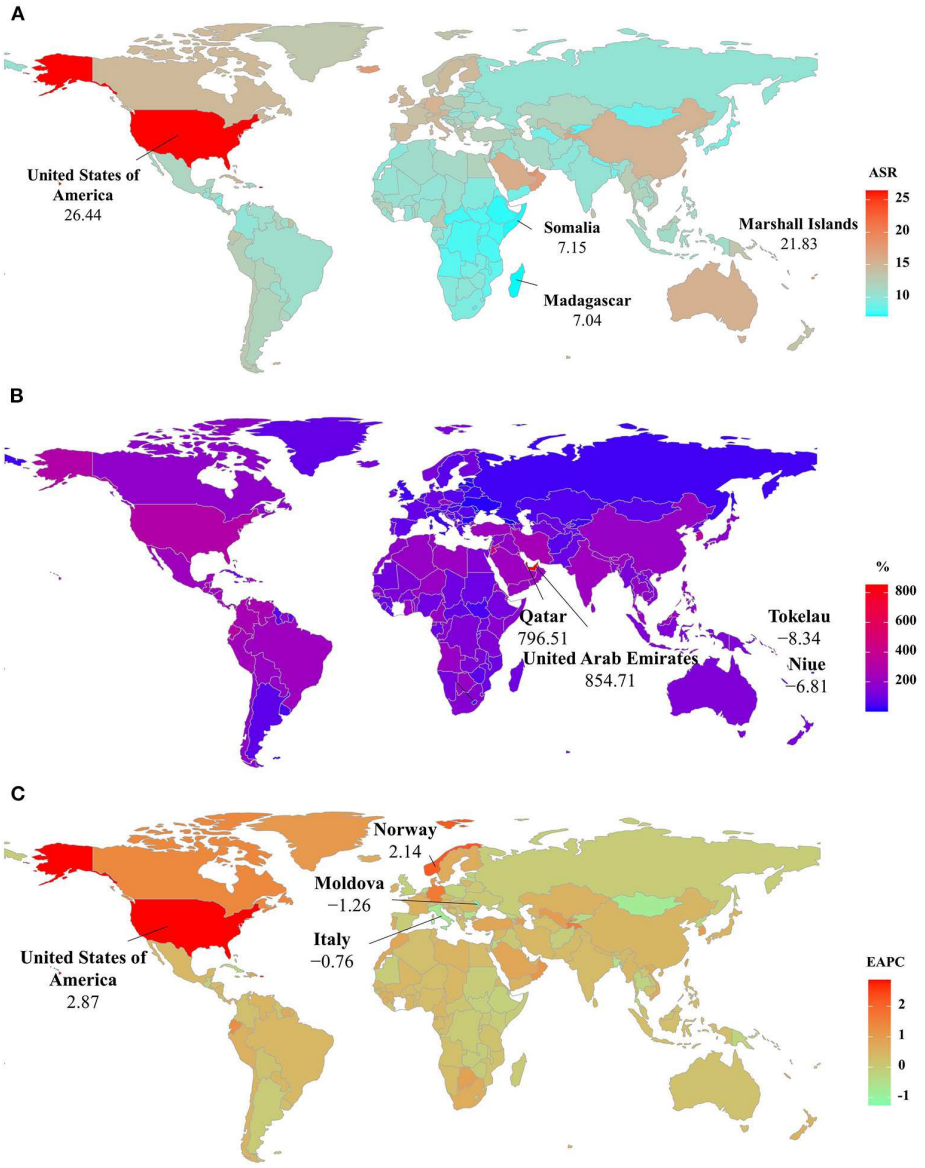

Figure 1.1: The distribution of ASRs, percentage changes, and EAPCs of Parkinson's disease incidence at the national level. (A) shows the ASR in 2019; (B) the percentage changes in number between 2000 and 2019; (C) the EAPCs in countries/territories, respectively. Countries/territories with an extreme value are annotated (Zejin Ou et al., [4]).

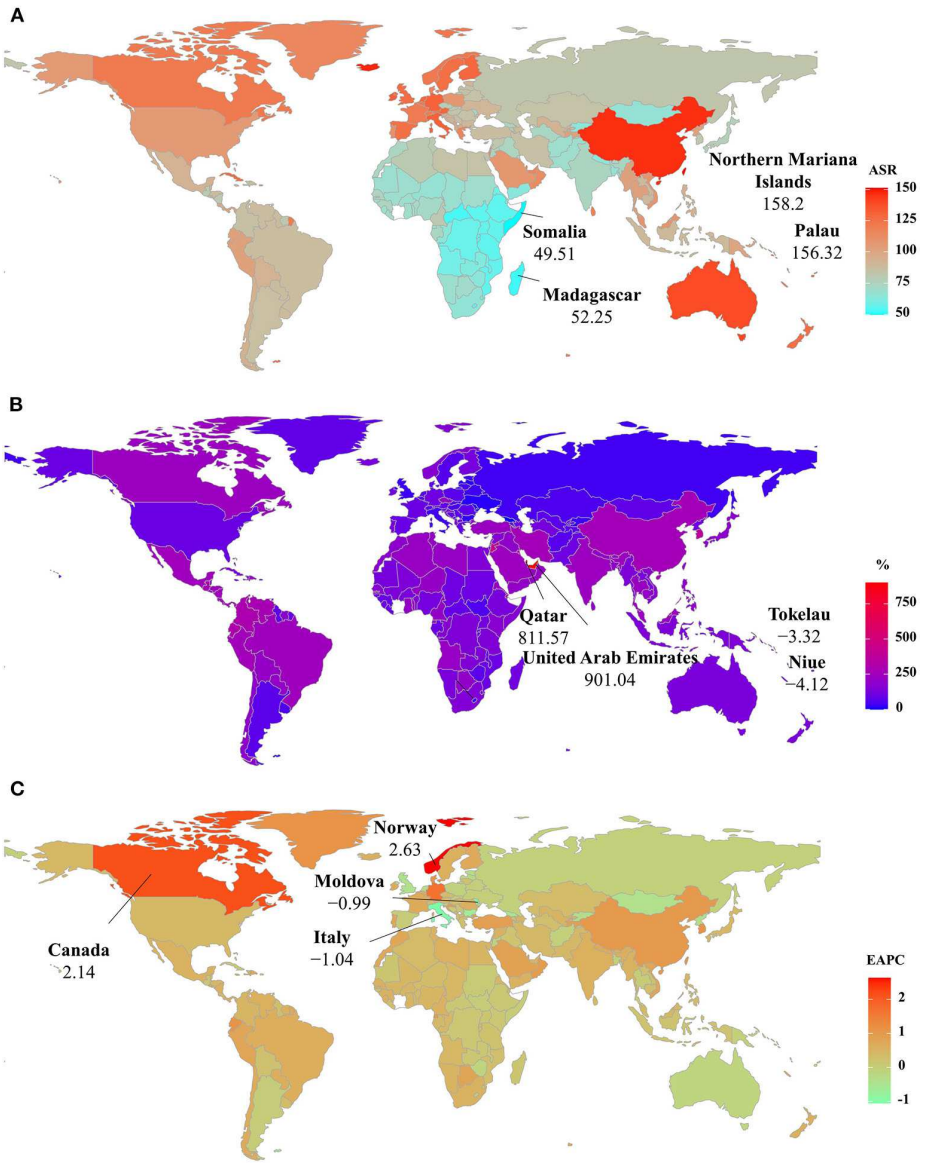

Figure 1.2: The distribution of ASRs, percentage changes, and EAPCs of Parkinson's disease prevalence at the national level. (A) shows the ASR in 2019; (B) the percentage changes in number between 2000 and 2019; (C) the EAPCs in countries/territories, respectively. Countries/territories with an extreme value are annotated (Zejin Ou et al., [4]).

rare (less than 1% of all PD patients) [10]. PD, then, can be considered a sporadic disorder.

Nowadays, there is evidence that PD is a disorder that involves multiple functional and neurotransmitter systems, moreover its pathological characteristics are similar in each of the targeted neuron groups, suggesting a common neurodegenerative process [3].

In 1960 it was discovered that in PD subjects the level of dopamine, which is a neuromodulatory molecule functioning as a neurotransmitter in brain, was much lower in comparison to that of healthy subjects. Consequently it was possible to start thinking of a treatment with levodopa, at that time known as a precursor of dopamine, and still used today [10].

The causes are still largely unknown [11], although they are mostly attributed to both genetic and environmental factors and, in some cases, to a prolonged exposition to one or more toxic substances (i.e. 1-methyl-4-phenyl-1,2,3,6-tetrahydropyridine, named MPTP). It also appears that moderate exercise is associated with a slightly reduced risk of disease [3]. Furthermore, various group of foods and specific nutrients have been investigated as a potential risk factors of PD and, on the other hand, it has been studied the possibility to obtain beneficial effects on longevity and age-related diseases through some specific diets, for example the Mediterranean one [4].

1.2 Symptoms

Nowadays PD diagnosis is still a clinical diagnosis since there are no specific biochemical and neuroradiological markers. The classic symptomatological picture is described by the presence of some main traits such as [3]:

tremors are present in approximately 70% of patients, they mainly occur at rest at an average frequency of 3-6 Hz. They may arise at the onset of the disease and they are usually unilateral, occurring firstly at the upper limb level. Later they can spread to the controlateral side nevertheless

maintaining a certain asymmetry.

stiffness is characterized by an augmented muscular tone both in flexors and extensors muscles. It is present in 89-99% of PD subjects.

bradykinesia consists in a slowdown of the speed of movement execution, it occurs in 77-98% of cases usually together with akinesia (inability to initiate movement) and hypokinesia (movement amplitude reduction). Early indicators can be observed in distal muscle groups with manifestations of reduced dexterity and impaired repetitive finger movements or prone-supination of the hand. In more advanced stages of the disease, akinesia takes over, making it difficult to perform movements of daily life.

postural changes occur as a result of a balance disorders present in PD patients. Balance is controlled by the extrapyramidal motor system from information derived from vision, the vestibular system and the proprioceptive system. There is a sensation of balance when the visual image is stabilized. Patients with Parkinson's disease tend to perceive as "good" a position that is actually pathological, thus causing the postural changes. As the disease progresses, there is also a loss of postural straightening reflexes.

These primary symptoms, that, if lateralized, can be clinically diagnostic of PD [10], are often accompanied by various non-motor symptoms related to the neurovegetative system (sialorrhea, seborrhea, constipation, orthostatic hypotension) and psychic (depression, memory disorders). Therefore it seems reductive to refer to PD exclusively as a motor disorder, since it is also a neurological disease and can involve all the districts in which neurotransmitters are present. In patients with Parkinson's disease, in fact, in addition to the motor symptoms mentioned above, there is also a degeneration of neurons in the substantia nigra of the brain that are responsible for the production of dopamine (DA), which is in turn responsible for the activation of circuits that control movement and balance. In the substantia nigra and noradrenergic

locus coeruleus of PD subjects, single or multiple, spherical, acidophilic masses presenting a dense nucleus with a peripheral halo, termed "Lewy bodies", are frequently found [3]. Consequently, a definitive diagnosis of Parkinson's disease requires pathological confirmation of two invariant features, namely the presence of the Lewy bodies (LBs) in regions of predilection and a reduced number of DA neurons in the substantia nigra pars compacta [10]. Furthermore, in order to assess the presence of PD, in addition to the classical clinical diagnosis which has a high margin of error [12], it is possible to achieve greater specificity using functional neuroimaging techniques for evaluation, such as positron emission tomography (PET) or single photon emission computed tomography (SPECT) [3].

1.3 Treatment and rehabilitation

There are many therapeutic options for treating PD, some of the most common ones are:

- anticholinergic treatment, the first pharmacological treatment used for PD [3], now specifically used for resting tremors [7]
- pharmacological substitutional treatment with levodopa, a precursor of dopamine, and, more recently, with substances that act directly on dopaminergic receptors
- deep brain stimulation (DBS) or other surgical approach
- rehabilitation

Choosing one or more of these options depends on the type of Parkinson, the stage of the disease and they are in some cases applied together, depending on the need. For example, rehabilitation is strongly recommended in every stage of the disease and independently on the motor symptom of the patient [7].
In general, levodopa is used to treat motor symptomps in almost all PD subjects, whereas for young subjects with prominent tremor, anticholinergic agents can

be used, being mindful of potential cognition-related adverse events.

Selection of the optimal therapy requires a thorough evaluation of the risks and benefits of each possible treatment. Levodopa, for example, has shown excellent results in terms of functional improvement, such that patient response to this therapy has itself become one of the diagnostic criteria for PD [3]. However, levodopa has increased dyskinesia risks, particularly with higher doses. In contrast, therapy with monoamine oxidase-B (MAO-B) inhibitors and dopamine antagonists is associated with lower risk of dyskinesia but, at the same time, has a lower efficacy [7]. As the disease progresses, PD subjects could require even higher doses of drugs and a possible addition of other therapies with complementary mechanism of action, like DBS or therapy with levodopa-carbidopa enteral suspension (via percutaneous endoscopic transgastric jejunostomy). However, thalamic procedures (unilateral focused ultrasound thalamatomy or DBS) are usefull only for the tremor but not for other parkinsonian features [7]. A general summary diagram describing a proposed therapy for Parkinson's motor symptoms is shown in figure 1.3.

Currently, there is no pharmacological therapy that prevents or delays PD progression, for this reason a physical therapy is considered as an adjuvant to pharmacological and surgical treatments in a way to maximize functional ability and minimize secondary complications [13]. Indeed, there is much evidence that rehabilitation and exercise bring beneficial effects to people quality of life, especially that of the elderly and those with neurological disorders [7]. Moreover, exercise has been associated with a reduced risk of developing PD [14].

There is no unique physical treatment for PD. A wide variety of rehabilitation methods can be found in literature, such as general physiotherapy that includes stretching, muscle strengthening, balance and postural exercises, gait and aerobic activity, or other types of training as resistance or strength training [7], treadmill training [15] and underwater training [16]. Certainly, different exercise approaches may enhance different motor aspects of PD. For example, resistance training can increase muscle strength and thus improve gait performance, while stretching can help to adjust the abnormally flexed posture in PD [13]. Moreover, a study

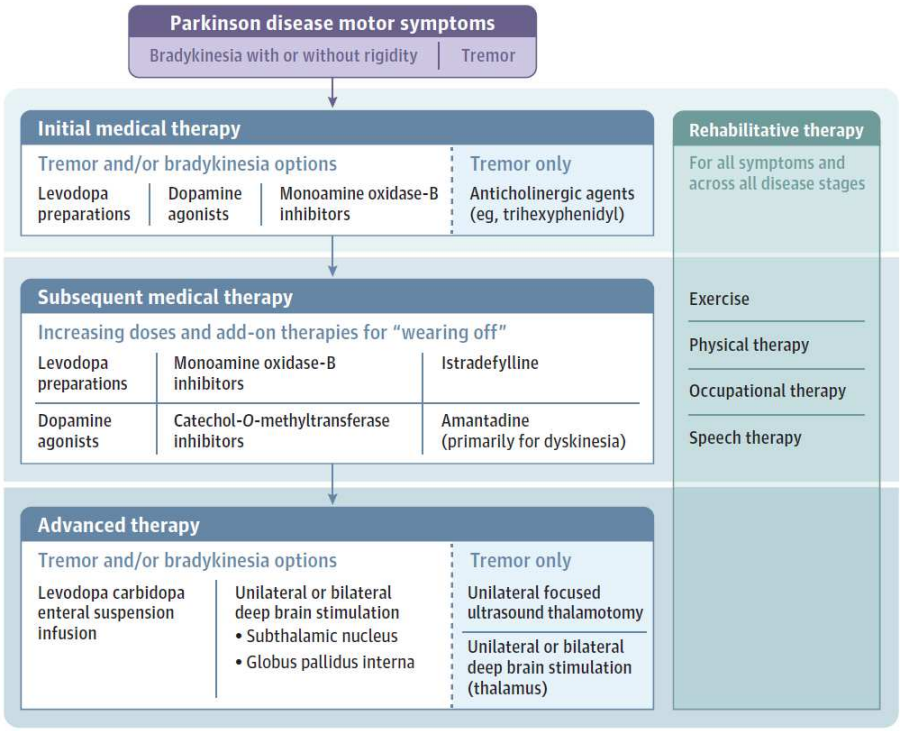

Figure 1.3: Proposed general approach to treat motor symptoms in Parkinson disease (M. J. Armstrong and M. S. Okun, [7]).

on treadmill training [15] reports significant results of clinical benefits on motor symptoms in PD subjects undergoing high intensity training. Furthermore, it is known that providing external temporal or spatial stimuli, can facilitate the initiation and maintenance of ongoing motor activities, particularly the rhythmic ones, such as gait, as they may help to compensate the defective generation of internal signals in PD that usually lead to loss of balance.

Alongside rehabilitation strategies, non conventional strategies, like music and dance therapy or Tai Chi, were tested too. Tai Chi has shown an enhance of postural control and a decrease in falls [13].

PD is characterized by relatively large phenotypic heterogeneity, and it is not known yet whether there are types of PD that are better suited to specific therapy. Nevertheless, a relatively preserved ability in motor learning has been found in subjects with PD, although consolidation of learned material may sometimes be

defective. Thus, both frequency and intensity of training are very important, since these elements seem to have an influence on short and long-lasting effects of motor performance [13], and so a poor training schedule might limit the benefit of the physical therapy or its maintenance over time.

Chapter 2

Motion capture and gait analysis

Newtonian mechanics is the oldest branch of physics devoted to the study of motion, the forces that causes the motion and the internal forces that act within the body. Biomechanics is the application of Newtonian mechanics to the study of the neuromuscular skeletal systems and one important branch of Biomechanics is the motion analysis of human gait. Indeed, Biomechanics is widely used in orthopedics, physical medicine and rehabilitation characterizing both functions and dysfunctions of the muscular skeletal system [17].

2.1 History

The science of gait analysis has its origin in Europe in the 17th century even if the first know written reference to the analysis of walking was made by Aristotle around 384-322 BCE [18]. The discoveries done in this field provided a solid scientific foundation for the understanding of human walking. These are attributed to some important scientists like Borelli who in *De Motu Animalium* (1679) analyzed the action of the muscles, the movement of the limbs, the

activities of man and animals and some aspects of human physiology, Galvani who wrote *De Viribus Electricitatis In Motu Musculari* (1791), where the earliest electrical experiments on animals' muscles can be found, Newton to whom are attributed his dynamic laws and study of forces in *Philosophiae Naturalis Principia Mathematica* (1687), and many others like Descartes, Marey, Carlet and the Weber brothers. Then, in the 19th century also Braun and Fischer created a representation of the gait of military subjects carrying backpacks employing the principles of Newtonian classical mechanics, the coordinate geometry of Descartes, and mathematical concepts of Borelli for muscles action estimation [2].

The basis of modern gait analysis originated in Europe during the Renaissance. At that time, Cardan studied the properties of three-dimensional angles, Galileo introduced deductive reasoning by experimental observation, and Descartes devised an orthogonal system for describing the position of objects in space. A few years later, Borelli performed the first experiment in gait analysis. However, in Borelli's work there were some mistakes in physical laws which were correctly formulated by Isaac Newton only few years later [18].

In 1836, the Weber brothers combined knowledge of mechanics and physiology in their publication *Mechanik der Gehwerkzeuge* in which they reported the presence of a correlation between walking speed and step cycle parameters including stride length and cadence. Moreover, they were the first ones to provide illustrations of limbs segment position at different walking instants. In the same period, electrophysiology was born in parallel with human movement studies, and attributed to Duchenne, who was at the time a student of human movement [18].

In 1872, Gaston Carlet designed the first shoe with three pressure sensors placed inside the sole and published the first accurate description of healthy human gait. Then, in addition to human movement, animal movement was also studied, expecially that of the horses. Carlet's teacher, Jules Etienne Marey, adapted pressure measurement devices in order to detect equine cannon bone pressure during gallop. Hence he discovered the existence of a short period when no

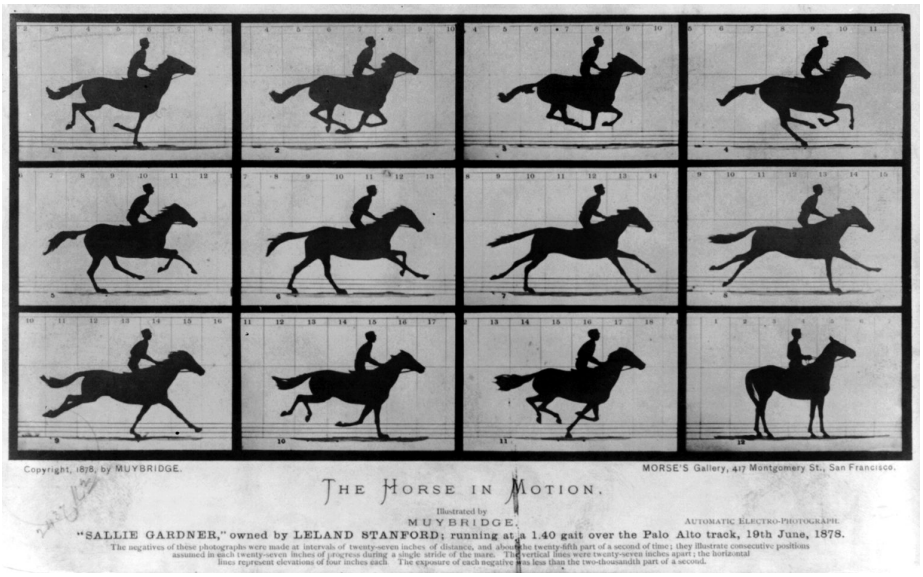

Figure 2.1: The Horse in Motion by Eadweard Muybridge, 19th June 1878 (Wikimedia Commons, [19]).

hoof rests on the ground. In order to further prove this findings, Stanford and Muybridge took multiple pictures of the whole trot (Fig. 2.1); their work was published in 1878 [18].

In the following years, Marey refined the imaging technique and used it for human movement pathological studies. Then, his work was continued by Charles, Robert, Jean and Pierre Ducroquet, culminating in the book *Walking and Limping: A study of Normal and Pathological Walking* (1965). Further, Mary introduced the use of force plates during gait analysis, though the first commercially available force plates were developed in 1969.

Marey, however, always focused on the study of two-dimensional measurements. Braun and Fisher were the first ones to conduct a three-dimensional analysis of gait, and their work remained a definitive study of kinematics for several decades [18].

In 1945 a group of 40 scientists of the University of California at Berkeley worked on the study of amputee gait, introducing the need of distinguishing normal from pathological gait. Through their studies, gait analysis began to be used

as a clinical tool. Later, two surgeons, Jacquelin Perry and David Shutherland, separately made major contributions to the development of clinical gait analysis by combining EMG with kinematics and kinetics. Dr Perry, then, focused on lower extremity function of human body, developing an unique instrumentation for monitoring EMG, foot floor contact, joint motion and energy cost of walking. This incorporation of computer processing of foot switch and EMG helped the identification of some gait parameters, like stance and swing percentages, walking velocity, stride length and stride frequency [2].

Nowadays, with technology development and a growing interest in motion analysis, motion capture is becoming more and more sophisticated allowing for an accurate identification of walking instants and a comprehensive understanding of the muscle activation associated with them. Moreover, such systems are capable of measuring in real time the three-dimensional movement of a subject, with accuracy greater than half a millimeter.

2.2 Instrumentation

Motion capture systems aim to objectively measure the movement of body segments (kinematic) and, in some cases, ground reaction forces and joint moments (kinetics), and muscles activation (EMG). Motion capture is able to reconstruct trajectories of anatomical landmarks in space during a movement execution. The most common method requires a laboratory where the analysis is performed. However, the expanding use of wearable devices [20] and the introduction of innovative methods have facilitated motion capture analysis outside of a laboratory.

Currently, many tools support motion capture analysis. The use of these tools depend also on the type of application for which motion capture is intended (clinical, sports, research, movies, etc.).

The systems used for acquisition can be divided into two main groups: optical and non-optical systems.

2.2.1 Non optical systems

Non-optical systems are systems that do not require the use of cameras. These systems use sensors attached to body parts to send data about their position in space. They can be divided into different categories: mechanical, electromagnetic systems and inertial.

Mechanical systems use electrogoniometers or rigid structures attached to the joints of the body that articulate as subject's body in motion [21]. These systems are low cost but they are quite cumbersome and could reduce the naturalness of movement.

Electromagnetic systems are composed of small electric coils, which acquire signals along the three space dimensions. Measurements are detected by a continuous magnetic flux generation and an external generation of a small voltage or current due to the movement [21].

Inertial systems are based on the use of small sensors containing accelerometers often combined with gyroscopes and magnetometers. Accelerometer consists of a mass whose weight is known and which is free to move inside the instrument due to the inertial forces. This instrument is capable to transduce acceleration into an electrical signal; therefore, for subjects in static position, is able to measure angular rotations. In order to analyze dynamic movements, instead, gyroscopes and magnetometers are combined with accelerometers through sensor fusion algorithms. Generally, these systems are compared to the optical ones as reference criterion or used in conjunction with them to complement data [21].

2.2.2 Optical systems

Optical systems are systems that requires the use of cameras. There should be at least two cameras to be able to calculate the three-dimensional position of a point and they have to be in a fixed position. For each camera it is possible to draw the straight line passing through the optical center of the lens to the position were the point is projected in the sensor. The intersection of two of these straight lines drawn for the same point for two cameras set at a fixed

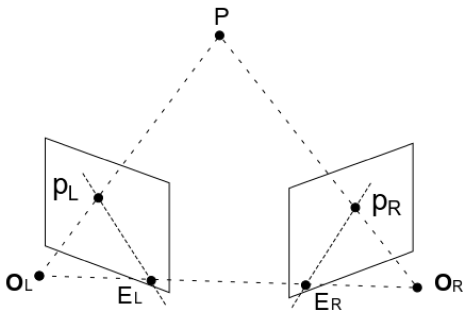

Figure 2.2: Principles of stereophotogrammetry. Two cameras, with their respective focal points OL and OR, observe a point P. The projection of P onto each of the image planes is denoted pL and pR. Points EL and ER are the epipoles. If the position and projection angles of the cameras are known, the location of any object in three dimensions can be determined (Wikimedia Commons, [22]).

position represents the position of that point in space (Fig. 2.2). However, before carrying out the reconstruction it is necessary to calibrate cameras. There are two different types of calibration. The first one is performed placing a set of axes representing the reference system in the data collection area (static calibration), the second one consists in moving an object of known dimensions, usually a wand, in the volume of cameras (dynamic calibration). For each camera, the position and orientation, as well as the focal length, the position of the optical center and distortion parameters are then calculated. Having these parameters, it is possible to perform the three-dimensional reconstruction.

Thus, optical motion capture systems require at least two cameras for triangulation, which must be synchronized with each other, and a software for image reconstruction and processing.

Optical systems can be then divided into two different categories:

- marker-based
- markerless

Marker-based optical systems

Marker-based optical systems are widely use, especially for clinical applications. This approach requires the use of markers that are applied on subjects' skin. Markers can be either active or passive. Active markers are generally LED markers and emit their own light so that they can be easily detected. They usually have different color or frequency of illumination to make them easily

distinguishable. In contrast, passive markers are retroreflective, therefore infrared cameras are used with this type of markers. The reflective material that covers the surface of the markers is called Scotchlite and it reflects infrared light emitted by diodes mounted on cameras back to the camera lens. There are pros and cons on the choice of active or passive markers. Active markers are immediately and automatically recognizable but require a local power supply, on the other side passive markers are to be recognized on the basis of the initial static positioning and a "model" of anatomic arrangement is required but they not require continuous power supply [23]. Although there are many advantages to using active markers, to date the most widely used ones are passive markers, since current hardware, and software, have nearly eliminated problems with marker identification and tracking, thus removing the principal objection to passive marker systems [24].

Marker-based optical systems are principally used for gait analysis since they are known to provide accurate results. Generally, eight or more cameras are necessary for full-body capture through different marker sets comprising around 40 markers applied to specific anatomic landmarks [21]. Markers are attached to subject's skin following specific protocols. Gait analysis protocols presented in literature are different in number of markers to be applied and in positions where they have to be attached but they all lead to define the position and orientation of the body segment on which they are placed. A good choice of protocol is important for the purpose of the experiment and for ensuring reproducibility of marker application. One of the major problems related to the use of the marker-based technique is soft tissue artifacts, for this reason all protocols provide an arrangement of markers aimed at minimizing this error, some providing the application of markers on anatomical landmarks where the movement of the bone under the skin is minimal, others act directly on the static calibration of the position of the marker during the execution of the two extremes of the movement [23].

In the laboratory configuration, cameras are placed at a fixed distance from each other and all directed toward the center of the room. In some cases, image

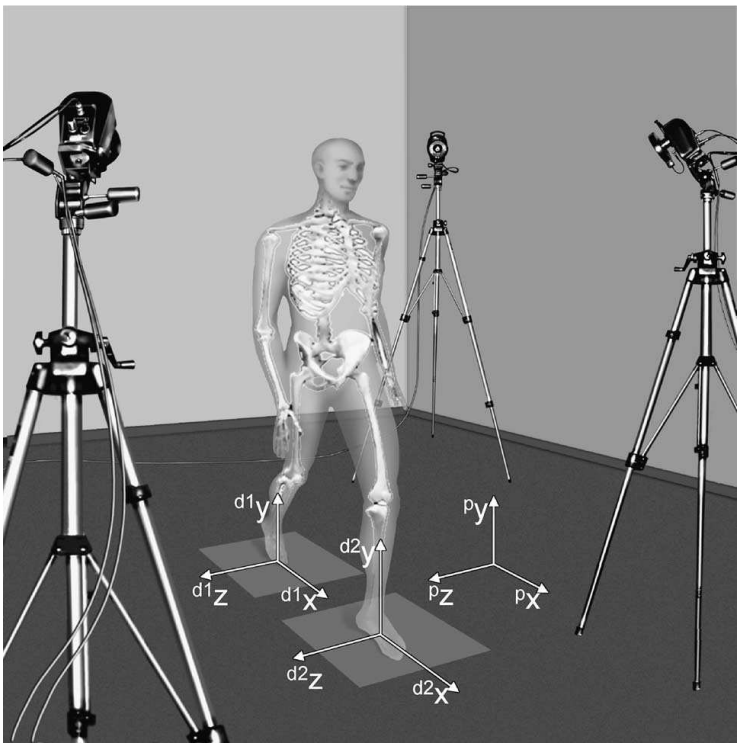

Figure 2.3: The human movement analysis laboratory. Basic measurement instruments are depicted together with their systems of axes (p: photogrammetry; d: dynamometry). If level walk is analyzed, the motor task frame may coincide with the frame of one of the two force plates (A. Cappozzo et al., [25]).

acquisition is combined with the use of two force plates placed in the center of the laboratory with known position with respect to the reference system. An example of the setup of a laboratory for gait analysis is shown in Fig. 2.3.
In gait analysis, the subject is asked to walk back and forth across the room. When he/she steps on the platform, it is possible to determine force and moment components acting during the foot stance phase and combine this information with the body segments position at each instant. In addition, another type of information is usually combined; in fact, in some cases during gait analysis, EMG acquisitions are also performed. In this case, EMG sensors are applied on the subject's skin with reference to the position of the muscles of lower body. From these measurements, it is possible to associate each instant of step cycle

with the presence of certain force and moment components and specific muscle activations.

Markerless optical systems

Markerless optical systems are able to reconstruct subject movements without the use of markers. They consists of sophisticated computer image processing techniques that reconstruct the three-dimensional motion from video of cameras. The employed cameras generally comprise one or two regular video cameras, and they are used together with infrared and ultrasonic sensors. This instrumentation is also employed for videogame and entertainment and is used to identify human forms from which to extract body segments and joints [21]. Markerless techniques allow the reduction of errors derived from the use of markers, including soft tissue artifacts. These artifacts can be distinguished into relative errors that are due to relative movement between two or more markers defining a rigid segment and absolute errors that are instead due to the movement of a marker relative to the bone landmark it represents [23]. However, the type of cameras used for markerless motion capture have usually lower resolution and acquisition frequency than those used in the laboratory, thus reconstructing the trajectory of a body segment during gait results in less accuracy [21].

2.3 Gait analysis

The most common application of movement analysis is gait analysis [17]. The act of walking relies on the repetition of a sequence of limb motions to simultaneously move the body forward while also maintaining stance stability.
Nowadays, there are mainly three different approaches for the definition of significant gait events [1]:

- subdivision of gait cycle according to the variation of reciprocal floor contact by the two feet
- use of time and distance qualities of the stride

- events functional significance identification within the gait cycle

2.3.1 Gait cycle division

During walking, the support of the right foot is alternated with that of the left one. While one foot is resting on the ground, the other one moves forward until it advances to a new support site. The action is then repeated in a reciprocal and alternating manner.

Since walking is a cyclic movement, a single sequence performed by a limb is defined as a gait cycle (GC). Consequently, the instant of beginning and end of the cycle should be identified. Thanks to the fluency of movement, any instant could be defined as the onset of GC. However, the starting point of GC is generally identified in the first floor contact of the foot. For healthy subjects, this coincides with the first heel strike [1]. The end point of the cycle then coincides with the next heel strike.

GC can be divided into two periods: stance and swing phases (Fig. 2.5). The former identifies the entire period in which the foot is in contact with the floor, even partially, while the latter identifies the phase in which the foot is completely detached from the ground and moves forward. The stance begins with the initial contact of the foot and ends when the foot is lifted off the ground, which corresponds to the beginning of swing phase. Stance period can be divided into three different phases, distinguished by the presence or absence of the stance of the controlateral foot. The first and third parts of stance phases are characterized by a double limb support, indeed both the feet are in contact with the floor. In contrast, in the second phase only the foot taken in exam is in contact with the floor. These phases are defined in order: initial double limb stance, single limb support and terminal double limb stance [1]. Initial double limb stance begins with the initial contact of the foot, single limb support when the opposite foot is lifted and terminal double limb stance with the initial contact of the controlateral foot.

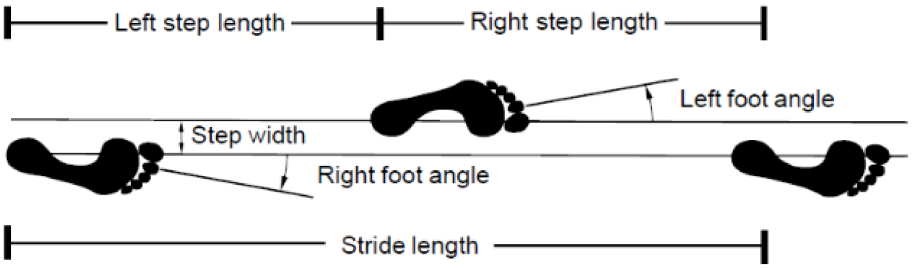

Figure 2.4: Stride and step comparison (PressureRef4PIL, [26])

2.3.2 Gait cycle timing and distance

The generic normal distribution of GC phases consists of 60% of GC for stance and 40% for swing. However, the precise duration of gait cycle intervals depend on subject's walking speed. The duration in time of stance and swing periods shows an inverse relationship to walking velocity; indeed as walking speed increases, GC time decreases. Nevertheless, there is a different relationship between the division of stance periods. An increase in walking speed leads to an increase in the duration of total stance duration of single stance but a decrease in the length of double stance intervals, whereas a decrease in speed causes the opposite effect. The single limb support matches the swing of controlateral limb, as they are occurring at the same time. When there are no double stance, subject is supposed to be in running mode [1].

Finally, gait cycle can also be defined in terms of stride and step length. Thus, it is important to define the difference between "stride" and "step". Stride corresponds to the GC, so it is defined for the action of a single limb. The length of a stride is the interval between two sequential initial contacts by the same limb. The step instead defines the interval between two sequential initial contacts of the two limbs. At the midpoint of one stride, the other foot hits the ground to start its next stance period. Stride and step can be measured in terms of length and time duration [1]. A clear representation of step and stride can be seen in Fig. 2.4.

Then, together with stride and step length and time, other parameters derived

from the concept of GC are usually defined. They are: cadence, speed, step width and single support percentage.

Cadence is the frequency of walking and the reciprocal of stride time, it is generally expressed in steps per minute. Speed represents the mean speed of the center of mass of the subject over the course of the gait. Step width is the distance between two feet when they are both on the floor perpendicular to the direction of walking. Lastly, single support percentage is the percentage of the GC time supported by a single limb [27].

Primitive interpretations of a subject's gait may be conducted solely using spatio-temporal parameters. Most of the times they are integrated with all other information and signals acquired during the performing of gait analysis. However, comparison of those parameters with that of healthy subjects could be a diagnostic tool [27].

2.3.3 Phases of gait

A single stride contains 8 functional patterns (Fig. 2.5), that are [1]:

Initial contact (0-2% GC)

This phase includes the instant in which the foot touches the floor and the reaction of body to the weight transfer.

Loading response (3-12% GC)

This phase is part of the initial double limb stance and ends when the other limb is lifted for swing.

Mid stance (13-31% GC)

This phase is the first phase of single limb support. It begins as the controlateral foot starts the swing period and ends when the body weight is aligned with the forefoot.

Terminal stance (32-50% GC)

This phase begins when the heel rises and ends when the other foot reaches

the ground. This last event coincides with the end of single limb support interval. In this phase, the weight of the body goes forward to the forefoot.

Pre-swing (51-62% GC)

This is the final phase of stance. It begins with the initial contact of the other foot and continues until ipsilateral toe off. In this phase the body prepares itself to a transfer of weight on the other foot and contributes to the progression of forward movement while preparing the foot to swing.

Initial swing (63-75% GC)

This phase is the first one-third of swing period. It begins as the foot is totally lifted from the floor until the swinging foot is opposite to the stance foot.

Mid swing (76-87% GC)

This phase is the middle third of swing period. It begins when initial swing ends and continues till the swinging limb is forward and the tibia is vertical.

Terminal swing (88-100% GC)

The last phase of swing and of the entire gait cycle. It starts when the tibia is vertical and ends when the foot touches the floor.

Patterns from 1 to 5 are part of stance period, while patterns from 6 to 8 are of swing period. Each pattern directly identifies the functional significance of the different motions occurring at the individual joints. The phases of gait also provide a means for correlating the simultaneous actions of the individual joints into patterns of total limb function. This is significant for interpreting the functional effects of disability [1].

2.4 Underwater gait analysis

In recent years, the application of motion analysis in environments different than the one of the laboratory gradually increased. Therefore, in addition to

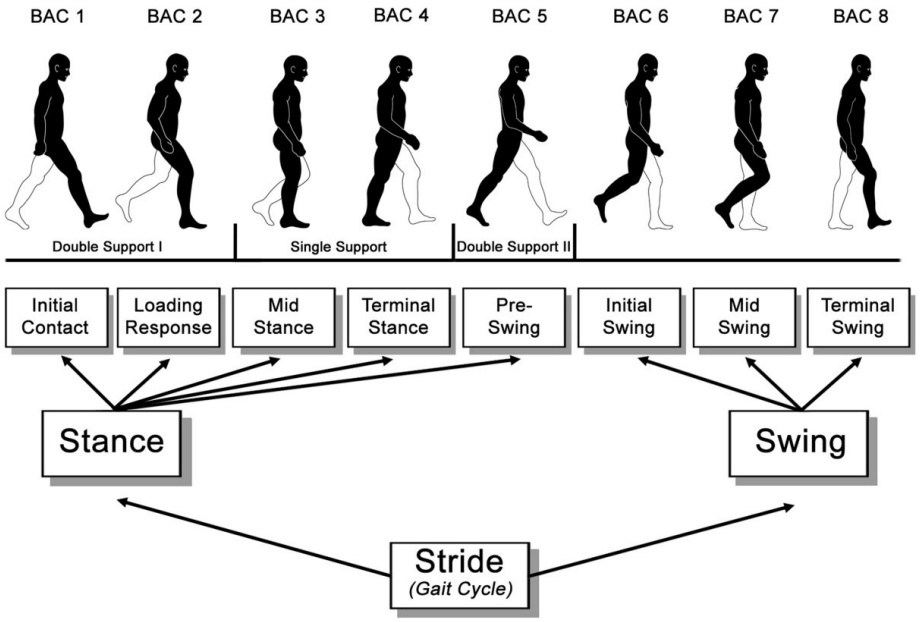

Figure 2.5: Functional division of gait cycle based on the work of Perry and Burnfield (2010) (ProtoKinetics, [28])

the opportunity of conducting motion analysis outdoors, it application is also performed in aquatic environments, usually in swimming pools.

The application of gait analysis in aquatic environment is due to the important role gained by both study on swimmers and in-water rehabilitation. Indeed, the aquatic environment provides an alternative option for active rehabilitation since it is shown to be effective in changing mobility, quality of life, dynamic balance and pain in some musculoskeletal conditions [29].

Underwater motion capture requires a few caveats compared to traditional stereophotogrammetric motion capture. This is due to the fact that in water it is not possible to use neither infrared cameras neither standard spherical markers. The latter can not be used because they can lead to problems of bulk and passive resistance of water since they have a non-negligible volume. Moreover, there is also an illumination issue in video recording, since in water there is presence of bubbles and turbulence that could affect the marker visibility. To that, in an aquatic environment is preferred the use of bi-adhesives or non-reflective markers

drawn on the subject's skin. Consequently, the impossibility of using of infrared cameras underwater and the consequent use of non-reflective markers leads to the use of conventional underwater cameras which must be synchronized with each other, and then also the resulting video recordings should be analyzed using a specific feature tracking software [30].

Moving in this direction, some underwater cameras were tested to verify that they provided results comparable to those obtainable on land. In [31] the authors tested GoPro Hero3+ for 3D reconstruction resulting in low variability and good accuracy in both the environments and better results as the image resolution increases.

Walking in water is supposed to be quite different to on land gait, due to buoyancy and water drag. Thus, considerations on spatio-temporal parameters during underwater walking have also been done [29, 32, 33]. The most evident results for self-selected walking speed were that subjects generally walk slower and take shorter steps in water, cadence resulted lower compared to on land GC. Furthermore, also the maximum walking speed resulted lower in water than on land. From a kinematic point of view, the range of movement of subjects walking at self-selected speed were similar in both environments. Then, force outcomes showed a consistent reduction in vertical ground reaction force in water at self-selected speed of walking in both weight acceptance and the propulsive phase of stance. Finally, average and peak of muscle activity at self-selected speed were shown to be similar in water and on land environment in the majority of studies and muscle groups, whereas they appear lower for walking at maximum speed [29]. In the work of Barela et al. [33], however, muscle activation patterns in water versus on land were shown to be different for most of the muscles examined. This was justified by the fact that the subjects in water walked at a self-selected speed, so it was likely that the speed of walk in water was much lower than on land, in addition, the reduction in weight in the water due to buoyancy may lead to a decrease in the intensity of the load and propulsive events requiring less muscle activation. Indeed, it is known that different speed of walking can influence spatiotemporal parameters and muscular activation

patterns [1, 33, 34, 35].

2.5 Gait analysis in Parkinson's disease

Healthy gait appears coordinated, efficient and effortless. A presence of either a motor or a neurological disease, or a trauma, can alter the precision, coordination, speed and versatility that characterize normal walking [1]. Thus, clinical gait analysis assumes great importance since there are many subjects affected by motor disorder which has its origin in neurodegenerative disease such as PD, multiple sclerosis, cerebellar ataxia, myopathies, brain tumours and some types of dementia. The comparison of spatio-temporal parameters between pathological and healthy subjects is a good tool for various application in clinical field, indeed, the first symptoms of neurological diseases generally comprise abnormality in walking, inability to coordinate balance, slower pace and frequent falls [36].
Many studies about gait of subjects with Parkinson's disease have been carried out [16, 37, 38, 39]. These works provided evidence for the existence of a central disorder in PD subjects in the correspondence between movement amplitude selection and execution, leading to a reduction in stride length, and significant variations in movement amplitudes [39]. In addition, compared with healthy subjects, reduction of stride velocity, increased gait cycle time and longer duration for stance and double support were observed in PD subjects [38]. Moreover, shuffling gait and freezing were observed, and are known to affect stride parameters. Freezing is a common problem for PD subjects, in particular at advanced stages. It consist in patient inability to perform walking or other motor tasks and, during gait, it occurs primarily when attempting to start walking, but it can also arise when turning or walking through a narrow passageway or doorway. Its possible causes can be identified in a combination of different factors such as an increasing inability to generate stride length superimposed on a dyscontrol of the cadence of walking [40]. Hence, increased double stance time could be a consequence of freezing, as PD patient may experience postural instability and thus keep both feet in contact with the ground, stopping or trying to drag them.

However, since walking abnormalities in PD are mostly due to akinesia, that is basal ganglia dopamine deficiency-related symptom, and to a lesser extent rigidity, some studies reported how drug treatments [39] or subthalamic nucleus deep brain stimulation [38] can improve some gait parameters of PD subjects.
The walking of subjects with PD, can also be used as a rehabilitation tool. Actually, rehabilitation approaches for PD are characterized by wide heterogeneity. This is because motor rehabilitation can be considered as a relearning process on how to move, indeed motor learning in PD subjects is feasible, but it is impaired in comparison to normal population [13]. Thus, cognitive status is a crucial factor in the outcome of rehabilitation.
An emerging rehabilitation approach for PD is underwater walking training [41]. As reported by *The American Parkinson Disease Association* [42] there are various advantages for PD subjects on performing water exercises. The first one reported is that buoyancy provides support to weak muscles for reassured balance and improves posture simply by standing in the pool, so the patient experiences a reduced fear of falling and movement is perceived as easier. Then, there is a muscular stiffness reduction and an improved posture and motor control. Furthermore, the freedom of movement promotes an increasing in range of motion. The latter is confirmed in work by Volpe et al. [16] where subjects performed a three-week underwater training session. The training consisted of walking at a self-selected speed back and forth within the pool for 40 minutes per day at the same time each morning. Movement analysis was performed before and after the training. From this, spatiotemporal parameters were extracted together with joint range of motion and compared. The results showed significant differences on spatiotemporal parameters and sagittal plane lower limb kinematics.

Chapter 3

Electromyography

Electromyography (EMG) is the recording of the electrical activity of muscles. This can be performed using different types of sensors: invasive or non-invasive electrodes. The former ones are usually composed by a needle or a fine-wire electrode that is inserted inside the muscle, while the latter ones are electrodes that are placed directly on the surface of the skin [43]. The detection of electrical activity by invasive electrodes is more accurate, however the use of surface EMG is often preferred as it is not painful to the subject and it is not necessary to anesthetize the subject before placing the electrode [44].
Therefore measuring the electrical activity of muscles during a task execution allows for the estimation of internal forces that cause the movement. EMG sensors are often integrated and used together in a more complex motion analysis system. Hence, the use of EMG as a clinical assessment tool is increasing its popularity.

3.1 Muscle physiology

Muscles can be classified according to their tissue type: cardiac, smooth, and striated (or skeletal). Unlike smooth muscle and cardiac muscle, skeletal muscle is under voluntary control [45].

Skeletal muscles are the most prevalent muscles in the body and are the responsible for the movement of the body's limbs. These muscles are attached to bones by tendons, and they are surrounded and supported by dense connective tissues, which are thin fibrous membranes called epimysium (or fascia) [46]. The muscle fiber is identified as the structural unit of skeletal muscle. It is a thin structure ranging from 10 to 100 μm in diameter and from a few millimeters up to 40 cm in length. A fascicle is defined as set of more muscle fibers arranged together. Fasciculi are the first subdivision of skeletal muscles, and they are surrounded by perimysium, a sheath formed by extensions of the epimysium into the muscle [46]. Each muscle fiber is formed by a bundle of thinner myofibrils [45]. The myofibrils are composed by a series of sarcomeres arranged end-to-end and composed by proteic filaments. Each sarcomere consists of filaments composed by two proteins: actin and myosin. Due to the precise arrangement of the myofibrils, characteristic landmarks can be identified. These are [46]:

- Z lines formed by the interconnections of the thin myofilament from adiacent sarcomeres;
- dark A bands where actin and myosin filaments are present;
- H bands, which are lighter parts of A bands where only myosin filaments are present
- I bands, adjacent to A bands, which instead contain only actin filaments.

The skeletal muscle organization is shown in Fig. 3.1.
In order to produce movement, muscles contract. During muscle contraction, the length of actin and myosin filaments does not change, but they slide over each other, resulting in a decrease in the width of H and I bands and the distance between Z lines, thus causing the shortening of the length of the muscle [45].
This mechanism of muscle contraction is due to the neat arrangement of actin and myosin forming cross-bridges between them (Fig. 3.2). The force generated by filaments sliding is transmitted both longitudinally and laterally within the fiber, reaching the Z line and continuing until myotendinous junction, tendons

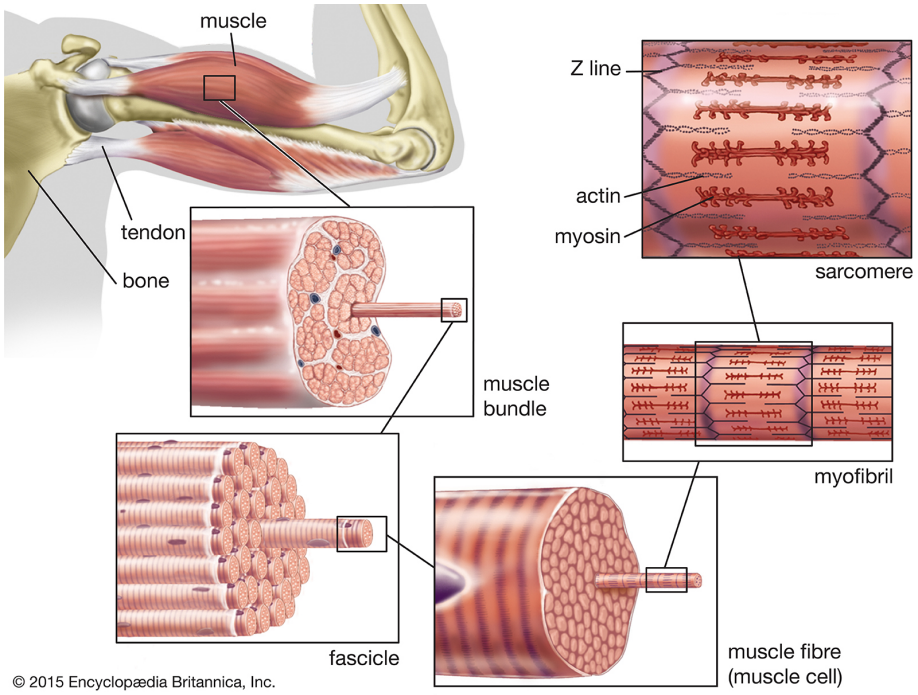

Figure 3.1: The structure of striated, or skeletal, muscle (Britannica, [45]).

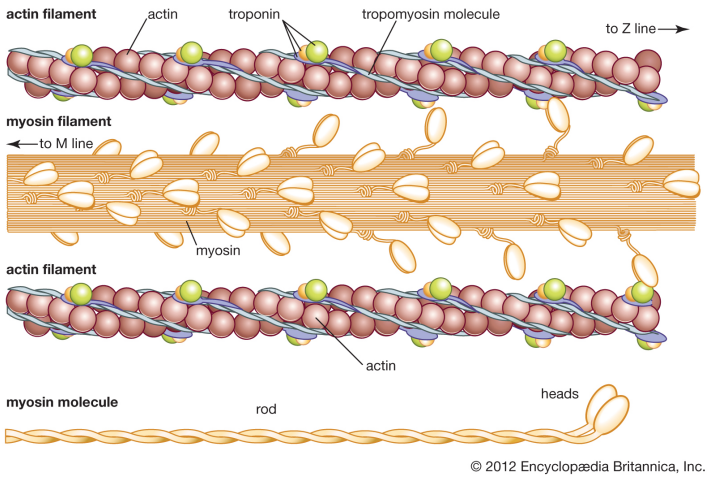

Figure 3.2: The structure of actin and myosin filaments (Britannica, [45]).

and joints [47]. The force generated by muscle contraction depends on the pennation angle, which is the angle at which muscle fibers insert into the tendon, on the muscle size and on the number of actin-myosin cross-bridges formed.
In order to briefly describe the causes that generates muscles contraction, the use of energy, in the form of ATP, is crucial in these phases. It allows to generate the sliding of myosin filaments heads of on those of actin and then to create new bonds between them in a different point from the previous one, thus promoting the approaching of the ends of the sarcomere. ATP binds to myosin head and is hydrolyzed, cleaving the cross-link with actin. The release of phosphate from ATP due to hydrolysis provides the necessary energy for myosin to move to a new, closer actin molecule. As a result of this power stroke, force is then generated. The amount of force that is generated by the muscle depends on multiple factors. These include dependence on the length of the muscle at the time of activation and on the velocity of the movement [47].

3.1.1 Origin of electromyographic signal

The electrical component has origin during contraction, however, also when muscle is at rest, it has been shown the presence of a resting potential. The muscle resting potential, is defined as resting membrane potential, and it is due to the different ion concentrations of extra and intra cellular fluids. Intra and extra cellular fluids are different for composition, they are present in and between muscle fibers respectively, and are divided by a semipermeable membrane, called sarcolemma. Sarcolemma surrounds muscle fibers and present channels for ion transport [46].
Intracellular fluid has high concentration of potassium (K^+) and an organic anion (A^+), while extracellular fluid has high concentration of sodium (Na^+) and chloride (Cl^-). Therefore, because of the higher concentration inside the sarcolemma, K^+ diffuses through the membrane to extracellular fluid, however, organic anions are too large to flow in the membrane channels. Similar problems have Na^+ ions that have difficulties in flowing through membrane due to their

size. Because of this, a positive charge is then produced outside the membrane, creating a voltage difference of $-80\ mV$ between inside and outside the muscle fiber and thus achieving equilibrium in the resting state. Variations from this equilibrium state occur when an internal or external stimulus occurs [46].

3.1.2 Motor unit action potential

All voluntary movements start from the brain. Muscle contraction is triggered by cortical signals that travel from the brain to the motor unit needed for the movement. Each motor unit, consists of a set of muscle fibers, and it is innervated by a motor neuron. Each motor neuron can innervate one or more motor units; for this reason some muscles appear to work together in a coordinating manner [48]. When a muscle fiber contraction is requested, the central nervous system initiates a depolarization in a motoneuron. This depolarization is transmitted along the axons of the neuron to the end plate of the muscle fiber, where the neuro-muscular junction is located. The latter is the synapse between motor neurons and skeletal muscle fibers. Here, acetylcholine is released in proximity to the active zone of the muscle where receptors for this chemical are present. This event causes a subsequent, rapid depolarization of the muscle fiber. Each depolarization and subsequent repolarization of the muscle fiber represents thus an action potential [46].

When a muscle fiber is depolarized, a potential difference is established between its active site and adjacent areas. Consequently, to restore balance, a ionic current is generated and propagated to the inactive areas. Therefore, the action potential propagates in both directions throughout the muscle fiber from the initial active region to the adjacent regions. This is called "muscle fiber action potential". Finally, this action potential, propagates also through the adjacent fibers to the whole muscle, allowing muscle contraction to occur [46].

EMG is able to detect action potentials only of an entire group of fibers, that compose a motor unit. Therefore the overall action potential of a motor unit, that is the summation of single fiber action potentials, is called the motor unit

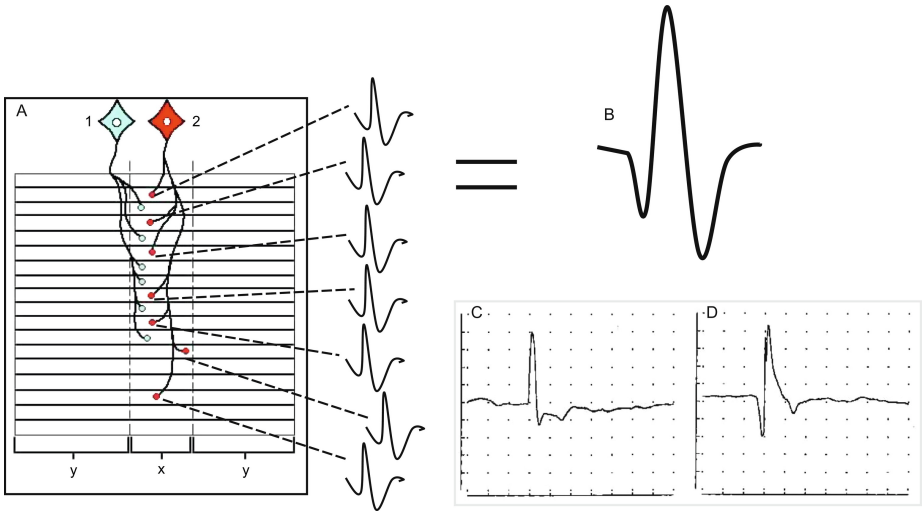

Figure 3.3: (A) Two different motorneurons that innervate various fibers of a single motor unit. Each fiber action potential contributes to MUAP generation. (B), (C) and (D) represent different MUAP shapes (M. Raghavan et al., [51]).

action potential (MUAP).

Surface EMG is then the recording of a train of one or more MUAPs in time domain. For example, if a generic function $f(t)$ for a single MUAP can be assumed, a MUAP train can be then described as follows [49]:

$$MUAPT_j(t) = \sum_i k_j \, f\big(\frac{t - \theta_{ij}}{\alpha_j}\big) \tag{3.1}$$

where i is the number of a single MUAP, j is a specific motor unit, k_j and α_j are an amplitude and a scaling factors, respectively, and θ_{ij} are the occurrence times of the MUAPs of the motor unit j.

Furthermore, each MUAP can have different shapes and duration. The shape can vary as a result of the position of the electrode on the skin and the contribution of the action potential of the individual fiber (Fig. 3.3). Instead, MUAP duration varies from approximately 5 to 15 ms and is defined as the time from the initial deviation from baseline to the final return of the MUAP to baseline [50].

3.2 Surface EMG

Internal forces created by muscles are responsible for externally measured forces. EMG allows to record the electrical activity of the muscle placing sensor on subjects' skin or directly within the muscle, using a needle. EMG electrode can be of different types and dimensions, indeed, according to the size, a sensor allows to detect the potential of a smaller or larger muscle area [23].

In surface EMG, sensors are directly applied on the region of skin in correspondence to the muscles under study. Surface EMG records the summation of fibers action potentials conducted from the muscle to the skin surface through ions movements. This recording allows for the detection of an attenuated version of the muscle action potentials since both skin and tissues act as a filter for the signal [46]. A typical EMG signals has amplitude between 1 μV and 1 mV and frequency content from 1 Hz to 500 Hz [23].

There are different configurations of surface EMG sensors: monopolar, bipolar (single differential) and double differential.

Monopolar configuration requires to apply a single electrode on the region of the skin closest to the muscle belly and a reference electrode to a region or prominence of bone. Bipolar configuration, instead, requires the use of two electrodes for measuring the EMG of the same muscle. A good choice of inter-electrodes distance (usually 1 or 2 cm) and electrodes position is determinant on the resulting quality of the acquisition [52]. Then, as for monopolar systems, a reference electrode is placed on a bony prominence. Finally, double differential configuration is similar to the single differential one but with one more electrode [23]. These last two types of configurations, since they involve the use of more electrodes, provide the advantage of removing common component and amplifing the differential, thus reducing noise more effectively than the monopolar configuration.

EMG acquisitions can provide information about the state of muscles during the execution of a movement; good interpretation of the signal can help identify which muscles are active and at which time interval. Indeed, muscles EMG of

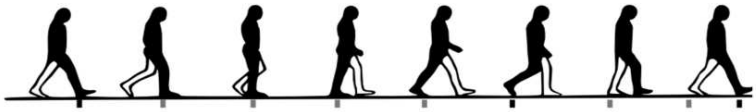

	Stance phase					Swing phase		
	Double support	Simple support			Double support			
		Initial	Middle	Terminal		Initial	Middle	Ter.
ILIACUS								
SARTORIUS								
GRACILIS								
RECTUS FEMORIS								
ADDUCTOR LONGUS								
VASTI								
GLUTEUS MAXIMUS								
GLUTEUS MEDIUS								
BICEPS FEMORIS								
TIBIALIS ANTERIOR								
EXTENSOR DIGITROUM LONGUS								
GASTROCNEMIUS								
SOLEUS								
FLEXOR HALLUCIS LONGUS								
TIBIALIS POSTERIOR								
PERONEUS LONGUS								

Figure 3.4: Representation of muscle activity during a gait cycle. The grey color indicates the periods where the muscles are active during the gait cycle (A. Bonnefoy-Mazure and S. Armand, [54]).

the lower limbs during walking is widely studied in clinical and research fields since it provides useful information even on the differences between healthy and pathological walking [1], e.g. Parkinson's disease [37, 53].

Therefore, one of the objectives of EMG is to identify the association between the different phases of gait and the muscle activation timing of different muscles involved in walking. This has been largely studied [2, 54] reporting the finding of characteristic pattern of muscle activation of healty subjects during a gait cycle, which is shown in Fig. 3.4.

3.2.1 Noise artifacts

Plenty of factors can influence the acquisition of EMG. Indeed, noise contaminations are very common in this signal, specially for dynamic acquisition, and

have different origins. First of all, the choice of single or double differential electrode configuration can lead to noise reduction due to common components and amplification of the differential one. In general, all configurations need ground electrode to be well adherent to the skin area relative to the bony prominence for external and internal noise reduction [23].

Another important noise component is due to movement artifacts. They often occurred when cables are handled or allowed to move during the activity execution [46]. Moreover, when the muscle contracts its length is reduced, and so the electrode placed on this muscle region is sensitive to skin movement, thus registering electrical activity due to this artifact. Frequency range of this type of contamination is usually 1-10 Hz and has a voltage comparable to that of EMG amplitude [44].

Another source of noise in EMG is the crosstalk contamination. This type of noise is due to the activation of muscles near to that of interest for which EMG sensors detect the electrical activity that is erroneously attributed. Therefore, crosstalk is an issue in particular when the aim is to determine muscular activation timing since this interpretation can be misleading. This artifact cannot be totally eliminated, but can be greatly reduced by placing the electrode in the midline of the muscle belly [55].

Moreover, as for all biological signals, electrocardiographic (ECG) artifacts are always present and are the most frequent endogenous common mode sources. They are not easy to remove since ECG frequency spectra are similar to those of EMG [44]. However, some techniques have been implemented to try to overcome this issue [56, 57].

Another noise component is the powerline interference, that is due to the stray capacitive coupling between a subject and the power line source [57] found at a frequency of 50 or 60 Hz (depending on the country). This component can be removed using a notch filter.

Finally, anatomical, biochemical, and physiological factors can also influence signal acquisitions. These are part of the internal noise and directly affect the quality of the EMG. They are mainly related to muscle fibers type, number per

unit, depth and position [44].

3.2.2 EMG data processing techniques

In order to extract useful features and information from EMG acquisition, it is necessary to remove or, at least, reduce the noise components. Many methods for noise removal and feature information extraction exist in the literature. [44, 57, 58].

Usually, the raw emg signal has a low voltage bias or offset due to its characteristic oscillation. This bias can be easily removed computing the signal mean value and subtracting it to the original signal [23]. There is not an unique filtering technique for EMG signals. Then, it is important to choose an appropriate filtering technique in order to remove noise components. This choice can be done having a look at the raw signal and its frequency component. In general, since frequency components of movement artifacts and instability of the electrode-skin interface are typically lower than 20 Hz a high-pass filter can be applied to the signal in the first stage of processing. The recommended cutoff frequency for high-pass filter is 10-20 Hz [59], however in movement, gait analysis, or clinical situations involving patients with movement disorder cutoff frequency should be augmented to 25-30 Hz [58, 59]. Then, high frequency noise artifacts can be reduced using a low-pass filter with cutoff frequency in the range of 350-400 Hz [57].

In all cases of filtering, it should be taken into account that the application of filters causes a reduction of the amplitude of the signal and consequently a reduction of some of its harmonics and possible loss of information, therefore for a good choice of cutoff frequencies a trade-off is needed [57, 58].

Demodulation techniques

The EMG signal has both positive and negative components because of its oscillatory nature and it is often rectified. The rectification consist in converting the whole EMG signal into positive. This is done by first squaring the signal and

then calculating its square root. Typically this technique is used for determining a threshold that establishes whether the muscle is active or not [23].
From the rectified signal, the linear envelope of the signal can be defined. As a matter of fact, this is extracted from the rectified signal which is filtered with a low-pass filter. This combination is called the linear envelope detector [46]. Of course, different filters provide different envelopes. However, the low-pass filter cutoff frequency typically ranges from 6 to 25 Hz [23]. The linear envelope is then represented by a curve that can be more or less smooth. When the muscle contracts the envelope increases, on the opposite when the muscle relaxes envelope returns to the baseline. Therefore, although an increasing on envelope curve is not always due to muscle but may be due to noise, envelope helps on muscle activation identification by setting a threshold whose value depends on the mean power of the background noise [60] and so give information about the onset duration. This technique was widely applied in locomotion studies where periodic activity is present and for which repetitions can be averaged over an interval of time [46]. However, the choice of a single threshold is generally unsatisfactory since it strongly depends on the choice of the threshold value [43], thus a double-threshold detection approach has been proposed in 1998 by Bonato et al. [61] resulting in better accuracy.
Another feature that can be extracted from EMG signal is the root-mean-square (RMS) voltage. This is calculated in three steps: first each signal samples is squared, then average value over a specified window length is computed and finally square root is applied to it [23]. Hence RMS is similar to envelope but is computed using a moving window, so it gives a linear envelope of voltage or a moving average over time. The RMS output values provide instantaneous measure of EMG signal power and depends on motor unit characteristics [46].

Fast Fourier transform

The envelope and the RMS of EMG signals are characteristic features of the signal in the time domain. By transforming the signal in the frequency domain,

additional information can be obtained. Indeed, EMG signal can be viewed as a random stochastic process since its oscillations are produced by the continuous contraction and relaxation of muscle fibers. These contractions can be considered in the range between 20 and 400 Hz without loss of information [59]. A representation of signal in frequency domain can allow to find out if there are dominant frequencies in that particular EMG trace. This can be done using Fast Fourier Transform (FFT), that is an implementation of a discrete Fourier transform.

In general, FFT is represented by its power spectrum as a function of frequency. For this reason, it has been used in particular for the study of muscle fatigue [62], since it is known that a variation in muscle force causes a modification of the frequency content of the signal [43], resulting in a frequency shift of the power spectrum and in its compression as the conduction velocity of the fibers decreases during a sustained muscle contraction [63].

The two most reliable measures of power spectrum are the mean and the median frequency [46]. The former is the average of all frequencies weighted by their power. The latter is the frequency at which the power density spectrum is divided into two regions with equal power, and appears to be less sensitive to noise than the mean frequency. These parameters are linearly related to the conduction velocity of muscle fibers and are a good tools to monitor frequency shift [62] or determine muscle force and fatigue [63]. The Fourier transform however assumes the stationarity of the signal, so it can be used only in cases where it meets this condition. In general being EMG a non stationary signal the use of different methods, like wavelet transform, can be more effective [64].

Wavelet transform

As an alternative to the Fourier transform, the wavelet transform has gained popularity. This type of transform is linear and transforms efficiently the signal with flexible resolution in both time and frequency domains [44]. Indeed, its application has been found to be very effective for surface EMG signals, which

have non-stationary and multicomponent nature [43].

Wavelet transform (WT), as for Fourier transform, can be either discrete or continue. Both ones are efficient in EMG signal processing and analysis. The discrete wavelet transform (DWT) requires little time for analysis, but introduces downsampling, while continous wavelet transform (CWT) is more consistent and is less time-consuming [44].

Assuming that the acquired EMG signal is represented by the function in time $s(t)$, then the CWT of the signal can be calculated through its general formula as follows:

$$CWT(a,\tau) = \frac{1}{\sqrt{a}} \int_{-\infty}^{\infty} s(t)\, w^*\big(\frac{t-\tau}{a}\big)\, dt \tag{3.2}$$

where τ is a translation time index, a is a scale parameter ($a > 0$) related to the frequency content and $w(t)$ is a function called mother wavelet [49].

The tuning of parameters a and τ allows to modify frequency and time resolution of the transform. Indeed, WTs are able to study high frequency components with sharper time resolution than low frequency components [65]. Thus, WT is a useful tool for EMG signal decomposition and has a huge advantage over the Fourier transform techniques which are time invariant.

The choice of the mother wavelet to use in CWT computation, however, is determinant for the result [66]. Mother wavelet can be considered as a band-pass function that has different characteristics since it can assume different time-frequency structures [44]. For this reason it also allows for multiresolution analysis, having focus on different signal frequency components. The parameter scale a is fundamental for extracting information at different time and scales [66].

There is no well-defined rule for mother wavelet function choice related to specific task execution, but it has been proved that some functions provide better results than others in EMG processing. Some of the popular standard families of wavelet basis functions are Haar (Fig. 3.5a), Daubechies, Coiflet, Symmlet, Morlet, and Mexican Hat. Each of these function is different in shape and characteristics. For example, Coiflet is ideal for data compression while Daubechies is more

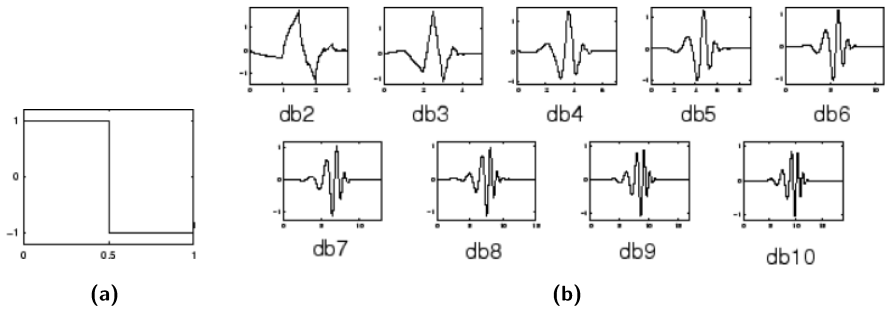

Figure 3.5: (a) Two different types of mother wavelet and (b) the same mother wavelet of different order (MathWorks, [68]).

suitable for feature extraction [66].

CWT can be seen as a measure of similarity of the shape of the considered signal in a specific time interval to the shape of the mother wavelet. Therefore, it has been theorized that if mother wavelet matches the MUAP shape, the resulting WT produces the best possible localization of its energy in the time scale plane [43]. Moreover, it has been demonstrated that the WT is useful for MUAP detection in the presence of additive white noise and that it is not affected by cross terms [67].

After an investigation done by Chowdury et al. [44], they have concluded that using Daubechies function as mother wavelet the analysis of surface EMG signals lead to successful results. However, Daubechies's wavelet can have different orders. Their differences can be seen in Fig. 3.5b by visual inspection. Daubechies of order 1 is coincident with the first and simplest wavelet, the Haar wavelet (Fig. 3.5a), that resembles a step function. On a related note, in case of EMG signals with both high and low frequency noise, the Daubechies wavelet of order 4 seems to be the best compromise.

3.3 Underwater EMG

Hydrotherapy refers to the execution of exercises in water as a therapeutic intervention. One of the exercise consists of underwater walking. This has

been proposed as an innovative rehabilitation strategy for the treatment of axial disorder in PD subjects, particularly for balance and gait impairments [69]. However, in literature, there is not yet much experimental evidence to confirm this.

A possible way to confirm the benefits of underwater walking is EMG underwater recording. This may help to have a broader understanding of gait dynamics during underwater walking, as it is quite different from walking on land. The differences are mostly due to the buoyancy and water drag. So, EMG of walking in shallow or deep water has been evaluated both in healthy [32, 33, 70] and pathological subject [53, 69].

Underwater surface EMG is usually acquired using specific EMG sensors for underwater acquisitions to be applied directly on the skin of the subject or using special techniques to make them water resistant or using fine wired electrodes. For example, some EMG sensors have a completely waterproof coating or taping that guarantees an acquisition similar to that obtainable out of the water [71]. However, in addition to the classic observations made for surface EMG, EMG signals acquired underwater can be affected by other sources of noise. Therefore, in order to obtain a correct understanding of this type of signal, possible confounding factors due to underwater recording should be taken into account.

Rainoldi et al. [71] stated that the lack of a standard protocol for underwater recording have led to different results in underwater versus on land EMG acquisition. Indeed, some authors found a difference in EMG amplitude when performing the same task on land and in water, resulting in lower amplitude in water [72, 73]. On the other hand, other authors found a greater amplitude in the water compared to the signal acquired in dry environment [74]. However, this may be due to multiple factors. For example, some studies acquired the EMG signal of an isometric contraction for which only one limb was immersed in water, while others compared the acquisitions of the entire walk for which the body was completely immersed and consequently was subjected to a greater drag force [75]. In addition, for underwater gait analysis, walking speed, walking direction and existence of water current seems to influence the results [72].

As reported from Veneziano et al. [74], there are three main factors to consider in the aquatic environment: the buoyancy force, water temperature and the choice of waterproofing technique. Buoyancy causes a force pointing upwards that reduces the actual force exerted in water with respect to air. This could explain the finding of lower amplitude in wet environment. Water temperature, on the other hand, may affect the temperature of muscles, which normally have a higher temperature than the skin. This occurs since the transfer of heat from the surrounding environment to the body is more intense, and tissues closer to the skin tend to become colder than in a dry environments. Consequently, a decrease in muscle temperature can cause a decrease in muscle fiber conduction velocity. Finally, the use of waterproof techniques is discussed. Indeed, to be able to compare signals acquired on land and in water, the authors suggest using the same waterproofing technique for both data acquisition setups. In this way, artifact due to coating or taping can be reduced. However, the use of same taping both on land and in water have not often been used in literature.

Chapter 4

Materials and methods

The main goal of the research was to study muscle activations of patients with PD before and after undergoing an underwater (UW) rehabilitation program. The aim of this thesis instead was to study UW muscle activations of patients comparing different methods for signal processing and muscle activity detection in order to compare which methods work best for the signal acquired in water. Indeed, EMG signals were acquired directly in water while subjects were walking. Consequently, different signal processing methods were used in combination with two muscle activity identification algorithms. These methods were then also used for signals acquired on land (OL) from healthy subjects used as controls (CS).

In this chapter subjects demographic data, signals acquired, the protocol used, the conditions where data were collected and the methods applied to identify muscles activations are illustrated.

4.1 Participants

In this work surface EMG signals acquired from 4 PD subjects and 5 healthy subjects during walking were analyzed.

Variable (*Unit of measurement*)	**Mean value** ($\pm$ *SD*)
Age (*years*)	$63,00\ (\pm 1,58)$
Weight (kg)	$67,60\ (\pm 10,76)$
BMI (kg/m^2)	$25,01\ (\pm 0,78)$
Height (m)	$1,64\ (\pm 0,12)$

Table 4.1: Healthy subjects data

4.1.1 Healthy subjects

Motion analysis was performed for 5 CS subjects and electrical signals of lower body muscles were acquired during on land (OL) walking by surface EMG. The average registry data of the subjects is reported in Table 4.1.

Data acquisition on CS involved the application of EMG sensors placed on lower limbs following a mixed acquisition protocol. sensors were placed in both right and left limbs in correspondence to the muscles belly. Table 4.3 shows the protocol used for 4 CS, whereas table 4.4 shows the protocol used for one CS that was the same used for PD subjects. *BTS Free EMG 1000* (BTS Bioengineering S.P.A., Italy) sensors were used with a sampling frequency of 1000 Hz.

Subjects were asked to walk at a self-selected speed in the laboratory room. Subsequently, through the use of specific motion analysis equipment and software, two consecutive initial contacts of the GC were identified for both the right and left sides of all subjects. Accordingly, all EMG acquisitions were analyzed and processed and finally muscle activation intervals during GC were identified.

4.1.2 PD subjects

In this work 4 PD subjects have been involved; their demographic data and their clinical characteristics are reported in table 4.2.

PD subjects acquisitions used were those taken before to start the UW rehabilitation program of three weeks. In this program subjects were asked to walk at self-selected speed, back and forth in a swimming pool with a level of immersion

Variable (*Unit of measurement*)	**Mean value** ($\pm$ *SD*)
Age (*years*)	$72,50\ (\pm 11,90)$
Weight (kg)	$72,50\ (\pm 16,58)$
BMI (kg/m^2)	$25,72\ (\pm 4,18)$
Height (m)	$1,67\ (\pm 0,13)$
UPDRS TOT	$58,25\ (\pm 15,86)$
UPDRS III	$33,75\ (\pm 14,77)$
Hhoehn & Yahr	$3\ (\pm 0,82)$

Table 4.2: PD subjects data

between the mammillary line and the shoulders. The program was performed for 40 minutes on a daily basis at the same time of day for a total of four weeks. All participants underwent UW motion analysis before the start of hydrotherapy program. All subjects underwent also OL motion analysis before to start the program. However, in this work it was considered only the OL acquisition of one PD subject, given that the exact same protocol was used for both OL and UW acquisitions for this subject only. The protocol followed for EMG sensors application for PD subjects is shown in table 4.4. It consisted of placing 8 *Mini Wave Waterproof* (Cometa srl, Italy) EMG sensors on the skin area corresponding to the belly of specific muscles of the lower body of the PD patients (Fig. 4.1). These sensors sampled at a frequency of 2000 Hz. Thereafter, as for healthy subjects, all EMG data were analyzed and processed and finally muscle activation intervals during 3 GCs were identified.

4.2 Methods

Currently, there is no general agreement in the literature regarding the methods for UW signals processing. Therefore, in order to assess the muscle electrical activity of PD subjects walking in water, signal processing was performed following some methods present in literature regarding the OL EMG analysis

(a) (b)

Figure 4.1: OL experimental setup of PD subject.

during motion analysis. In particular, the two main methods used in this work were:

- the double threshold statistical method of Bonato et al. [61], developed specifically for gait analysis and which has been shown to be significantly better than single-threshold methods;
- the technique implemented by Merlo et al. [49] based on the identification of the action potentials of individual motor units by using the continuous wavelet transform.

Finally, the results of these methods were compared in term of number of activations and percentage of activations for each muscle-specific EMG during GCs. Moreover, two different filtering techniques were employed the first using Butterworth filter of fifth order and the second using a bandpass filter with cutoff frequency of 30-300 Hz and 3dB bandwidth.

Muscle's name	Acronym
Right Peroneus longus	RPL
Right Tibialis anterior	RTA
Right Gastrocnemius lateralis	RGL
Right Extensor digitorum	RED
Right Gluteus medius	RGM
Right Rectus femoris	RRF
Right Biceps femoris caput longus	RBF
Left Peroneus longus	LPL
Left Tibialis anterior	LTA
Left Gastrocnemius lateralis	LGL
Left Extensor digitorum	LED
Left Gluteus medius	LGM
Left Rectus femoris	LRF
Left Biceps femoris caput longus	LBG

Table 4.3: Protocol 1 for EMG acquisition

Muscle's name	Acronym
Right Tibialis anterior	RTA
Right Rectus femoris	RRF
Right Biceps femoris	RBF
Right Gastrocnemius lateralis	RGL
Left Tibialis anterior	LTA
Left Rectus femoris	LRF
Left Biceps femoris	LBF
Left Gastrocnemius lateralis	LGL

Table 4.4: Protocol 2 for EMG acquisition

4.2.1 Experimental Setup

UW gait analysis for PD patients was performed in a swimming pool. Inside the pool, four GoPro Hero 8 were placed just below the water level at a known and pre-determined distance (two on one side and two on the other side of the pool), fixed on dedicated tripods. The cameras were oriented towards the center of the pool and their video acquisitions were synchronized later between the different cameras using a TrackOnField software [76]. The GoPro cameras acquired underwater videos at 30 fps. Camera calibration was performed using a checkerboard of known size placed at the bottom of the pool immediately before the start of each experiment.

Adhesive markers made with double colored tape were placed on the skin of patients following the IOR gait protocol [77], and 8 EMG sensors (4 bilaterals) were placed following protocol shown in table 4.4. EMG sensors did not require the use of cables since they were connected wireless to the amplifier. EMG recordings were made online and were stored in an internal memory. Sensors were synchronized and controlled by a remote controller that allowed acquisition to be started simultaneously for all sensors.

All sensors had a waterproof body so no additional protection was required, whereas the electrodes required the application of a proper insulation sheath for the waterproofing during UW acquisitions. However, one PD patient (PD1 of table 4.5) was analyzed without the insulation sheath during both the UW and OL acquisitions.

During the UW experiment, all PD patients were asked to walk back and forth the pool. In addition, during the same acquisition, the patients were asked to perform the Romberg test with both eyes open and eyes closed while remaining stationary in the center of the pool (Fig. 4.2). The same test was also performed during the OL acquisition of the PD patient. In contrast, the OL acquisitions of healthy subjects did not involve the execution of the Romberg test. A general summary of the modality of acquisition and sensors used for both CS and PD subjects is shown in table 4.5.

Figure 4.2: A PD subject during UW Romberg test execution

In order to identify the instants of GC in EMG acquisitions, synchronization between EMG and video acquisitions was needed. In order to do this, a video recording taken outside the pool was used, capturing the instant of the start of EMG signal acquisition (whereby the light from the sensors changed from green to red). While both the outside and underwater cameras were recording, the light inside the pool was turned on and immediately turned off. This allows to identify a common instant for the two cameras (external and underwater) and to scale the time axis in order to know for which instant, according to the UW cameras, the EMG acquisition started. An example of an entire acquisition of a PD subject can be see in figure 4.3, where all the 8 EMG channels are shown, synchronized with the time of the main UW camera.

4.2.2 Data Processing

The entire signal processing steps were performed using Matlab 2020a. The first step regarded the synchronization of the time axis of UW EMG acquisitions with the instants of the UW camera video. Then, for all subjects, the temporal

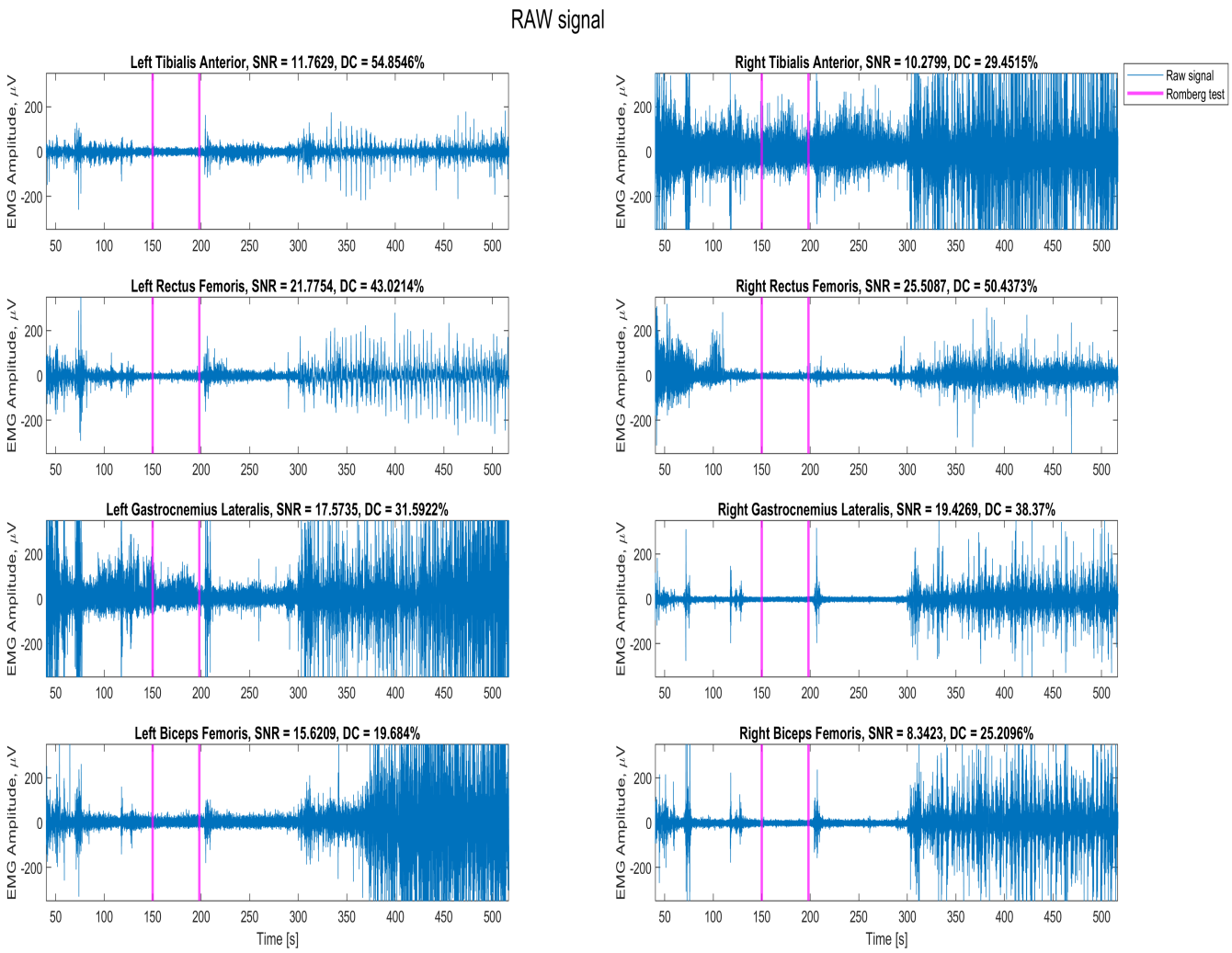

Figure 4.3: Raw EMG channels of a PD subject during underwater walking and Romberg test execution. The two vertical lines indicate an interval selected for the application of one of the algorithm used for muscle activity identification in which the subject was performing Romberg test.

Subject ID	Modality	EMG sensors name	f_c [Hz]	Channels	Protocol
CS1	OL	BTS Free EMG BTS Bioengineering S.P.A., Italy	1000	14	1
CS2	OL	BTS Free EMG, BTS Bioengineering S.P.A., Italy	1000	14	1
CS3	OL	BTS Free EMG, BTS Bioengineering S.P.A., Italy	1000	14	1
CS4	OL	BTS Free EMG, BTS Bioengineering S.P.A., Italy	1000	14	1
CS5	OL	BTS Free EMG, BTS Bioengineering S.P.A., Italy	1000	8	2
PD1	OL	Mini wave Waterproof, Cometa srl, Italy	2000	8	2
PD1	UW	Mini wave Waterproof, Cometa srl, Italy	2000	8	2
PD2	UW	Mini wave Waterproof, Cometa srl, Italy	2000	8	2
PD3	UW	Mini wave Waterproof, Cometa srl, Italy	2000	8	2
PD4	UW	Mini wave Waterproof, Cometa srl, Italy	2000	8	2

Table 4.5: General summary of EMG acquisition modality for healthy subjects (CS) and Parkinson subjects (PD).

instants of 3 right steps and 3 left steps performed during the UW gait analysis for the same gait direction were identified from the video. The initial instant of the step cycle was matched to the moment of initial foot contact on the pool bottom and the final instant to the moment of the next initial contact of the same foot.

The same preprocessing pipeline was applied to each EMG signal of both UW and OL signals of CS and PD subjects. For each EMG acquisition, the mean value of the entire acquisition was calculated and subtracted from it. Then, a notch filter was applied to remove the 50 Hz power frequency and a first-order filter was applied to remove heart beat artifacts. From the filtered signal obtained, two different muscle activity identification methods were implemented and applied for all subject acquisitions.

Double threshold detection method

The first method used for the identification of muscles' activations was the double threshold (DT) detector of Bonato et al. [61]. This method is a statistical method that focuses on adjusting three main parameters: the value of the first threshold (ζ), the value of the second threshold (r_o) and the length of the observation window (m). These parameters contribute to determine the detector

performance since their choice is strictly correlated to the false alarm probability (P_{fa}), which is the probability of misclassifying noise samples as signal, the detection probability (P_d), which is the probability of correctly classify signal samples albeit corrupted by noise and the temporal resolution, which depends on the choice of the observation window length. A longer observation window length generally increases the probability of a correct detection, but the more it increases the lower the temporal resolution of the detector is. The second threshold defines the number r_o of m successive samples that are above the first threshold ζ needed to acknowledge the presence of signal. The first threshold can then been chosen to maximize the probability of detection and minimize the probability of false alarm and it depends on signal-to-noise ratio (SNR) and noise power.

However, since this method required knowledge of the SNR of the signal, an estimate of this parameter was made for all signals using the algorithm described by Agostini and Knaflitz [78]. Therefore, for each EMG channel, the steps followed for muscle activity identification with this method were:

1. Noise power estimation (P_{noise}) and signal power estimation (P_{signal}) using an auxiliary time series obtained subdividing the signal samples in M epochs constituted by r consecutive samples and considering the normalized sum of square of each epoch. In this case, the desired time resolution was of $t_{resol} = 5$ ms so the number of consecutive samples was set as $r = f_c \cdot t_{resol}$, where f_c is the signal sampling frequency, and the number of epochs as $M = \frac{N}{r} - 1$ for all signal channels.

2. Computation of root-mean-square value of the background noise e_{noise} as:

$$e_{noise} = \sqrt{P_{noise}} \tag{4.1}$$

3. Estimate the SNR (in dB) as:

$$SNR = 10 \cdot \log_{10} \frac{P_{signal} - P_{noise}}{P_{noise}} \tag{4.2}$$

4. Generation of Gaussian white noise simulation using the estimated noise power information.

5. Filtering of simulated noise with a 5th-order Butterworth filter using as cutoff frequencies combinations of values between 15 and 20 Hz and between 465 and 479 Hz, respectively. Computation of the second threshold r_o using noise variance of white filtered simulated noise for all combinations. Selection of the second threshold value that maximize P_d.

6. Signal filtering with a 5th-order Butterworth filter using the same cut-off frequencies used for noise filtering corresponding to the value selected for the second threshold.

7. Computation of the first threshold ζ value using SNR estimate of point 3 and the desired false alarm probability.

8. Application of the selected threshold ζ to the filtered signal.

9. Determination of the presence or absence of activation using a cascade post processor. The detector starts a primary count when its logical state has been stable for at least $30\,ms$. If the output level remains stable for $30\,ms$ the transition is accepted. Otherwise, the instant of second transition is memorized and a secondary count is initiated.

The steps described above from 1 to 3 referred to the algorithm of Agostini [78] for SNR estimation, while steps from 4 to 9 referred to the double threshold method of Bonato et al. [61].

The post processor of point 9 is useful since the detector output of point 8 may show erroneous transitions (false positives) due to spurious high levels of output or false negatives for spurious low levels. Therefore, a post processor is cascaded to the output in order to eliminate these erroneous transitions that generally have a duration of few signal samples. Since it is generally accepted that a muscle activation shorter than 30 ms has no effect in controlling the joint motion during gait, the post processor rejects all transitions that last less than 30 ms [61]. An example of the output of this algorithm is shown in Fig. 4.4.

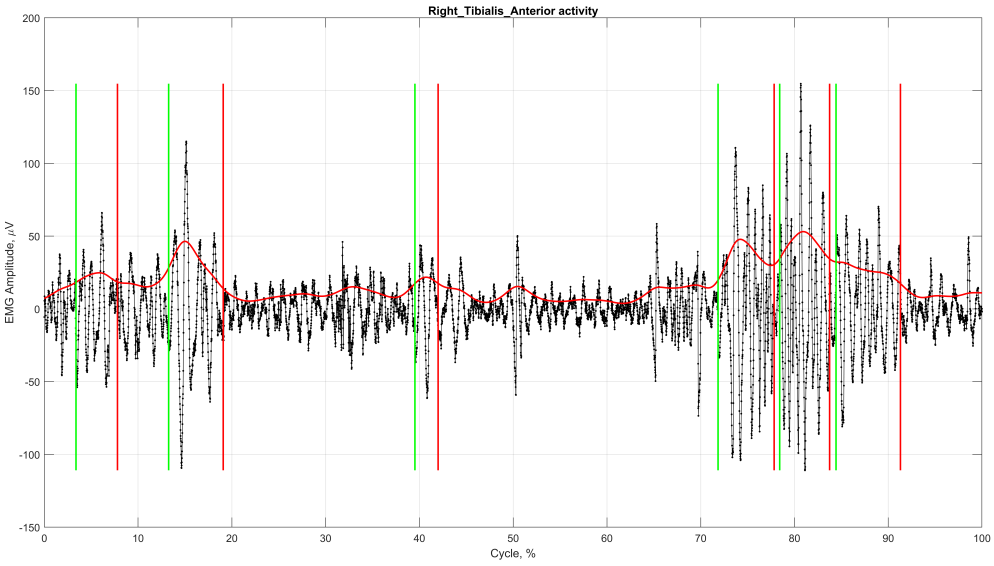

Figure 4.4: Detection of muscle activity using DT method. The green lines represent the instants of the activation onset, whereas the red ones indicate the instants where the muscle turns to the off state.

Continuous Wavelet Transform

Another method developed that has been shown to be effective for identifying muscle activity is that of Merlo et al. [49]. This algorithm, unlike the DT method which is a probabilistic method, is based on the construction of a physical model describing the waveforms of the motor units of the EMG signal. The goal of the method is to find where EMG signal matches the waveform of a single action potential thus identifying the presence or absence of muscle activity. This is done applying CWT to the EMG signal, selecting as mother wavelet the one that best approximates the shape of an action potential.

In this thesis, the fourth-order Daubechies ($db4$) wavelet was used as mother wavelet to compute the CWT of the signal (see Fig. 3.5b). This choice is justified by a more recent article [44] which, after investigating several research studies, has observed that better results are obtained with the Daubechies function.

For each EMG signal, the steps followed for muscle activity identification with

this method were:

1. Filtering of the signal with a bandpass filter (3-dB bandwidth: 30-300 Hz).

2. CWT computation for the entire signal using equation (3.2):

$$CWT(a,\tau) = \frac{1}{\sqrt{a}} \int_{-\infty}^{\infty} s(t)\, w^*\big(\frac{t-\tau}{a}\big)\, dt$$

   for 10 different scale parameters a and using as mother wavelet w^o the $db4$. The scale parameter a was varied so that the w^* function was scaled to remain within the physiological duration of a MUAP, i.e., between 5 and 40 ms, in this way CTW acted as a bank of filters matched to the MUAP shape. An example of CWT computation for the 10 different scale parameters is shown in Fig. 4.5.

3. Application of a classic event detection scheme, defined by the function $\eta(t)$:

$$\eta(t) = \max_{a}\{CWT(a,t)\} \tag{4.3}$$

4. Setting of a threshold using the maximum of the function in a defined range:

$$M = \max\{\eta(t)\}, \quad \text{for } t \in [t_{1_{noise}},\, t_{2_{noise}}] \tag{4.4}$$

$$th = \gamma\, M \tag{4.5}$$

   where $[t_{1_{noise}},\, t_{2_{noise}}]$ is an interval in which EMG activity is not present and γ is a scale parameter ($\gamma > 1$).

5. Signal values above the threshold have been classified as ON and those below as OFF.

6. Events identified and separeted by a temporal distance smaller than 125 ms were considered as belonging to the same contraction and merged. This value corresponds to a global muscular firing rate of eight pulses per second (pps), which is arbitrary assumed as the lowest effective muscle activity.

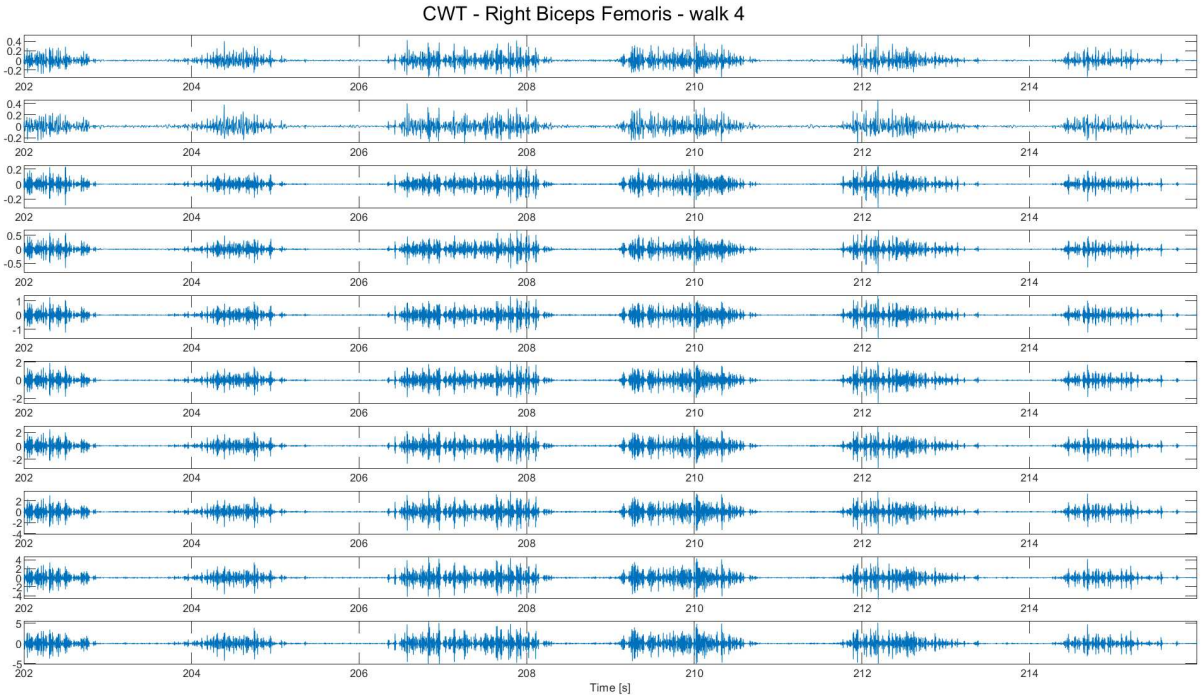

Figure 4.5: CWT of the right biceps femoris EMG signal during the performance of UW walking. CWT was calculated for 10 different scaling parameters such that the overall wavelet duration was maintained between 5 and 40 ms. Each raw corresponds to CWT computed with a different scale parameter a.

7. The detected events shorter than 5 ms were attributed to either isolated MUAPs or noise related spikes and disregarded.

Therefore, the intervals for which muscle activity was present or absent were obtained for all channels of the EMG signal.

However, all signals acquired from both healthy and PD subjects, had no acquisition interval where only noise was acquired that instead is required by equation (4.4). Therefore, two different intervals of signal for the calculation of the threshold at point 4 were used and results compared. These intervals were:

- the interval coincident with the execution of the Romberg test, in which muscle activity is assumed to be absent than during walking;

- a noise interval extracted through the application of an algorithm implemented by Ying and Wall [79] specific for rhythmic EMG signals behaviors.

The latter is based on a statistical method with an adaptive algorithm that discriminates noise regions from EMG and allows multichannel data to be processed. The method is a reinterpretation of Texton's single threshold algorithm [60] that roughly distinguished the amplitude of the noise region and that of EMG. In this case, the signal for which the subject was performing only walking activity was provided to the algorithm as the input signal, since this method works well for cyclic signals. Parameters required for the application of the algorithm were scaled according to authors indications in dependence of EMG sampling frequency. At the output, the algorithm provided the regions where only noise was present and the raw EMG signal in a form ready for further analysis. The longest of these noise regions was then used as the interval $[t_{1_{noise}}, t_{2_{noise}}]$ in (4.4). An example of the application of the method described above that uses this noise interval is shown in Fig. 4.6.

Another parameter to set was the scale parameter γ of equation (4.5). The choice of this parameter was made following the results reported by Merlo et al. [49], i.e. using a low gamma ($\gamma = 1.1$) in case of low SNR and higher γ in case of higher SNR ($\gamma = 1.6$). For CS EMG signals both $\gamma = 1.1$ and $\gamma = 1.6$ were used and compared, while for UW signals only $\gamma = 1.1$ was used.

Finally, it was intended to verify how much the type of filtering applied in step 1 affected the determination of muscle activation instants. Therefore, all subsequent steps were re-performed using instead of simple bandpass filtering, the filtering implemented for the DT method (from point 4 to point 6 of DT method).

4.2.3 Comparison

In order to compare the results obtained from the two different methods and type of filtering, two parameters were extracted from each step of each subject for which muscle activity was detected. These parameters were:

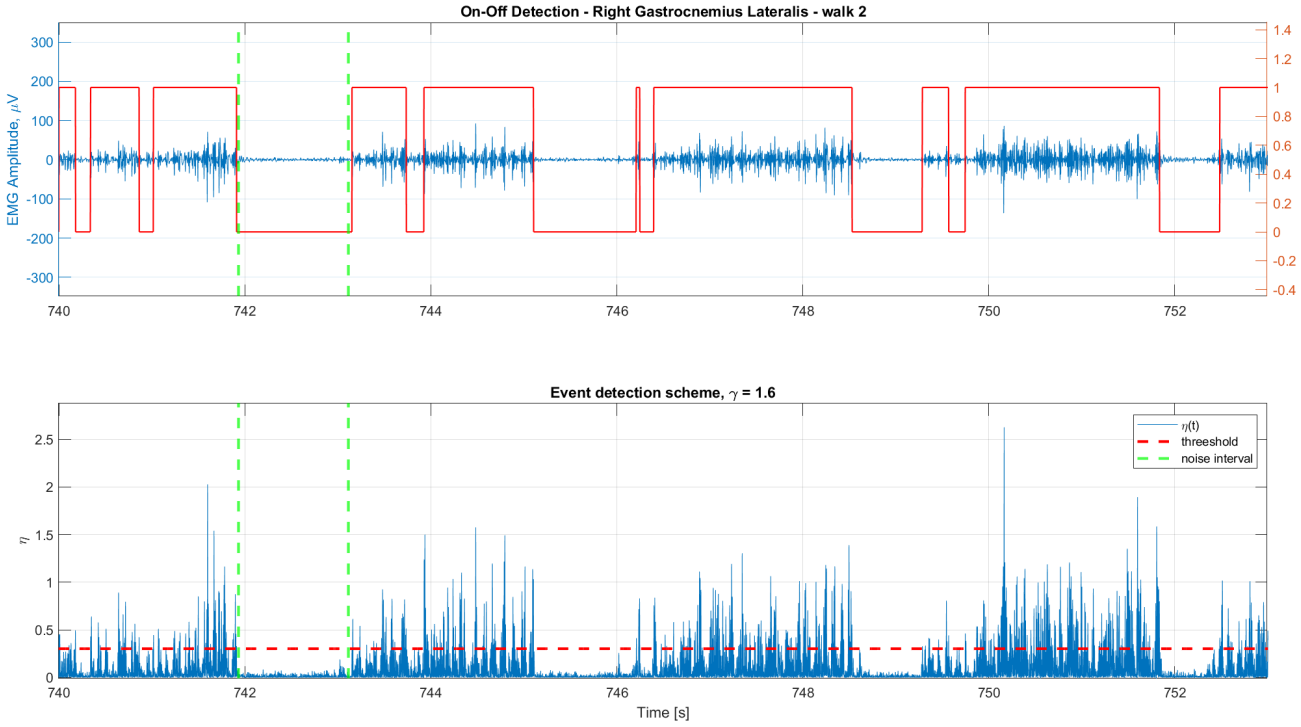

Figure 4.6: Detection of muscle activity using CWT method. The first figure shows the signal in blue and activations are represented by red line. The second figure shows the function $\eta(t)$ computed as specified by the algorithm. The dotted green lines define the noise interval selected as $[t_{1_{noise}}, t_{2_{noise}}]$ using noise extraction method and the dotted red line represents the threshold applied to $\eta(t)$ computed using $\gamma = 1.6$ multiplied by the maximum of $\eta(t)$ within noise interval.

- Number of activations, that is the number of times within the same GC that the muscle goes from inactive to active state;
- Percentage of activation that represents the overall normalized percentage over the duration of the GC for which the muscle is in an active state.

These two parameters were subsequently averaged for the three steps in order to compare the results of the different methods used (DT, CWT, and CWT using Butterworth filter). Then an overall average and standard deviation of these parameters were calculated for all muscles of the CS subjects and the PD subjects.

Chapter 5

Results and discussion

In this chapter the results obtained for both CS (section 5.1) and PD (section 5.2) subjects are reported in terms of number of activations and percentage of activations.

5.1 Results of healthy subjects

Instants of CS muscles activation were extracted using both DT (Fig. 5.1a) and CWT methods. However, since Romberg test was not acquired for CS subjects, only the noise interval identified by the noise extraction (NE) algorithm [79] described in the previous chapter (4.2.2) was used as noise interval required for the CWT method.

CWT was tested for two different values of γ namely $\gamma = 1.1$ (CWT 1.1, Fig. 5.1b) and $\gamma = 1.6$ (CWT 1.6, Fig. 5.2a). Finally, in order to compare the different filtering techniques, the same filtering technique used for DT method was used for CWT with $\gamma = 1.6$ (CWT 1.6 Butterworth, Fig. 5.2b).

All detected muscle activations were represented by reporting the EMG corresponding to one GC and the time scale normalized over the entire duration of the GC, in order to have a representation of the signal by GC percentage, as shown in Figure 5.1 and 5.2.

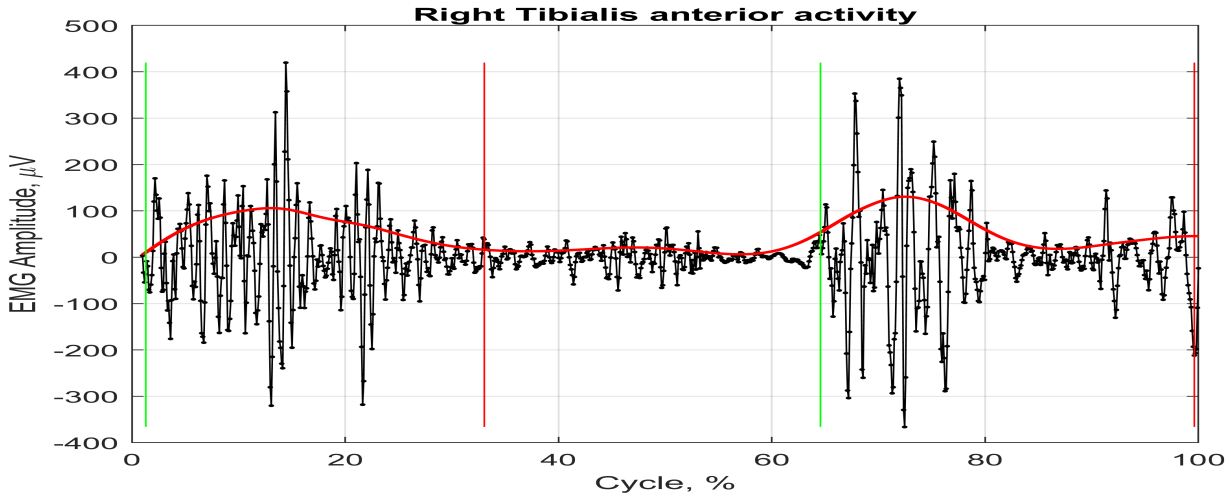

(a)

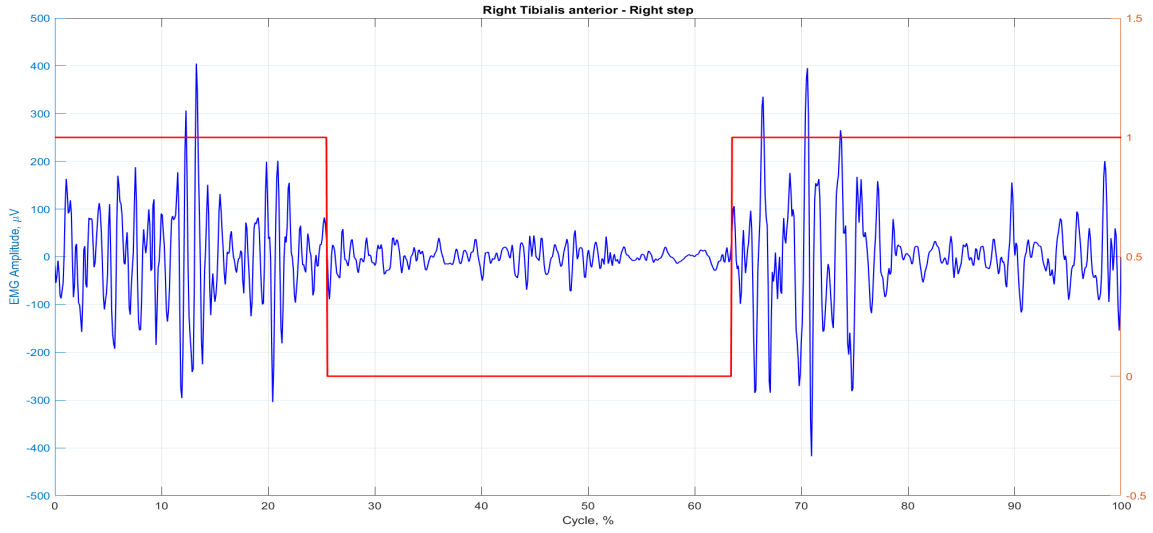

(b)

Figure 5.1: (a) RTA activity identified with DT method for subject CS2 during the GC, (b) RTA activity identified with CWT 1.1 (NE) method for subject CS2 during the GC.

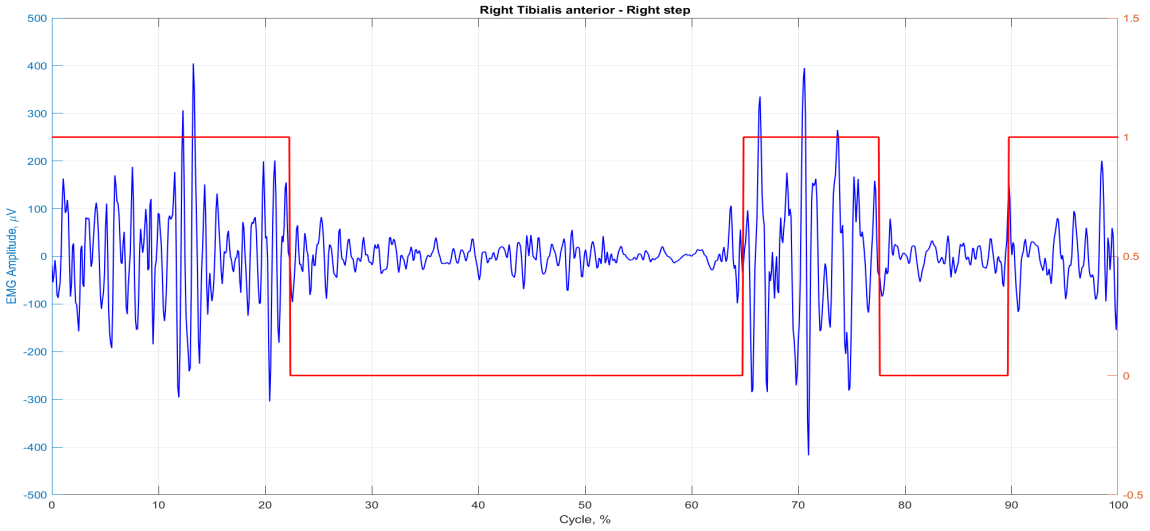

(a)

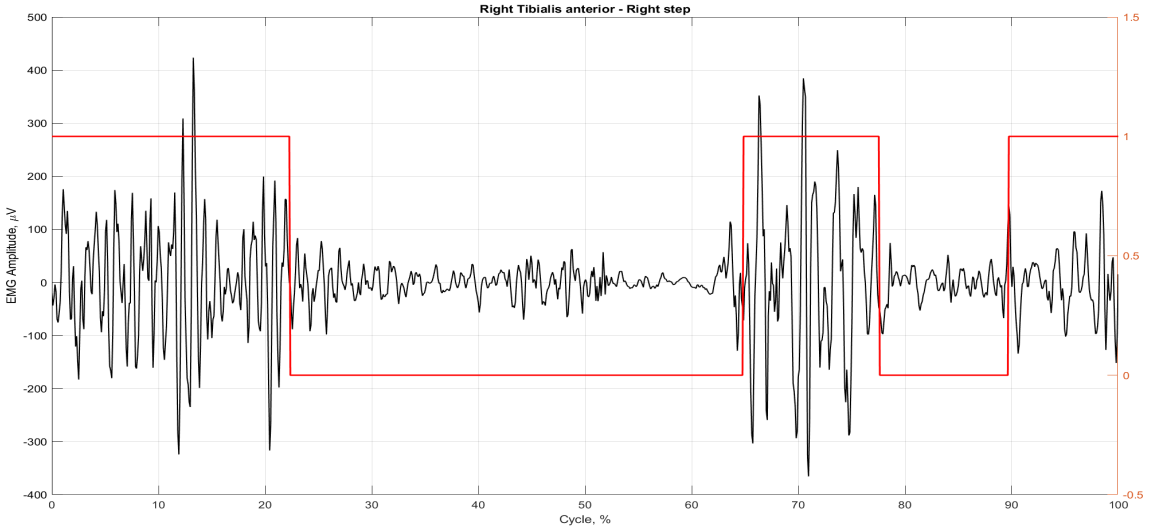

(b)

Figure 5.2: (a) RTA activity identified with CWT 1.6 (NE) method for subject CS2 during the GC, (b) RTA activity identified with CWT 1.6 Butterworth (NE) method for subject CS2 during the GC.

The overall results of the number of activations and percentage of activations of all muscles of protocol 1 are shown for subject CS5 for all 3 steps considered in Fig. 5.3. It can be seen that there are some differences between the DT and CWT methods in both the number of activations detected and the activation percentage. In some cases CWT gives as output a 100% activation percentage, this is related both to the choice of the scaling factor for the threshold determination and to the noise interval considered. In fact, decreasing or increasing the value of the scale factor γ, results into more or less percentage of activation respectively. In addition, the noise interval considered is selected specifically for each muscle, therefore, the calculated maximum of the detection function may vary depending on how the CWT signal was identified within the period as the noise-only interval by NE method. An example of this difference is shown for RTA of CS5's third step. Indeed, in this specific case the choice of $\gamma = 1.1$ and $\gamma = 1.6$ provided the results shown in Fig. 5.4.

Another noticeable point is that in some cases, CWT method failed to detect muscle activity, resulting in 0 number and percentage of activation as it can be seen for CWT 1.6 and CWT 1.6 Butterworth of step 2 and 3 of CS5 LRF in Fig. 5.3. This may be due to mainly two factors. The first one was that the chosen γ parameter turned out not to be appropriate for that specific signal and thus the threshold was set too high to allow detection of muscle activity. The second aspect was that, in some cases, within the noise-only interval there could be peaks of noise component not eliminated by the filtering technique that the CWT detected as a match for the MUAP. Therefore, the maximum of the detection function in that noise range resulted similar or sometimes even higher than the value of the function in the remaining range, resulting in a threshold selection too high even in the case of low γ. Another possibility, although not verifiable, could be a misidentification of the noise interval computed by the NE algorithm .

Moreover, it can be seen that the application of a different type of filtering to the signal, using the same method and scaling parameter, can also affect the identification of muscle activations. An example can be seen for the third GC of

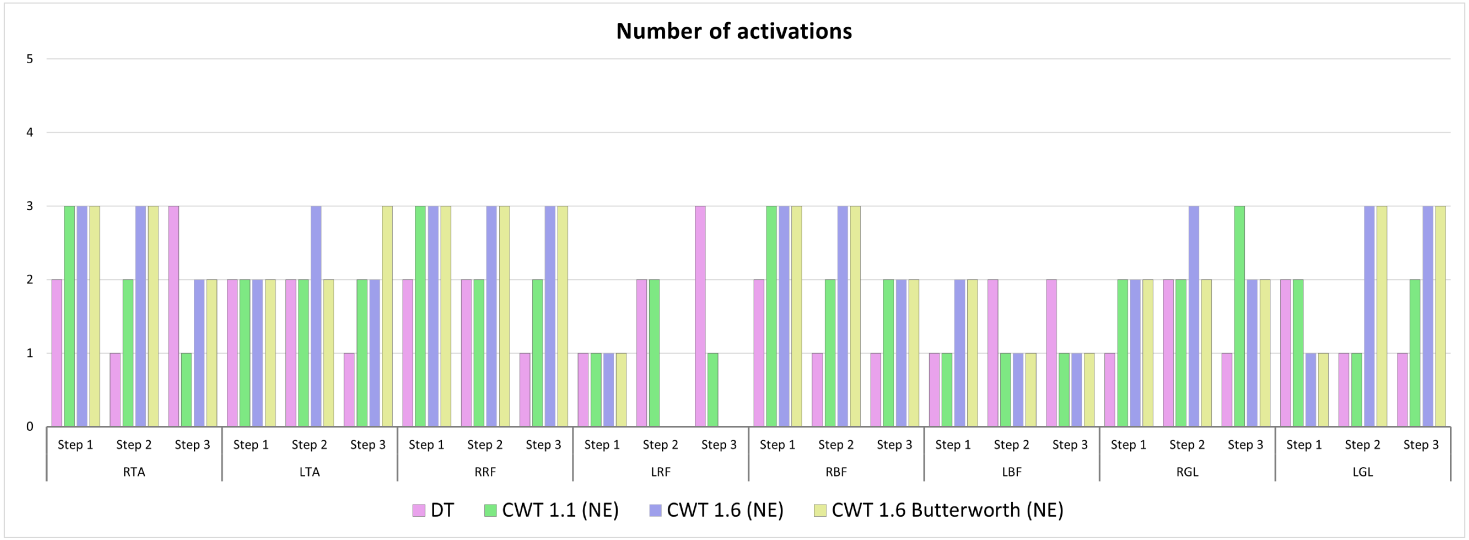

(a)

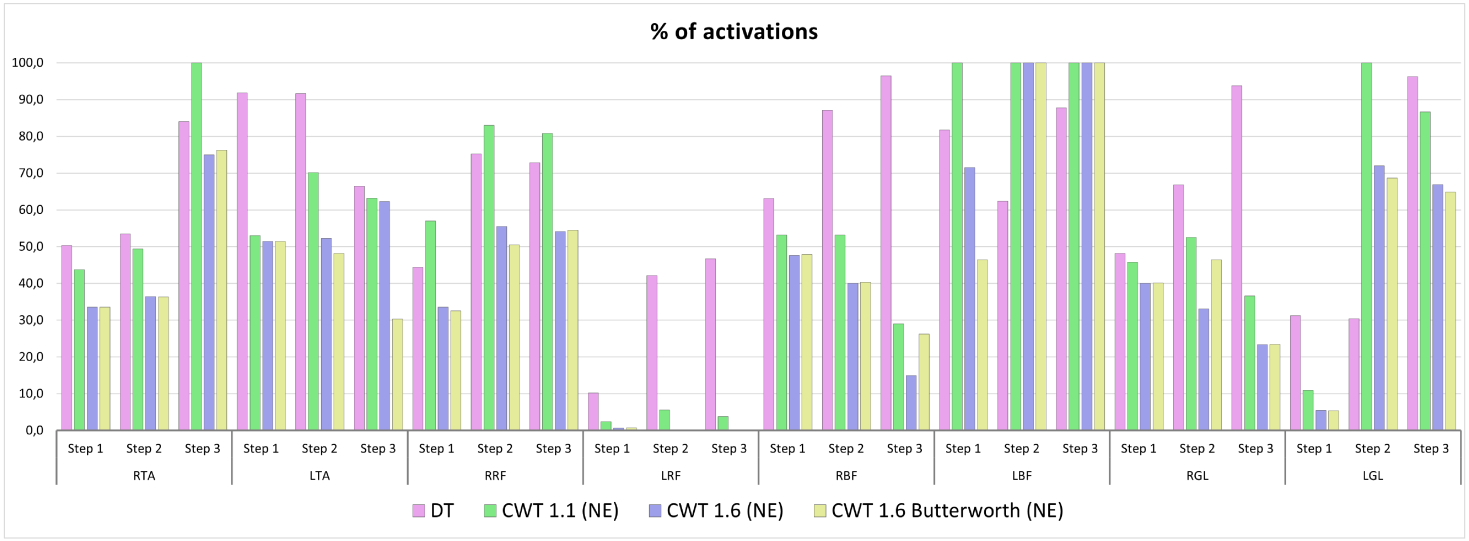

(b)

Figure 5.3: (a) Number of activations of 3 GCs of CS5 subject for all muscles. (b) Percentage of activation of 3 GCs of CS5 subject for all muscles.

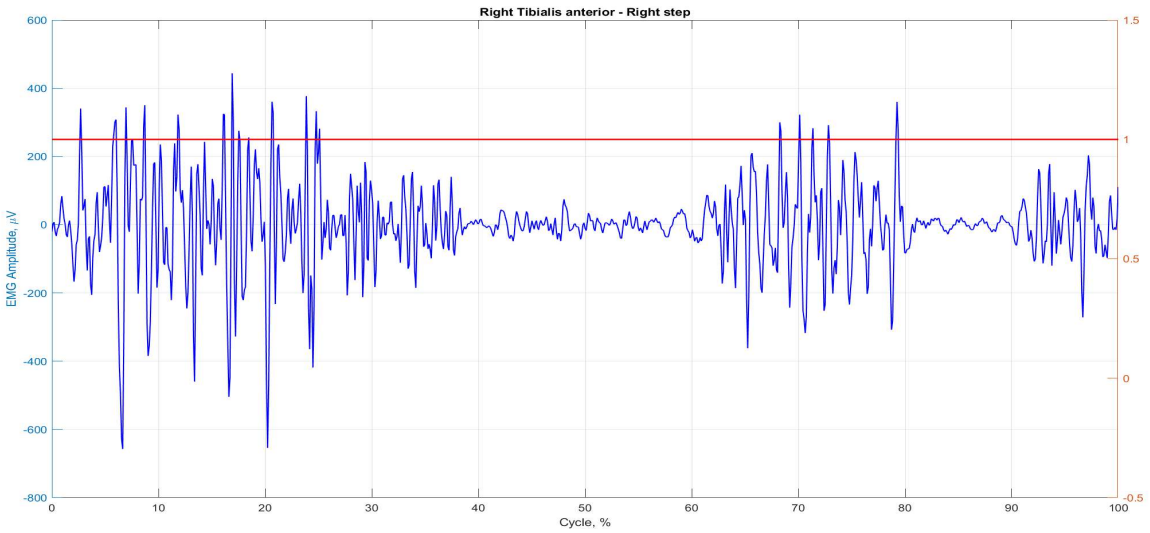

(a)

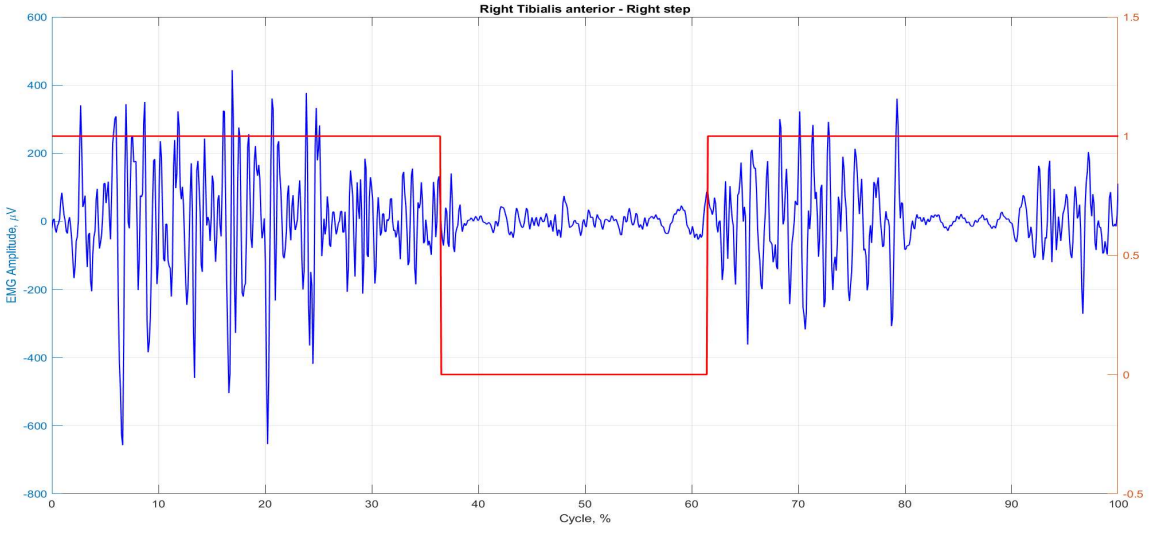

(b)

Figure 5.4: Influence of the scale factor γ in the identification of muscle activity with (a) CWT 1.1 method and (b) CWT 1.6 method

LTA of CS5 in Fig. 5.5. This difference occurs since the different type of filtering affects the signal amplitude and consequently the noise range over which the CWT is calculated and the resulting detection function may also appear different. Therefore, a different maximum value M of the noise range is obtained which leads to a different threshold selection and consequently the muscle activity identification could be different.

Then, the two different methods using the same preprocessing technique are compared in Fig. 5.6 for CS5 RTA of the third GC where the CWT method appears more restrictive.

Finally, when comparing DT with CWT it can be noted that in some cases the choice of $\gamma = 1.1$ is the one that provides results most similar to those of DT, while in others it is that of $\gamma = 1.6$. This might suggests basing the choice of γ according to the specific signal under investigation instead of fixing it globally a priori.

A general summary of all muscles and for all GCs of CS subjects is reported in Fig. 5.7. Here, data obtained are reported in boxplots in order to visually compare results obtained for the different methods employed. It can be observed that the CWT 1.6 and the CWT 1.6 Butterworth methods in many cases provided the same results for the number activations while there were some differences in the percentage. Moreover, for RBF these two methods provided the same values both for number and percentage of activation. This might suggest that the algorithm provides similar results for the two different types of filtering. However, it can be observed that the CWT 1.6 butterworth method did not find activations in some GCs for both RPL and LBF, while the CWT 1.6 method where bandpass filter was used did not find activations only for LBF.

Finally, it can be said that in most cases the DT method is the one that reports more variability in the number of activations but less variability in the percentage of activation. This can be seen in particular for RPL, LTA, LED and LBF. In general, the CWT method reports more variability in percentage of activations. This can be explained since for some GCs the percentage of activation detected was 100% while for others GCs of the same muscle no activations were found,

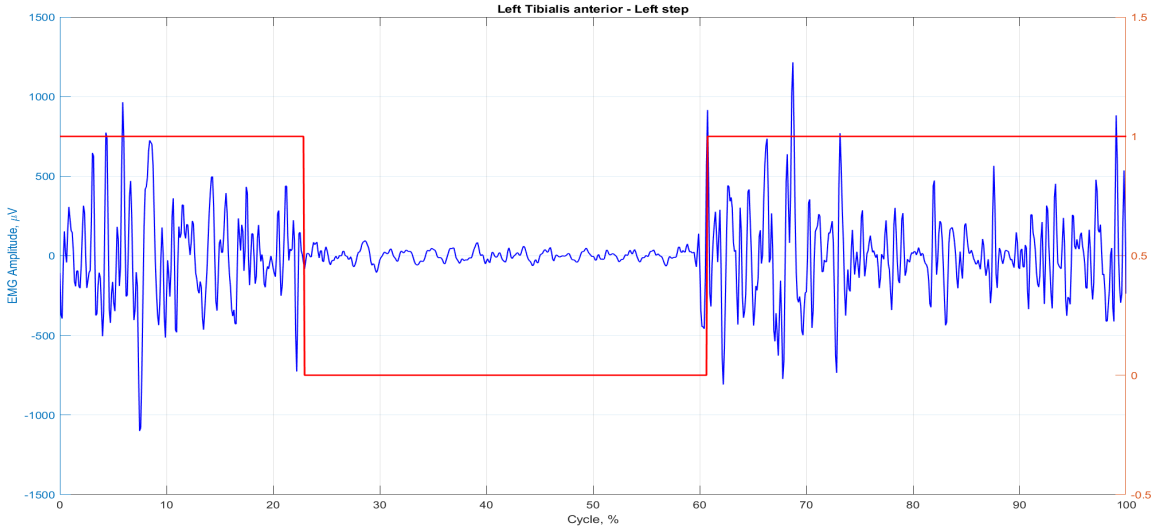

(a)

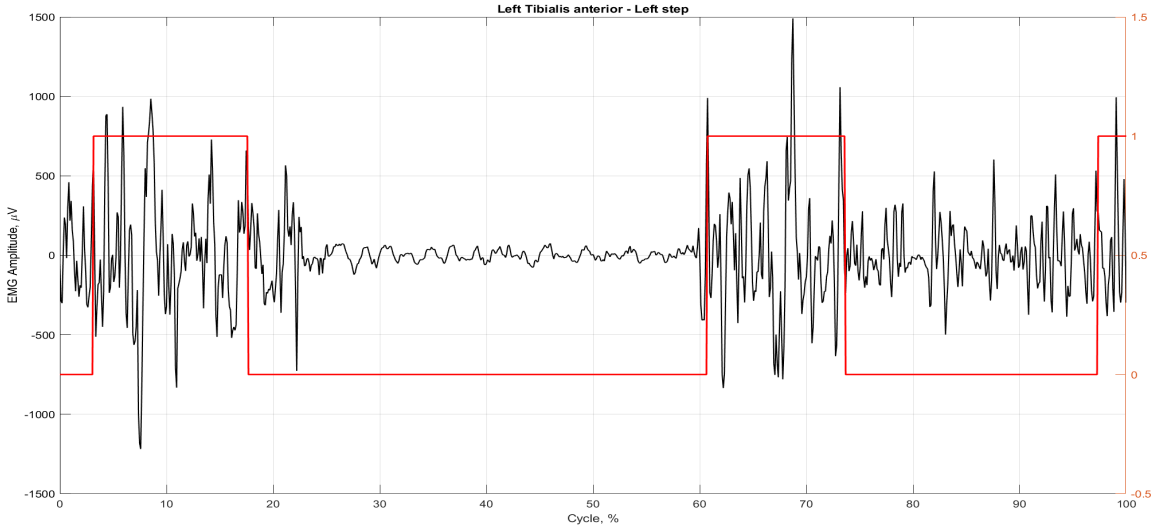

(b)

Figure 5.5: Influence of different preprocessing in the identification of muscle activity with (a) CWT 1.6 method and (b) CWT 1.6 Butterworth method

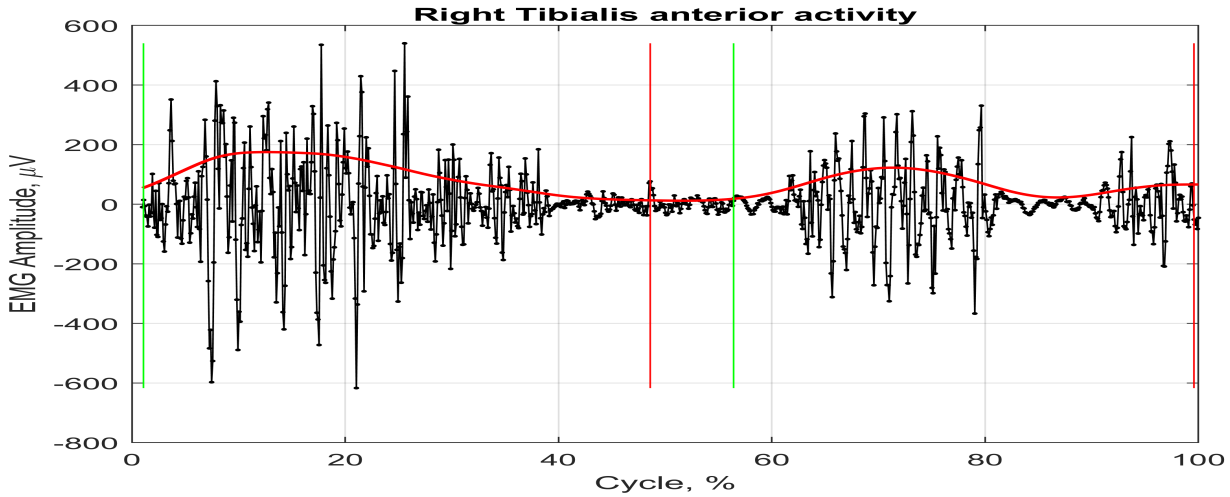

(a)

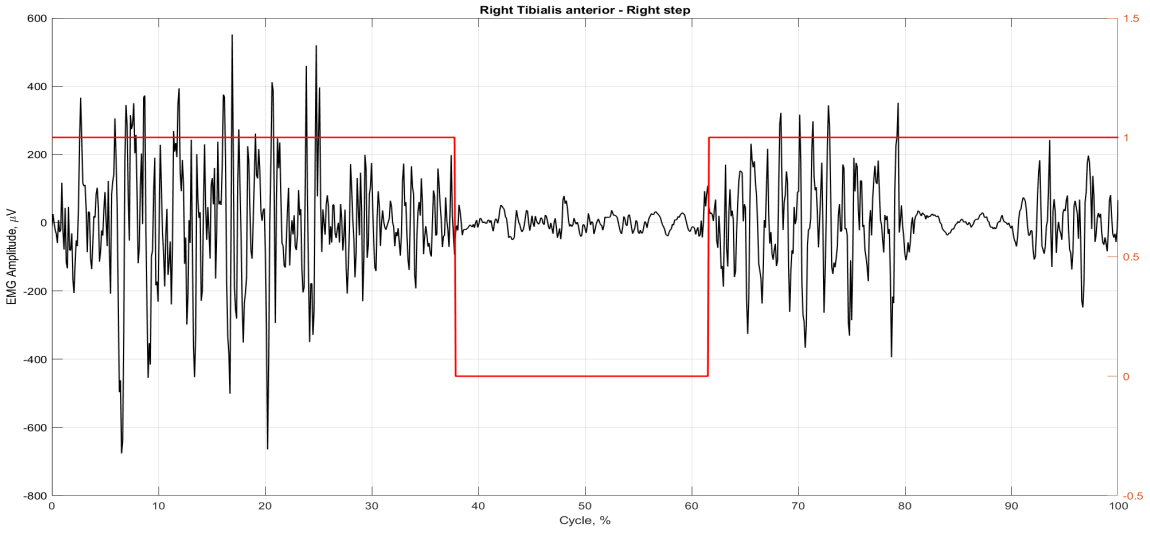

(b)

Figure 5.6: DT and CWT methods comparison with the application of the same preprocessing technique: (a) DT method and (b) CWT 1.6 Butterworth method

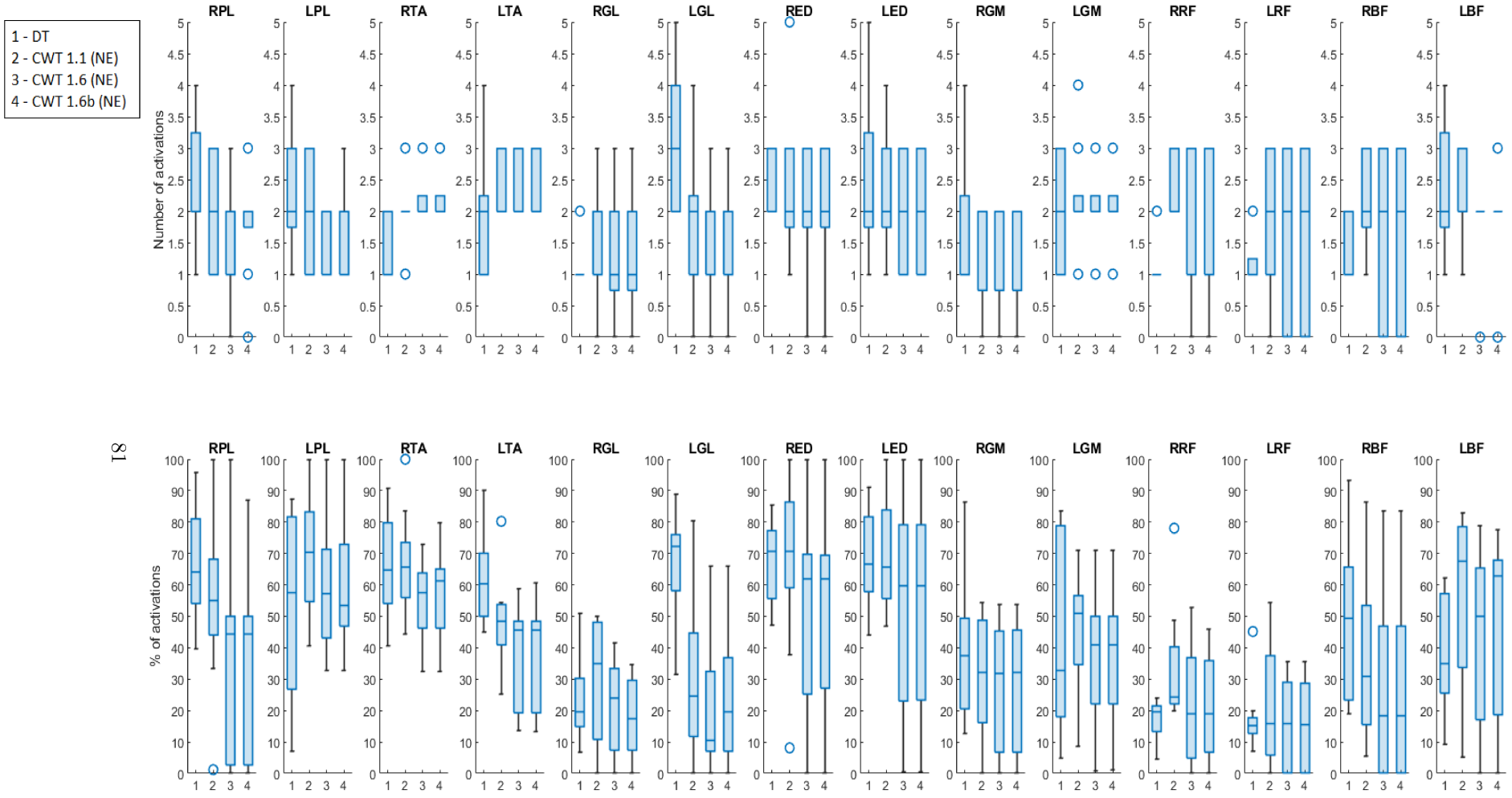

Figure 5.7: Boxplot of CS subjects results. Each boxplot reports the results obtained for all GCs of the CS subjects using a specific muscle activity identification method. Each graphic reports the results obtained for a specific muscle. X-axis values correspond to the application of a different method; in order: DT, CWT 1.1 (NE), CWT 1.6 (NE) and CWT 1.6 Butterworth (NE). In the first line the results are reported in term of number of activations. In the second line the results are reported in terms of percentage of activations. Outliers are represented by circles.

resulting in higher variability. This can be observed for example in RED and LED for both filtering methods and in RPL only in the case of CWT 1.6 with bandpass filtering.
The results of the average and standard deviation values of number of activations and percentage of activation are reported in tables 6.3 and 6.4 of the appendix 6.

5.2 Results of PD subjects

A similar comparison as that made for CS subjects was performed also for PD subjects. Instants of PD subjects muscle activation were extracted using both DT and CWT methods. This was done both for UW EMG acquisition of the 4 PD subjects and OL EMG acquisition of PD1 subject. In all these cases, Romberg test was performed. Therefore, the CWT method was applied using as noise interval either the interval extracted with NE method or the interval while subjects were performing Romberg test.
CWT method was applied to UW signals setting the scale factor $\gamma = 1.1$, whereas gamma was set to 1.3 when considering OL signals. Therefore, the methods applied to UW signals were: DT, CWT 1.1 (Romberg), CWT 1.1 Butterworth (Romberg) and CWT 1.1 (NE). While the methods applied to PD1 OL signals were: DT, CWT 1.3 (Romberg) and CWT 1.3 Butterworth (Romberg). An example of the application of the above methods to UW signals is shown in Fig. 5.8.
In Fig. 5.9 the results are reported in terms of number and percentage of activation for all muscles of subject PD1 for 3 different OL GC. In Fig. 5.10 the results are reported in terms of number and percentage of activation for all muscles of subject PD1 for 3 different UW GC.
Similar observations done for the results found in terms of number and percentage of activation of CS subjects can be drawn for PD ones. Indeed, CWT methods did not find any activation in some cases while in others they found a 100% of activation. The possible causes of these inconsistencies could be the combination of the choice of the scaling parameter and the selected noise interval or a presence

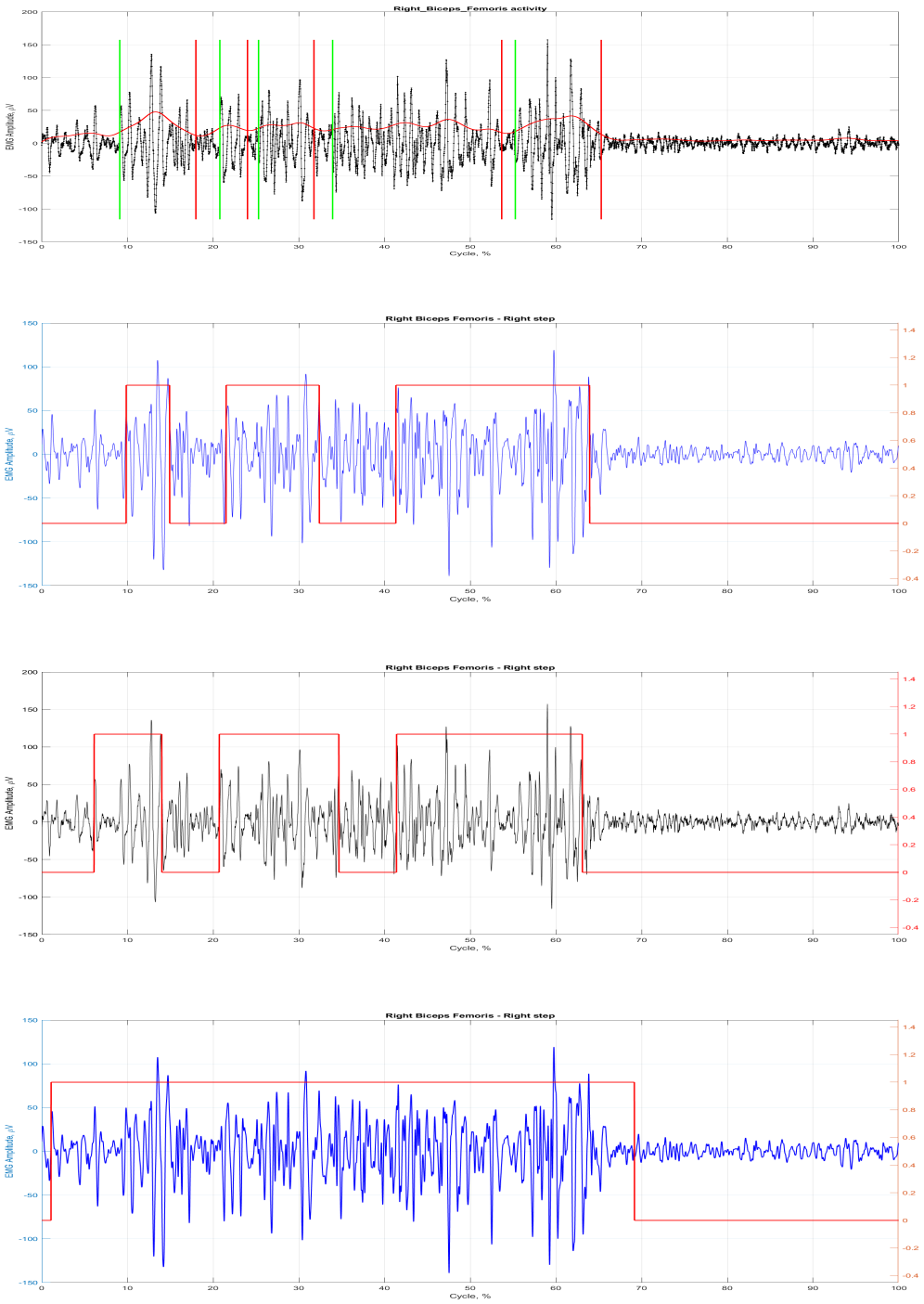

Figure 5.8: DT, CWT 1.1 (Romberg), CWT 1.1 Butterworth (Romberg) and CWT 1.1 (NE) methods comparison for RBF of PD2 during UW GC.

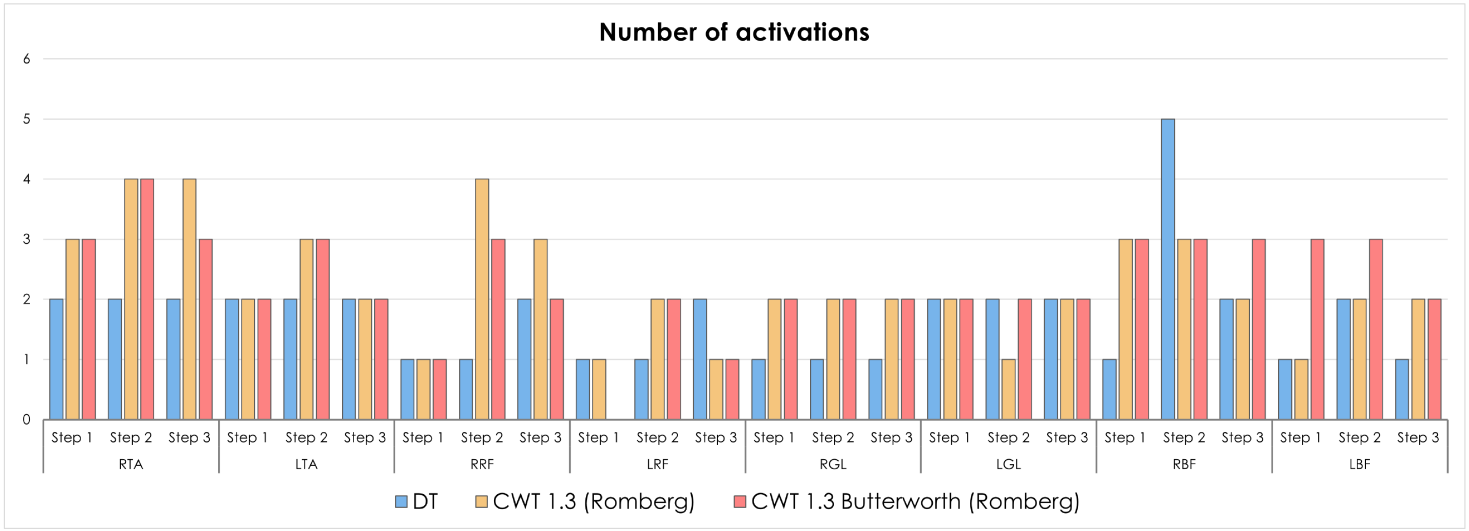

(a)

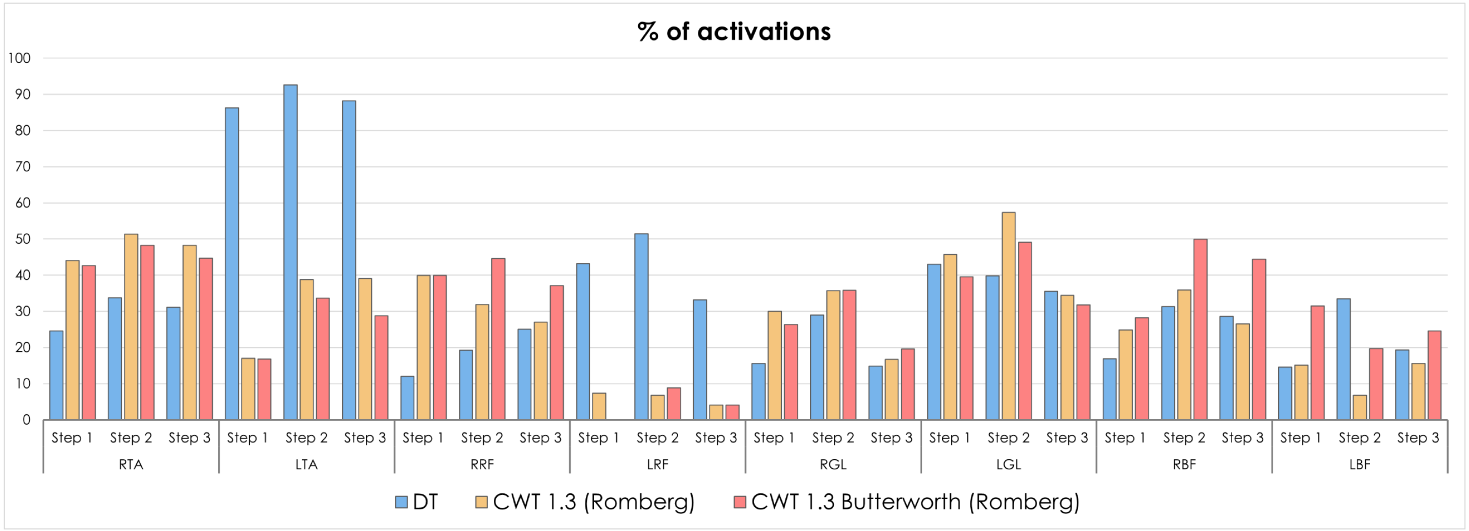

(b)

Figure 5.9: (a) Number of activations of 3 OL GCs of subject PD1 for all muscles. (b) Percentage of activation of 3 OL GCs of subject PD1 for all muscles.

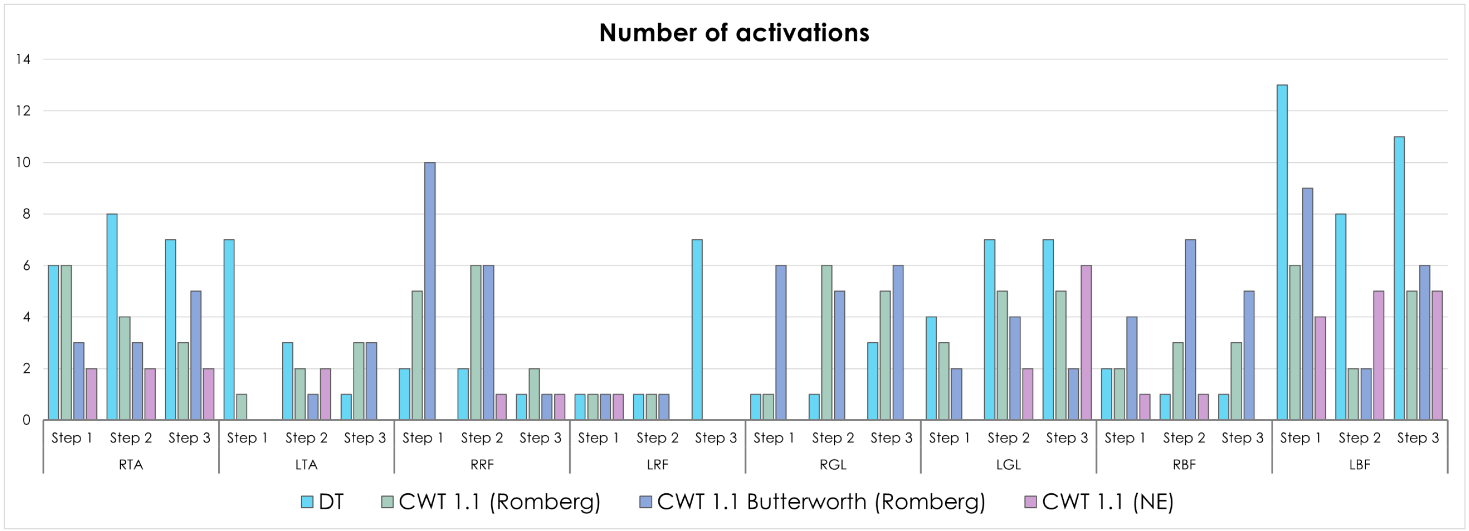

(a)

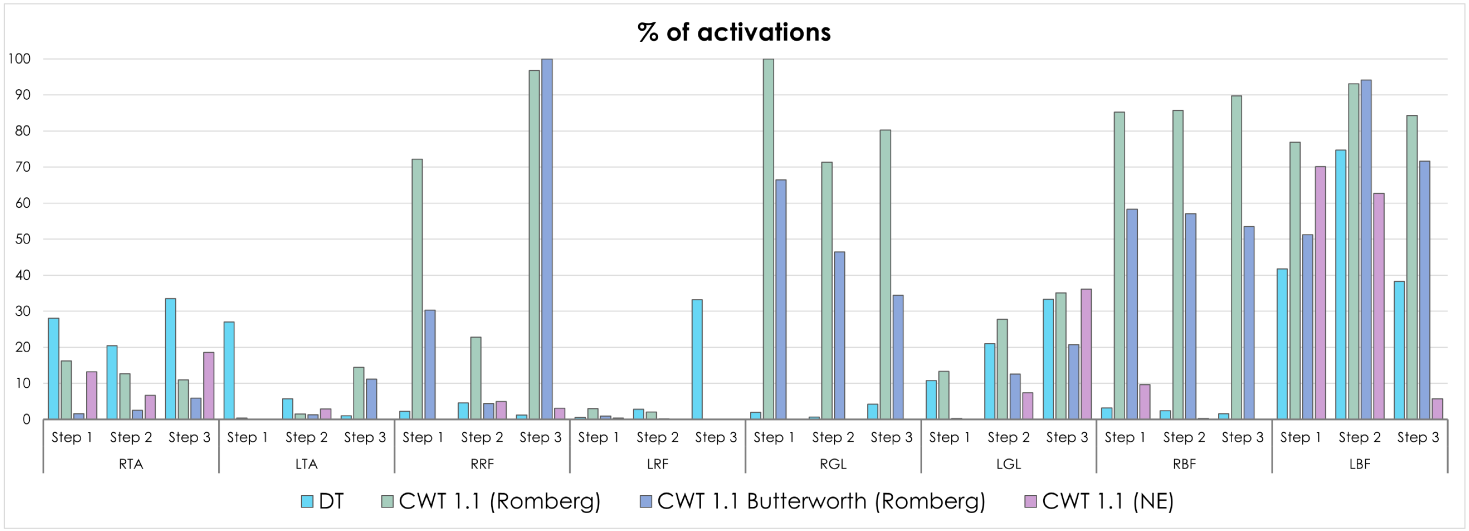

(b)

Figure 5.10: (a) Number of activations of 3 UW GCs of subject PD1 for all muscles. (b) Percentage of activation of 3 UW GCs of subject PD1 for all muscles.

of spurious peaks within the only-noise interval used for the analysis or even an erroneous identification of the noise interval with NE method. However, it was observed that in the OL date there were no cases in which the CWT method found 100% activations, and there was only one case in which it found no activations. The latter case used the CWT method with butterworth filtering. In contrast, in the UW analysis, 100% activation and 0% activation were found in both cases of CWT with bandpass filtering and with butterworth filtering. In some specific cases described below, however, it is possible that the detection of 0% activation was correct because for some patients' EMG channels the electrodes may have made poor contact. Therefore, although the subject was walking, no activation was recorded and then detected. Indeed, one observation that can be drawn from these analyses was that the UW signal appeared to be much corrupted by noise and artifacts than the OL signal. This could be due to the presence of confounding factors during the recording of the UW EMG signal. For example, all channels of EMG acquisitions of PD4 were corrupted by a regular artifact. This artifact repeated at a constant frequency of about 1,4 Hz (i.e. every 0,7 seconds), so it was probably generated by electronics or by the acquisition system, since it was present in all the acquisition both when the subject was walking and when he was executing the Romberg test. The artifact is shown in Fig. 5.11 for the Romberg test execution. In addition, for all channels acquired with the exception of RTA and LTA, sensors seemed to have a bad contact with the subject's skin since for almost all the acquisition the signal was close to zero. For this reason, in the subsequent calculation of the average for all subjects of the number and percentage of activations only the results obtained for RTA and LTA of PD4 were included. Moreover, to PD4 signals a notch filter was applied to remove the artifact above described before the application of CWT method, since the only bandpass filtering resulted not enough to reduce the artifact. The results of the different processing technique applied for PD4 signals are shown for RTA and RBF for a 10 seconds interval in which the subject was walking in Fig. 5.12 and 5.13 respectively.

Finally, in the case of CWT (Romberg) method, it must be stressed out that

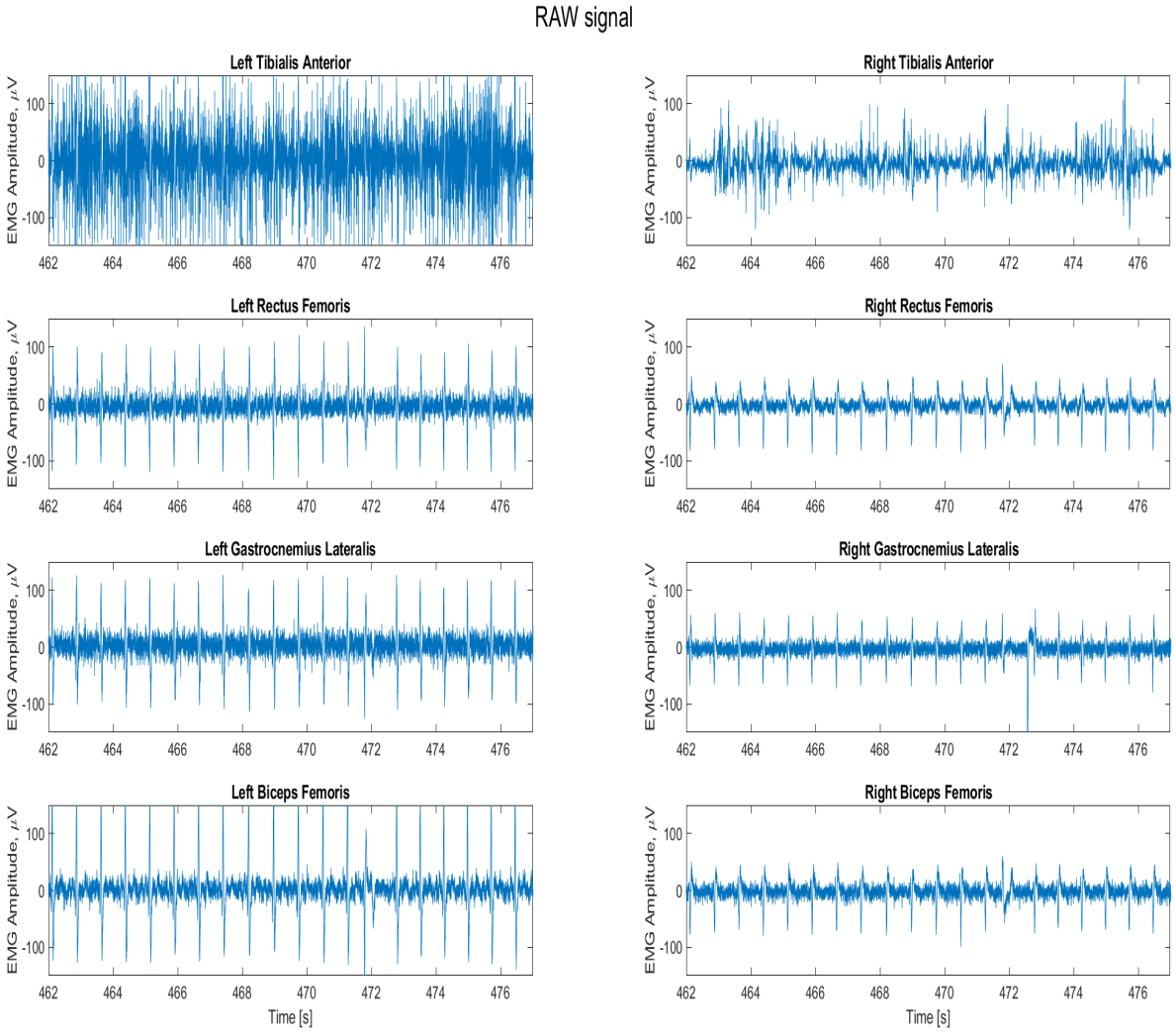

Figure 5.11: Raw signals of UW EMG acquisition for PD4 during Romberg test execution

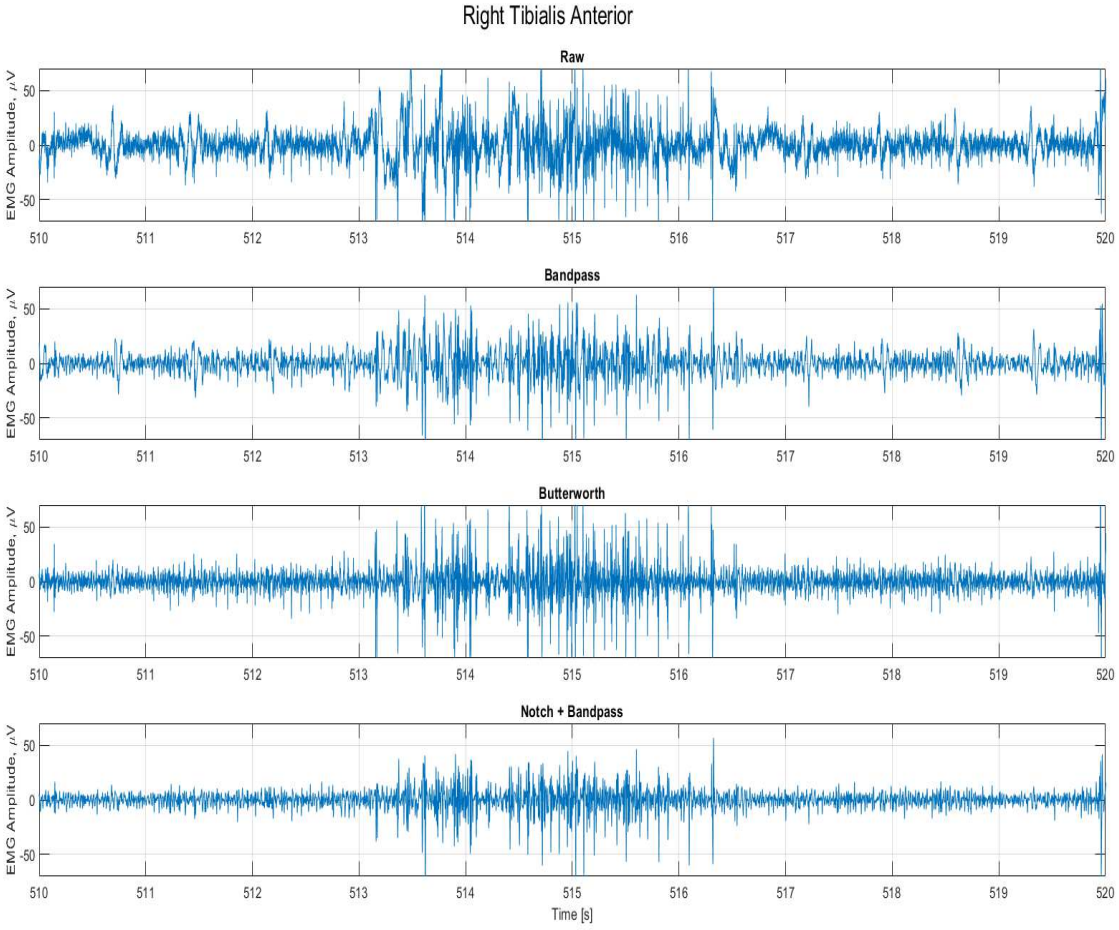

Figure 5.12: Comparison of filtering techniques to test the effectiveness of artifact removal in UW EMG acquisition of PD4 for RTA. The same interval of 10 seconds of EMG acquisition while the subject was walking is reported for the comparison.

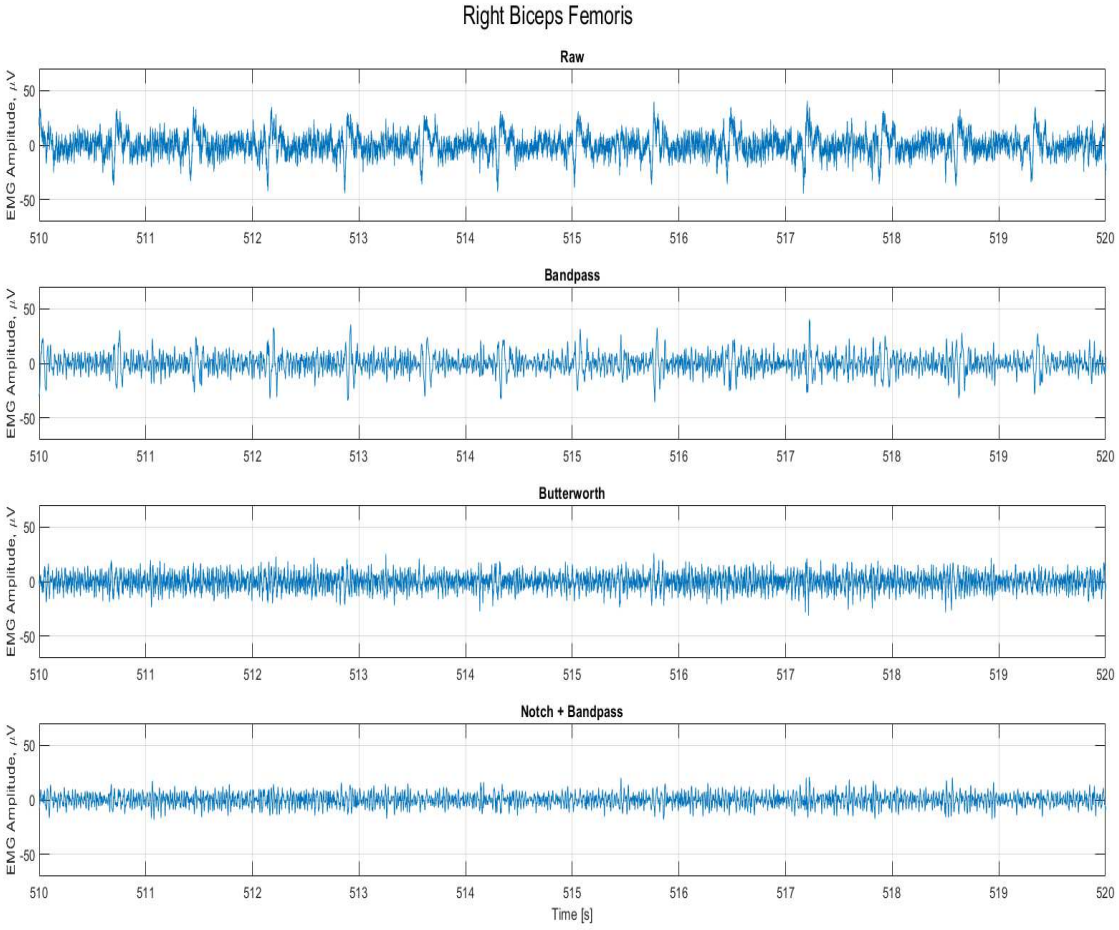

Figure 5.13: Comparison of filtering techniques to test the effectiveness of artifact removal in UW EMG acquisition of PD4 for RBF. The same interval of 10 seconds of EMG acquisition while the subject was walking is reported for the comparison.

using the Romberg test as a noise-only interval, could lead to detect lower activation rates. In fact, this was a methodological choice considering that a stationary subject presents no muscular activity. This is confirmed by the results obtained for OL signals in almost all cases. Indeed, results obtained for OL walking (Fig. 5.9) are comparable to those obtained with DT method. However, it was observed from the UW GoPro video that some PD patients struggled to remain completely still during the execution of the Romberg test. Indeed, some of them, during this phase, were taking small steps forward and backward and others were waving their arms in order to maintain equilbrium. As a result, this may have led to an higher muscle activity than that of OL. An example can be seen in Fig. 4.3 for RTA and LGL. However, further consideration and analysis should be done to prove the validity of this hypothesis.

A general summary of all muscles and all UW GCs for all PD subjects considered in the analysis is reported in Fig. 5.14. Here, for each muscle, data obtained for all GCs of all subjects with a specific method are reported in boxplots in order to visually compare results obtained for the different methods used. It can be seen that the DT method showed high variability in the determination of number of activations and in general it found higher number of activations with respect to CWT methods, recording up to 13 activations for LBF. Then, CWT 1.1 (NE) method shows in almost all cases the highest variability in the percentage of activation. As already hypothesized for CS, it might be due to the case where a 0% and 100% of activation are found for the same muscle in different GCs.

The results of the average and standard deviation values of number of activations and percentage of activation are reported in tables 6.1 and 6.2 of the appendix 6.

5.3 UW/OL comparison

The last analysis investigated regarded the comparison between the results obtained with the application of two different methods to UW and OL signals.

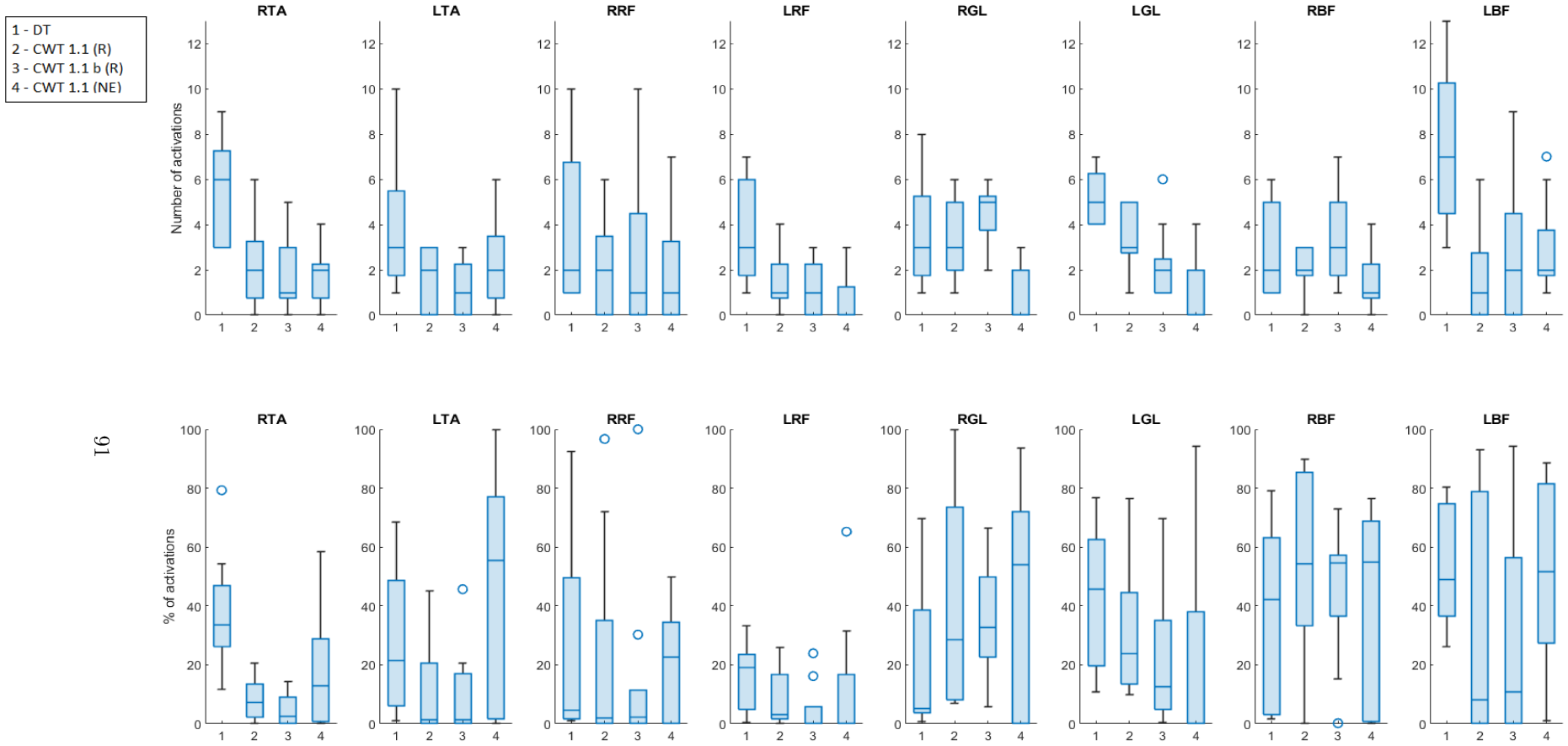

Figure 5.14: Boxplot of PD subjects results. Each boxplot reports the results obtained for all UW GCs of the PD subjects using a specific muscle activity identification method. Each graphic reports the results obtained for a specific muscle. X-axis values correspond to the application of a different method; in order: DT, CWT 1.1 (Romberg), CWT 1.1 Butterworth (Romberg) and CWT 1.1 (NE). In the first line the results are reported in term of number of activations. In the second line the results are reported in terms of percentage of activations. Outliers are represented by circles.

These methods were DT and CWT 1.1 (NE). The results are reported for the common EMG channels between protocol 1 and 2 for CS and PD subjects. It was observed that DT method applied on UW signals obtained in general a higher number of activations with higher variability than the number of activations found for OL signals. Indeed, for DT applied on UW signals the maximum number of activations found was 13 activations per GC, while for DT applied to OL signals it was 7. This was probably depended on the post-processor used by this method that classified transitions that remained stable for longer than 30 ms as muscle activity both for UW and OL EMG signals. However, the application of this method was over the entire GC which, in terms of time duration, was longer in water than OL. Therefore, by applying DT method to a longer time period it is possible to find a higher number of activations. However, this difference was not observed for the CWT method which never finds more than 7 activations per GC both for UW and OL signals. Finally, comparison between OL and UW results for PD1 using DT method is reported in Fig. 5.16. Each boxplot comprises the results obtained for the 3 GCs for UW and OL acquisitions respectively. It can be seen that in all cases, the number of activations was higher for UW results than OL while percentages of activations were lower in UW data than OL. The only exception was the biceps femoris since RBG had both lower number and percentage of activation, while LBF had both higher number and percentage of activation.

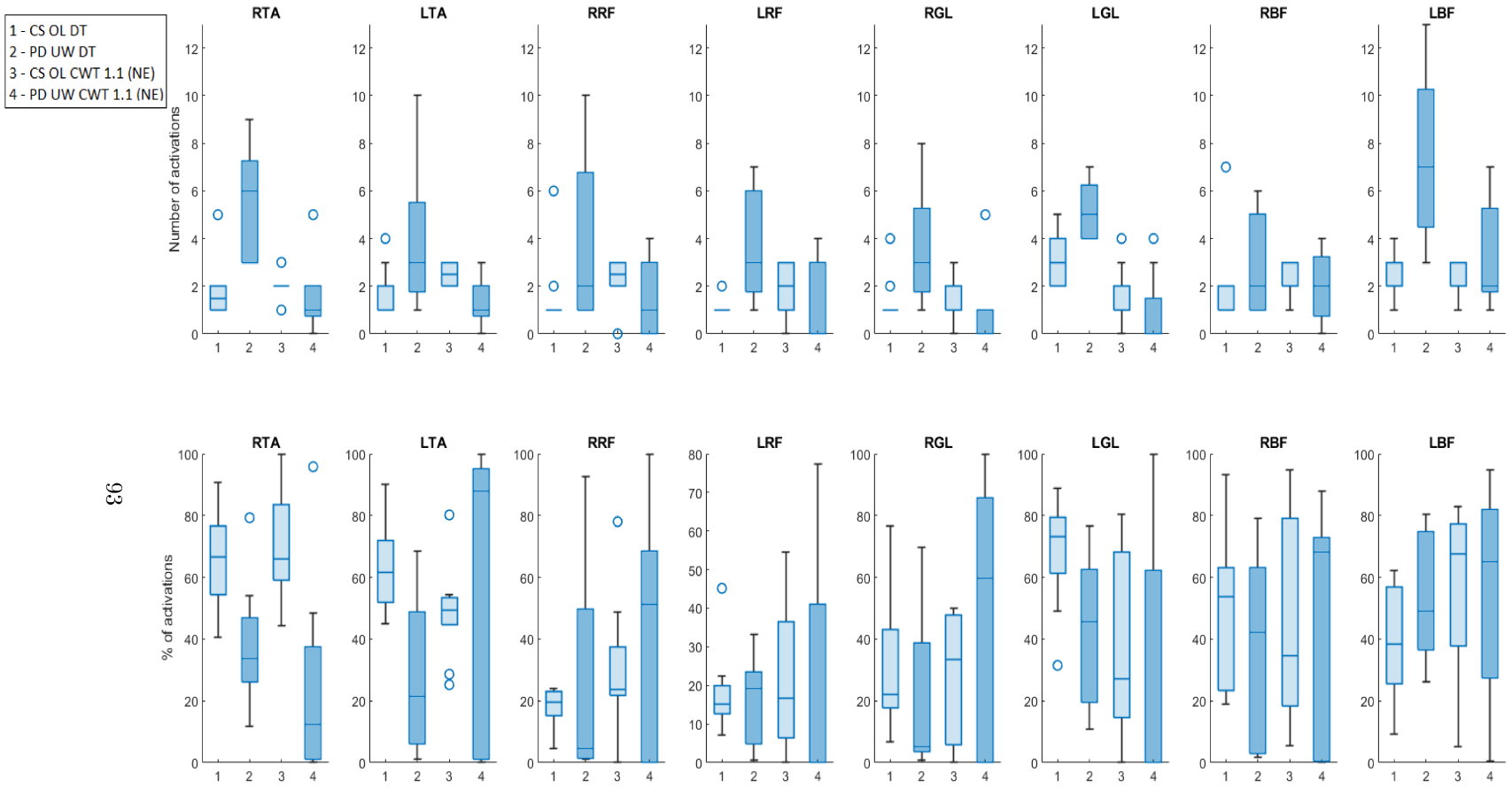

Figure 5.15: Boxplot of PD and CS subjects results for UW and OL analysis respectively. Each boxplot reports the results obtained for all GCs of CS and PD subjects using respectively DT and CWT 1.1 (NE) method. Each graphic reports the results obtained for a specific muscle. X-axis values correspond to the application of a different method to a different acquisition modality; in order: DT applied to OL EMG of CS subjects, DT applied to UW EMG of PD subjects, CWT 1.1 (NE) applied to OL EMG of CS subject and CWT 1.1 (NE) applied to UW EMG of PD subjects. In the first line the results are reported in term of number of activations. In the second line the results are reported in terms of percentage of activations. Outliers are represented by circles.

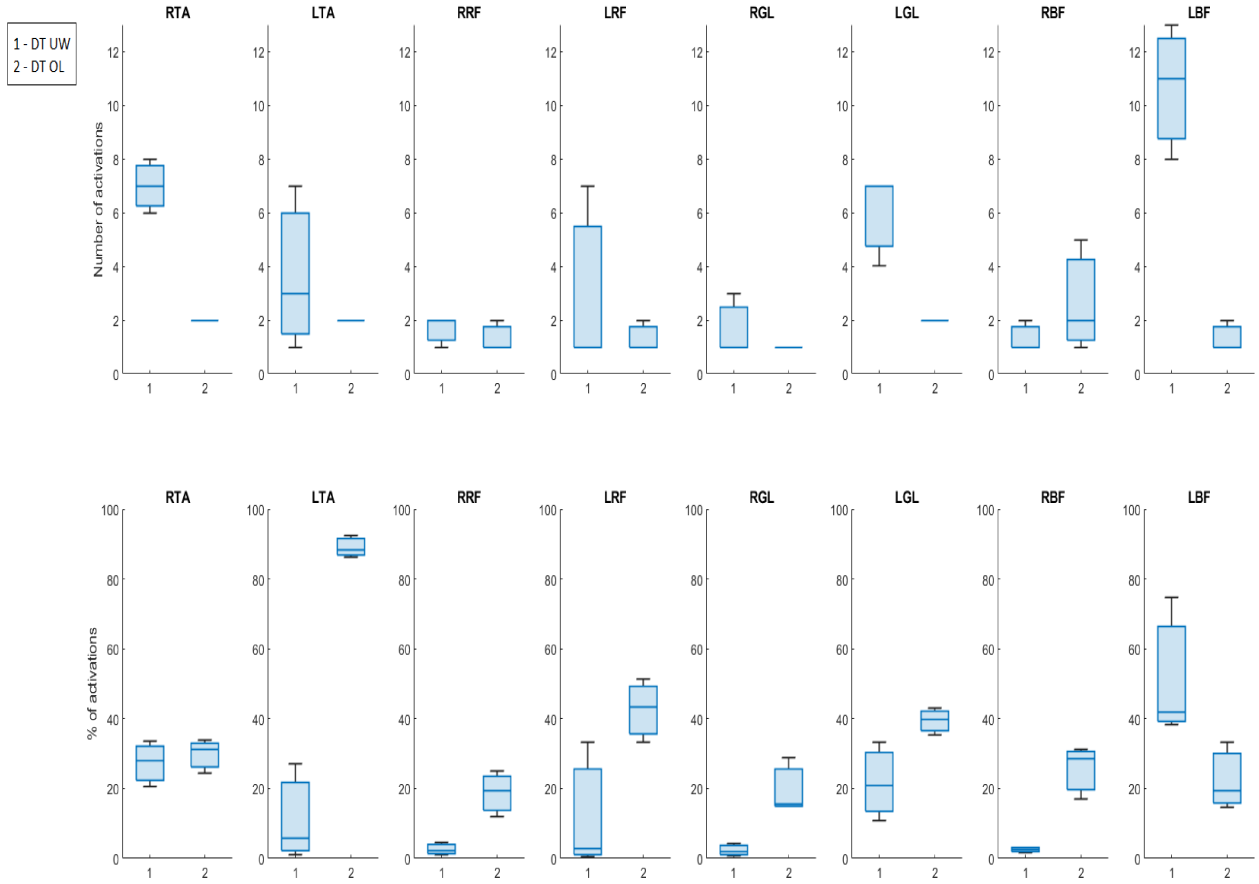

Figure 5.16: UW/OL comparison for PD1 using DT method. Each boxplot reports the results of the 3 UW and OL GCs respectively for each muscle. X-axis values correspond to the type of EMG acquisition. In the first line the results are reported in term of number of activations for the different EMG acquisition modality. In the second line the results are reported in terms of percentage of activations for the different EMG aquisition modality. Outliers are represented by circles.

Chapter 6

Conclusions

The present work had the aim of comparing different techinques for the elaboration of EMG signals acquired underwater on PD subjects. Firstly, healthy subjects were analyzed OL in order to validate the methodologies. Secondly, comparison among different preprocessing techniques and noise intervals extraction were performed on a cohort of 4 PD subjects who underwent EMG acquisition underwater. DT appeared to be the most robust technique. CWT, generally, selected narrower ranges of activation. The generalisability of these results is subject to certain limitations.

The main one was that no real UW noise-only acquisition was available, thus leading to the use either of the Romberg test execution interval or of an interval extracted through NE algorithm. Therefore, this choice may have led to lower effectiveness of the CWT detection algorithm. Moreover, the underwater setup played a key role in the elaborations; indeed, in some cases, bad contact of the electrodes to the skin seems be found in some acquired data.

Another limitation lies in the parameters choice. Firstly, the choice of the Romberg test as a noise-only interval UW. The obtained results showed in fact a possible presence of muscle activity while performing UW Romberg test in some cases comparable in amplitude to that of walking. However, further studies are needed to support this aspect. Secondly, gamma parameter choice in the

CWT method is crucial either considered alone or in combination with the other parameters to be set (e.g. filters). Different combinations of values were tested but no unique solution was found to be the best one in the analyzed cases. A possible future development for the use of this method is to automatically set the parameters in order to obtain reliable results and to decrease the occurrences of failure in detecting the activation.

On the other hand, DT method applied in UW signals found a higher average number of activations than OL signals and CWT methods applied to the same UW signals. Further research could be carried on the tuning of some parameters of this method, such as the minimum time period considered by the postprocessor for the identification of muscle activity or the observation window length for UW acquisitions.

Consequently, filters parameters must be taken into account. Current literature suggest to apply the same methodologies used in OL signals to UW ones. This can be a good practice to make both signals comparable but it must be kept in mind that different signal types may require different processing. Therefore, future research could be carried on this direction. Moreover, it is important to notice that walking UW is different than walking OL. In fact, it was found that during UW walking some PD subjects walked only on tiptoes without ever or almost never completely resting their foot or heel. This type of walking is different from that usually performed OL, so it is reasonable to expect some differences in muscle activity.

Finally, the methods described may be fine for detecting individual GC activations, however, a larger subjects database would be needed for a more in-depth comparison. The identification of muscle activity is then of fundamental importance to give a contribution to the gait analisys especially in patients with motor diseases. It is important not only to find the correct method for the identification of activations and the execution of a proper preprocessing of the acquired signal, but also to distinguish whether there are differences in the processing of the EMG signal depending on the environment in which it is acquired.

Appendix A

Muscle name	DT	CWT 1.1 (Romberg)	CWT 1.1 Butterworth (Romberg)	CWT 1.1 (NE)
	MEAN (± SD)	MEAN (± SD)	MEAN (± SD)	MEAN (± SD)
RTA	5,5 (± 2,4)	2,2 (± 1,9)	1,8 (± 1,6)	1,7 (± 1,3)
LTA	4,0 (± 3,0)	1,6 (± 1,3)	1,2 (± 1,3)	2,2 (± 2,1)
RRF	3,8 (± 3,6)	2,0 (± 2,3)	2,7 (± 3,5)	1,8 (± 2,4)
LRF	3,8 (± 2,3)	1,6 (± 1,3)	1,1 (± 1,3)	0,7 (± 1,1)
RGL	3,8 (± 2,4)	3,6 (± 1,7)	4,4 (± 1,3)	1,3 (± 1,1)
LGL	5,3 (± 1,2)	3,6 (± 1,5)	2,2 (± 1,7)	1,1 (± 1,5)
RBF	2,7 (± 2,0)	2,1 (± 1,1)	3,3 (± 2,1)	1,6 (± 1,3)
LBF	7,2 (± 1,9)	1,9 (± 2,2)	2,9 (± 3,1)	3,0 (± 2,1)

Table 6.1: Average number of muscle activations per GC for EMG UW signals of PD subjects

Muscle name	DT	CWT 1.1 (Romberg)	CWT 1.1 Butterworth (Romberg)	CWT 1.1 (NE)
	MEAN (± SD)	MEAN (± SD)	MEAN (± SD)	MEAN (± SD)
RTA	37,33 (± 20,0)	8,5 (± 7,2)	4,8 (± 5,2)	18,2 (± 19,4)
LTA	27,5 (± 23,3)	11,7 (± 15,9)	10,5 (± 15,4)	47,9 (± 38,5)
RRF	24,4 (± 32,6)	23,5 (± 36,1)	15,8 (± 33,0)	19,9 (± 20,7)
LRF	15,7 (± 11,1)	9,3 (± 10,2)	4,8 (± 8,9)	12,1 (± 22,5)
RGL	22,5 (± 24,7)	41,2 (± 35,8)	34,8 (± 20,5)	41,5 (± 38,5)
LGL	42,1 (± 23,3)	32,5 (± 25,0)	23,8 (± 26,6)	24,4 (± 35,8)
RBF	35,7 (± 30,2)	55,2 (± 31,7)	45,6 (± 23,1)	42,4 (± 33,1)
LBF	53,2 (± 20,5)	31,6 (± 40,6)	29,4 (± 35,0)	52,3 (± 31,0)

Table 6.2: Average percentage of muscle activation per GC for EMG UW signals of PD subjects

Muscle name	DT	CWT 1.1 (NE)	CWT 1.6 (NE)	CWT 1.6 Butterworth (NE)
	MEAN (± SD)	MEAN (± SD)	MEAN (± SD)	MEAN (± SD)
RPL	2,6 (± 1,0)	1,9 (± 0,9)	1,7 (± 0,8)	1,8 (± 0,8)
LPL	2,3 (± 0,9)	1,8 (± 0,9)	1,6 (± 0,5)	1,6 (± 0,7)
RTA	1,4 (± 0,5)	2,0 (± 0,5)	2,2 (± 0,4)	2,2 (± 0,4)
LTA	1,9 (± 0,9)	2,5 (± 0,5)	2,4 (± 0,5)	2,4 (± 0,5)
RGL	1,1 (± 0,3)	1,4 (± 0,8)	1,2 (± 0,9)	1,3 (± 0,9)
LGL	3,1 (± 0,9)	1,9 (± 1,0)	1,6 (± 0,8)	1,7 (± 0,8)
RED	2,3 (± 0,5)	2,4 (± 1,2)	2,1 (± 1,0)	2 (± 0,9)
LED	2,3 (± 1,3)	2,1 (± 0,9)	2,2 (± 0,9)	2 (± 0,8)
RGM	1,7 (± 1,1)	1,4 (± 0,8)	1,3 (± 0,8)	1,3 (± 0,8)
LGM	1,9 (± 0,8)	2,3 (± 0,8)	2,1 (± 0,5)	2,1 (± 0,5)
RRF	1,1 (± 0,3)	2,6 (± 0,5)	1,8 (± 1,1)	1,8 (± 1,1)
LRF	1,2 (± 0,4)	1,8 (± 1,0)	1,5 (± 1,3)	1,5 (± 1,3)
RBF	1,7 (± 0,5)	2,1 (± 0,7)	1,6 (± 1,3)	1,6 (± 1,3)
LBF	2,3 (± 1,0)	2,2 (± 0,6)	2 (± 0,9)	1,9 (± 0,7)

Table 6.3: Average number of muscle activations per GC for EMG OL signals of CS subjects

Muscle name	DT	CWT 1.1 (NE)	CWT 1.6 (NE)	CWT 1.6 Butterworth (NE)
	MEAN (± SD)	MEAN (± SD)	MEAN (± SD)	MEAN (± SD)
RPL	67,0 (± 17,4)	55,2 (± 26,7)	37,4 (± 30,3)	35,9 (± 27,5)
LPL	51,9 (± 27,4)	67,0 (± 20,9)	56,0 (± 22,3)	57,0 (± 22,5)
RTA	66,7 (± 15,8)	66,4 (± 16,3)	55,7 (± 11,6)	57,4 (± 13,1)
LTA	62,5 (± 13,4)	48,4 (± 14,3)	37,9 (± 15,9)	38,0 (± 16,3)
RGL	23,8 (± 14,1)	30,8 (± 18,7)	21,2 (± 14,4)	18,4 (± 12,5)
LGL	68,5 (± 16,2)	35,7 (± 28,2)	26,8 (± 25,8)	28,7 (± 25,4)
RED	67,8 (± 12,7)	67,9 (± 27,6)	52,4 (± 29,6)	52,2 (± 29,5)
LED	70,6 (± 16,0)	73,6 (± 19,5)	54,0 (± 33,4)	55,7 (± 33,8)
RGM	39,2 (± 22,0)	31,5 (± 19,5)	27,0 (± 20,2)	27,2 (± 20,4)
LGM	39,1 (± 28,6)	44,8 (± 19,2)	35,5 (± 20,4)	35,3 (± 20,5)
RRF	16,9 (± 6,3)	33,4 (± 18,1)	21,7 (± 17,6)	21,1 (± 15,9)
LRF	18,1 (± 9,9)	20,7 (± 16,9)	13,5 (± 13,3)	13,4 (± 13,2)
RBF	48,1 (± 25,1)	36,6 (± 27,6)	27,3 (± 28,9)	27,5 (± 28,9)
LBF	38,3 (± 16,3)	56,2 (± 25,2)	39,4 (± 25,6)	43,4 (± 27,6)

Table 6.4: Average percentage of muscle activation per GC for EMG OL signals of CS subjects

Bibliography

[1] J. Perry and J. M. Burnfield, *Gait Analysis. Normal and Pathological Function*, 2nd ed. SLACK Incorporated, 2010.

[2] D. H. Sutherland, "The evolution of clinical gait analysis part l: kinesiological EMG," vol. 14, no. 1, pp. 61–70, 2001, publisher: Elsevier.

[3] A. Costa and C. Caltagirone, *Malattia di Parkinson e parkinsonismi La prospettiva delle neuroscienze cognitive.* Springer, 2009.

[4] Z. Ou, J. Pan, S. Tang, D. Duan, D. Yu, H. Nong, and Z. Wang, "Global trends in the incidence, prevalence, and years lived with disability of Parkinson's disease in 204 countries/territories from 1990 to 2019," *Frontiers in Public Health*, vol. 9, 2021.

[5] S. L. Kowal, T. M. Dall, R. Chakrabarti, M. V. Storm, and A. Jain, "The current and projected economic burden of Parkinson's disease in the United States," *Movement Disorders*, vol. 28, no. 3, pp. 311–318, 2013.

[6] M. Wanneveich, F. Moisan, H. Jacqmin-Gadda, A. Elbaz, and P. Joly, "Projections of prevalence, lifetime risk, and life expectancy of Parkinson's disease (2010-2030) in France," *Movement Disorders*, vol. 33, no. 9, pp. 1449–1455, 2018.

[7] M. J. Armstrong and M. S. Okun, "Diagnosis and treatment of Parkinson disease: a review," *Jama*, vol. 323, no. 6, pp. 548–560, 2020.

[8] U. S. Kanmounye, L. Angelov, S. C. Pannullo, S. Z. Y. Ooi, R. d. Koning, A. J. Bourcier, Y. Zolo, E. Zusman, Y. J. Kenfack, L. Sebopelo *et al.*, "The role of neurosurgery in global health epilepsy, movement disorders, and psychiatric diseases," in *Neurosurgery and Global Health*. Springer, 2022, pp. 107–122.

[9] A. Cieza, K. Causey, K. Kamenov, S. W. Hanson, S. Chatterji, and T. Vos, "Global estimates of the need for rehabilitation based on the global burden of disease study 2019: a systematic analysis for the global burden of disease study 2019," *The Lancet*, vol. 396, no. 10267, pp. 2006–2017, 2020.

[10] G. E. Alexander, "Biology of Parkinson's disease: pathogenesis and pathophysiology of a multisystem neurodegenerative disorder," vol. 6, no. 3, p. 259, 2004, publisher: Les Laboratoires Servier.

[11] A. Wood-Kaczmar, S. Gandhi, and N. Wood, "Understanding the molecular causes of Parkinson's disease," *Trends in molecular medicine*, vol. 12, no. 11, pp. 521–528, 2006.

[12] A. J. Hughes, S. E. Daniel, L. Kilford, and A. J. Lees, "Accuracy of clinical diagnosis of idiopathic Parkinson's disease: a clinico-pathological study of 100 cases." *Journal of neurology, neurosurgery & psychiatry*, vol. 55, no. 3, pp. 181–184, 1992.

[13] G. Abbruzzese, R. Marchese, L. Avanzino, and E. Pelosin, "Rehabilitation for Parkinson's disease: Current outlook and future challenges," *Parkinsonism & Related Disorders*, vol. 22, pp. S60–S64, 2016, proceedings of XXI World Congress on Parkinson's Disease and Related Disorders, December 6-9, 2015, Milan, Italy.

[14] J. E. Ahlskog, "Does vigorous exercise have a neuroprotective effect in Parkinson disease?" *Neurology*, vol. 77, no. 3, pp. 288–294, 2011.

[15] M. Schenkman, C. G. Moore, W. M. Kohrt, D. A. Hall, A. Delitto, C. L. Comella, D. A. Josbeno, C. L. Christiansen, B. D. Berman, B. M. Kluger,

E. L. Melanson, S. Jain, J. A. Robichaud, C. Poon, and D. M. Corcos, "Effect of high-intensity treadmill exercise on motor symptoms in patients with de novo Parkinson disease: A phase 2 randomized clinical trial," vol. 75, no. 2, pp. 219–226, 2018.

[16] D. Volpe, D. Pavan, M. Morris, A. Guiotto, R. Iansek, S. Fortuna, G. Frazzitta, and Z. Sawacha, "Underwater gait analysis in Parkinson's disease," *Gait & Posture*, vol. 52, pp. 87–94, 2017.

[17] R. W. Soutas-Little, "Motion analysis and biomechanics," in *Gait Analysis in the Science of Rehabilitation*. Department of Veteran Affairs, 1998, p. 49.

[18] R. Baker, "The history of gait analysis before the advent of modern computers," vol. 26, no. 3, pp. 331–342, 2007, publisher: Elsevier.

[19] Wikimedia Commons. (2006) The horse in motion. [Online]. Available: https://commons.wikimedia.org/wiki/File:The_Horse_in_Motion.jpg

[20] B. Zhang, S. Jiang, D. Wei, M. Marschollek, and W. Zhang, "State of the art in gait analysis using wearable sensors for healthcare applications," in *2012 IEEE/ACIS 11th International Conference on Computer and Information Science*, 2012, pp. 213–218.

[21] B. Pueo, J. M. Jimenez-Olmedo *et al.*, "Application of motion capture technology for sport performance analysis," 2017.

[22] Wikimedia Commons. (2009) Projection of p on both cameras. [Online]. Available: https://commons.wikimedia.org/wiki/File:Epipolar_Geometry1.svg

[23] J. Richards, *Biomechanics in Clinic and Research*. Churchill Livingston Elsevier, 2008.

[24] D. H. Sutherland, "The evolution of clinical gait analysis: Part II kinematics," vol. 16, no. 2, pp. 159–179, 2002.

[25] A. Cappozzo, U. D. Croce, A. Leardini, and L. Chiari, "Human movement analysis using stereophotogrammetry: Part 1: theoretical background," vol. 21, no. 2, pp. 186–196, 2005.

[26] PressureRef4PIL. (2015) Measure of stride length. [Online]. Available: https://paginas.fe.up.pt/~ee10185/methodology

[27] A. P. Shortland, "Gait and clinical gait analysis," in *Clinical Engineering*. Elsevier, 2020, pp. 473–489.

[28] ProtoKinetics. (2018) Breakdown of the gait cycle into phases based on the work of perry and burnfield. [Online]. Available: https://www.protokinetics.com/understanding-phases-of-the-gait-cycle/

[29] S. Heywood, J. McClelland, P. Geigle, A. Rahmann, and R. Clark, "Spatiotemporal, kinematic, force and muscle activation outcomes during gait and functional exercise in water compared to on land: A systematic review," *Gait & posture*, vol. 48, pp. 120–130, 2016.

[30] F. A. Magalhaes, Z. Sawacha, R. Di Michele, M. Cortesi, G. Gatta, and S. Fantozzi, "Effectiveness of an automatic tracking software in underwater motion analysis," *Journal of sports science & medicine*, vol. 12, no. 4, p. 660, 2013.

[31] G. R. Bernardina, P. Cerveri, R. M. Barros, J. C. Marins, and A. P. Silvatti, "In-air versus underwater comparison of 3d reconstruction accuracy using action sport cameras," *Journal of Biomechanics*, vol. 51, pp. 77–82, 2017.

[32] A. M. Barela and M. Duarte, "Biomechanical characteristics of elderly individuals walking on land and in water," *Journal of electromyography and kinesiology*, vol. 18, no. 3, pp. 446–454, 2008.

[33] A. M. Barela, S. F. Stolf, and M. Duarte, "Biomechanical characteristics of adults walking in shallow water and on land," *Journal of Electromyography and Kinesiology*, vol. 16, no. 3, pp. 250–256, 2006.

[34] T. Andriacchi, J. Ogle, and J. Galante, "Walking speed as a basis for normal and abnormal gait measurements," *Journal of biomechanics*, vol. 10, no. 4, pp. 261–268, 1977.

[35] A. Den Otter, A. Geurts, T. Mulder, and J. Duysens, "Speed related changes in muscle activity from normal to very slow walking speeds," *Gait & posture*, vol. 19, no. 3, pp. 270–278, 2004.

[36] N. Prajapati, A. Kaur, and D. Sethi, "A review on clinical gait analysis," in *2021 5th International Conference on Trends in Electronics and Informatics (ICOEI)*, 2021, pp. 967–974.

[37] G. Albani, G. Sandrini, G. Kunig, C. Martin-Soelch, A. Mauro, R. Pignatti, C. Pacchetti, V. Dietz, and K. L. Leenders, "Differences in the EMG pattern of leg muscle activation during locomotion in Parkinson's disease," *Functional neurology*, vol. 18, no. 3, pp. 165–178, 2003.

[38] A. Salarian, H. Russmann, F. J. Vingerhoets, C. Dehollain, Y. Blanc, P. R. Burkhard, and K. Aminian, "Gait assessment in Parkinson's disease: toward an ambulatory system for long-term monitoring," *IEEE transactions on biomedical engineering*, vol. 51, no. 8, pp. 1434–1443, 2004.

[39] M. Morris, R. Iansek, J. McGinley, T. Matyas, and F. Huxham, "Three-dimensional gait biomechanics in Parkinson's disease: evidence for a centrally mediated amplitude regulation disorder," *Movement disorders: official journal of the Movement Disorder Society*, vol. 20, no. 1, pp. 40–50, 2005.

[40] A. Nieuwboer, R. Dom, W. De Weerdt, K. Desloovere, S. Fieuws, and E. Broens-Kaucsik, "Abnormalities of the spatiotemporal characteristics of gait at the onset of freezing in Parkinson's disease," *Movement disorders: official journal of the Movement Disorder Society*, vol. 16, no. 6, pp. 1066–1075, 2001.

[41] L. M. Carroll, D. Volpe, M. E. Morris, J. Saunders, and A. M. Clifford, "Aquatic exercise therapy for people with Parkinson disease: a randomized

controlled trial," *Archives of physical medicine and rehabilitation*, vol. 98, no. 4, pp. 631–638, 2017.

[42] J. See, *Aquatic exercise. An exercise program for people with Parkinson's Disease*. American Parkinson Disease Association, Inc., 2008. [Online]. Available: https://www.apdaparkinson.org/uploads/files/Aquatic-Book_8-08---edited-2015-oUM.pdf

[43] M. B. I. Reaz, M. S. Hussain, and F. Mohd-Yasin, "Techniques of EMG signal analysis: detection, processing, classification and applications," *Biological procedures online*, vol. 8, no. 1, pp. 11–35, 2006.

[44] R. H. Chowdhury, M. B. Reaz, M. A. B. M. Ali, A. A. Bakar, K. Chellappan, and T. G. Chang, "Surface electromyography signal processing and classification techniques," vol. 13, no. 9, pp. 12 431–12 466, 2013, publisher: Multidisciplinary Digital Publishing Institute.

[45] Britannica, The Editors of Encyclopaedia. (2018) Muscle. [Online]. Available: https://www.britannica.com/science/muscle

[46] G. L. Soderberg, *Selected Topics in Surface Electromyography for Use in the Occupational Setting: Expert Perspectives*. U.S. Department of Health and Human Services, 1992.

[47] W. R. Frontera and J. Ochala, "Skeletal muscle: a brief review of structure and function," *Calcified tissue international*, vol. 96, no. 3, pp. 183–195, 2015.

[48] Britannica, The Editors of Encyclopaedia. (2018) Higher-level mechanisms of movement. [Online]. Available: https://www.britannica.com/science/human-nervous-system/Higher-level-mechanisms-of-movement

[49] A. Merlo, D. Farina, and R. Merletti, "A fast and reliable technique for muscle activity detection from surface EMG signals," vol. 50, no. 3, pp. 316–323, 2003, publisher: IEEE.

[50] D. C. Preston and B. E. Shapiro, "15 - basic electromyography: Analysis of motor unit action potentials," in *Electromyography and Neuromuscular Disorders (Third Edition)*, third edition ed., D. C. Preston and B. E. Shapiro, Eds. London: W.B. Saunders, 2013, pp. 235–248.

[51] M. Raghavan, D. Fee, and P. E. Barkhaus, "Chapter 1 - generation and propagation of the action potential," in *Clinical Neurophysiology: Basis and Technical Aspects*, ser. Handbook of Clinical Neurology, K. H. Levin and P. Chauvel, Eds. Elsevier, 2019, vol. 160, pp. 3–22.

[52] L. Mesin, R. Merletti, and A. Rainoldi, "Surface EMG: the issue of electrode location," *Journal of Electromyography and Kinesiology*, vol. 19, no. 5, pp. 719–726, 2009.

[53] G. Pacini Panebianco, M. Fonsato, G. Frazzita, and R. Stagni, "EMG activation during walking in Parkinson's disease patients," *Gait & posture*, vol. 74, pp. S1–S39, 2019.

[54] A. Bonnefoy-Mazure and S. Armand, *Normal gait*, January 2015, pp. 199–214.

[55] C. J. De Luca, "The use of surface electromyography in biomechanics," *Journal of applied biomechanics*, vol. 13, no. 2, pp. 135–163, 1997.

[56] G. Lu, J.-S. Brittain, P. Holland, J. Yianni, A. L. Green, J. F. Stein, T. Z. Aziz, and S. Wang, "Removing ECG noise from surface EMG signals using adaptive filtering," *Neuroscience letters*, vol. 462, no. 1, pp. 14–19, 2009.

[57] R. Merletti and G. Cerone, "Tutorial. surface EMG detection, conditioning and pre-processing: best practices," *Journal of Electromyography and Kinesiology*, vol. 54, p. 102440, 2020.

[58] C. J. De Luca, L. D. Gilmore, M. Kuznetsov, and S. H. Roy, "Filtering the surface EMG signal: Movement artifact and baseline noise contamination," *Journal of biomechanics*, vol. 43, no. 8, pp. 1573–1579, 2010.

[59] R. Merletti, A. Botter, A. Troiano, E. Merlo, and M. A. Minetto, "Technology and instrumentation for detection and conditioning of the surface electromyographic signal: state of the art," *Clinical biomechanics*, vol. 24, no. 2, pp. 122–134, 2009.

[60] A. Thexton, "A randomisation method for discriminating between signal and noise in recordings of rhythmic electromyographic activity," vol. 66, no. 2, pp. 93–98, 1996, publisher: Elsevier.

[61] P. Bonato, T. D'Alessio, and M. Knaflitz, "A statistical method for the measurement of muscle activation intervals from surface myoelectric signal during gait," vol. 45, no. 3, pp. 287–299, 1998, publisher: IEEE.

[62] C. J. De Luca, "Myoelectrical manifestations of localized muscular fatigue in humans." *Critical reviews in biomedical engineering*, vol. 11, no. 4, pp. 251–279, 1984.

[63] M. M. Lowery, C. L. Vaughan, P. J. Nolan, and M. J. O'Malley, "Spectral compression of the electromyographic signal due to decreasing muscle fiber conduction velocity," *IEEE transactions on rehabilitation engineering*, vol. 8, no. 3, pp. 353–361, 2000.

[64] M. R. Canal, "Comparison of wavelet and short time Fourier transform methods in the analysis of EMG signals," *Journal of medical systems*, vol. 34, no. 1, pp. 91–94, 2010.

[65] I. Daubechies, "The wavelet transform, time-frequency localization and signal analysis," *IEEE transactions on information theory*, vol. 36, no. 5, pp. 961–1005, 1990.

[66] D. K. Kumar, N. D. Pah, and A. Bradley, "Wavelet analysis of surface electromyography," *IEEE transactions on neural systems and rehabilitation engineering*, vol. 11, no. 4, pp. 400–406, 2003.

[67] F. Laterza and G. Olmo, "Analysis of emg signals by means of the matched wavelet transform," *Electronics letters*, vol. 33, no. 5, pp. 357–359, 1997.

[68] MathWorks. (2021) Introduction to wavelet families. [Online]. Available: https://it.mathworks.com/help/wavelet/gs/introduction-to-the-wavelet-families.html

[69] D. Volpe, F. Spolaor, Z. Sawacha, A. Guiotto, D. Pavan, L. Bakdounes, V. Urbani, G. Frazzitta, and R. Iansek, "Muscular activation changes in lower limbs after underwater gait training in Parkinson's disease: A surface emg pilot study," *Gait & Posture*, vol. 80, pp. 185–191, 2020.

[70] H. Yokoyama, T. Kato, N. Kaneko, H. Kobayashi, M. Hoshino, T. Kokubun, and K. Nakazawa, "Basic locomotor muscle synergies used in land walking are finely tuned during underwater walking," *Scientific Reports*, vol. 11, no. 1, pp. 1–11, 2021.

[71] A. Rainoldi, C. Cescon, A. Bottin, R. Casale, and I. Caruso, "Surface EMG alterations induced by underwater recording," *Journal of Electromyography and Kinesiology*, vol. 14, no. 3, pp. 325–331, 2004.

[72] K. Masumoto and J. A. Mercer, "Biomechanics of human locomotion in water: an electomyographic analysis," *Exercise and sport sciences reviews*, vol. 36, no. 3, pp. 160–169, 2008.

[73] I. N. P. Santos, I. d. S. Mendes, M. O. Lima, A. R. d. Paula Junior, A. R. Simioni, P. R. G. Lucareli, and F. P. S. Lima, "Muscle electrical activity during exercises with and without load executed on dry land and in an aquatic environment," *Research on Biomedical Engineering*, vol. 31, pp. 19–25, 2015.

[74] W. Veneziano, A. F. da Rocha, C. Gonçalves, A. Pena, J. Carmo, F. Nascimento, and A. Rainoldi, "Confounding factors in water EMG recordings: an approach to a definitive standard," *Medical and Biological Engineering and Computing*, vol. 44, no. 4, pp. 348–351, 2006.

[75] M. F. Silva, J. M. Dias, L. F. D. Bela, A. R. M. Pelegrinelli, T. B. Lima, R. G. da Silva Carvalho, M. Taglietti, J. P. B. Júnior, L. M. Facci, J. G. McVeigh

et al., "A review on muscle activation behaviour during gait in shallow water and deep-water running and surface electromyography procedures," *Journal of Bodywork and Movement Therapies*, vol. 24, no. 4, pp. 432–441, 2020.

[76] Z. Sawacha, F. Spolaor, W. J. Piątkowska, F. Cibin, A. Ciniglio, A. Guiotto, M. Ricca, R. Polli, and A. Murgia, "Feasibility and reliability assessment of video-based motion analysis and surface electromyography in children with fragile X during gait," *Sensors*, vol. 21, no. 14, 2021.

[77] A. Leardini, Z. Sawacha, G. Paolini, S. Ingrosso, R. Nativo, and M. G. Benedetti, "A new anatomically based protocol for gait analysis in children," *Gait & posture*, vol. 26, no. 4, pp. 560–571, 2007.

[78] V. Agostini and M. Knaflitz, "An algorithm for the estimation of the signal-to-noise ratio in surface myoelectric signals generated during cyclic movements," vol. 59, no. 1, pp. 219–225, 2011, publisher: IEEE.

[79] R. Ying and C. E. Wall, "A method for discrimination of noise and EMG signal regions recorded during rhythmic behaviors," vol. 49, no. 16, pp. 4113–4118, 2016, publisher: Elsevier.